Characterization of coordination patterns in lower limb amputees and healthy controls with a handless crutch

By

S. Mukui Mutunga

M.S., University of Kansas, 2019

B.S., Robert Morris University, 2014

Submitted to the gradute degree program in Bioengineering ad the Graduate Faculty of the

University of Kansas in partial fullfillment of requirements of Degree of Philosophy

_____

Chair: Sara Wilson, Ph.D.

_____

Carl Luchies, Ph.D.

_____

Neena Sharma, Ph.D.

_____

Adam Rouse, Ph.D.

_____

Eduardo Rosa-Molinar, Ph.D.

Date Defended: Wednesday 6 July 2022

The dissertation committee for S. Mukui Mutunga certifies that this is the approved version of the following dissertation:

Characterization of coordination patterns in lower limb amputees and healthy controls with a handless crutch

_____

Chair: Sara Wilson, Ph.D.

Date Approved: Wednesday 6 July 2022

Abstract

Lower limb amputation (LLA) is an often traumatic and life altering event that can be accompanied by life-long musculoskeletal complications. This is particularly concerning when the approximately 150,000 people who undergo lower limb amputation each year in the United States are considered. From a biomechanical standpoint, unilateral or bilateral LLA impacts lower-limb architecture inducing changes to gait like slower preferred walking velocities, stance time and length asymmetries, and swing time asymmetries. Amputation also impacts trunk and pelvic range of motion. Given the upstream effects of amputation, it is not surprising that amputees experience low back pain (LBP) at higher rates than the general population. In fact, surveyed amputees report that their back pain is more bothersome than phantom limb pain and some more bothersome than residual limb pain. Interestingly amputees and those with low back pain (LBP) present with similar gait and trunk and pelvic range of motion changes.

In recent years, methods that characterize relative movements or coordination patterns between spinal segments such as the trunk/torso and pelvis have proven to be more sensitive to LBP status than traditional gait and range of motion measures. These studies have found that adults with LBP, with a history of LBP, and no LBP all have distinct pelvic/trunk coordination patterns. Understanding how LLA impacts coordination patterns could lend insight into the development of LBP in both amputees and the general population.

The goal of this dissertation is to begin characterizing the effects of LLA on upper-torso, torso, and pelvic coordination patterns during both running and walking. In addition, the three most ubiquitous continuous methods used for calculating coordination patterns are compared using computer generated signals. These three methods are: Continuous Relative Phase (CRP), Continuous Relative Phase using the Hilbert Transform (CRP_{HT}) and Relative Fourier Phase

analysis (RFP). This dissertation aims to provide a comprehensive comparison of these methods along with a set of best practices.

The studies in this literature review reveal three overarching conclusions concerning coordination patterns in unilateral LLAs. Firstly, unilateral LLA does not impact overall patterning of pelvic/torso coordination patterns. As walking and running velocity increases pelvic/torso coordination patterns in amputees transitions from a more in-phase pattern where the pelvic and torso rotate together, to an out-of-phase pattern where there is counter rotation between segments. This is particularly apparent in lateral (frontal plane) and axial coordination patterns. These velocity dependent changes in coordination are also seen in healthy controls. However, like subjects with LBP, amputees maintain in-phase coordination patterns longer or spend a longer proportion of the gait cycle adopting in-phase coordination patterns. Secondly, in walking there were significant decreases in coordination variability. Again, echoing a pattern seen in non-amputees with LBP. Thirdly, the fourth chapter of this dissertation analyzes data on a cohort of controls walking with and without the iWalk 2.0 which was used to mimic knee disarticulation. While this is an unconventional way of analyzing the effects of LLA on gait mechanics results of this study show that it was an effective means of isolating the effects of LLA.

A comparison of continuous methods used to calculate coordination patterns revealed similarities between CRP and $CRP_{HT.}$ While RFP consistently overestimated relative phase between computer generated signals, whether this is of concern would depend on the research question. If the research objective is to characterize changes in coordination patterns, then a 10-15º overestimation of relative phase may not be of great concern. However, if the purpose of the research is to characterize variability particularly as a proxy for stability, this overestimation

could impact interpretation. Also, because RFP relies on windowing and the fundamental frequency of a signal, it is best used to analyze data where multiple cycles are collected.

Overall, the work in this dissertation clarifies and provides key considerations for researchers who would like to use CRP, CRP_{HT}, or RFP to analyze coordination between body segments. In addition, it adds to the growing body of literature characterizing coordination patterns in various populations and identifies unique changes to them that are induced by LLA.

Acknowledgements

To God be the glory, forever and ever. Amen.

There are many people who I would like to thank for the roles they played in keeping me sane as I weathered the waves that are graduate school. First and foremost, to my family: Isaac Kivuva, Catherine Mutunga, and Winnie Mutunga. By the sheer volume of your support, your prayers, and countless late-night calls I have finished. I cannot thank you for the gentle pushes to keep going when things inevitably did not work out like I expected and reminding me that in the end it will indeed be well. I'm particularly thankful for Margaret Aña-Maria Harden who gave me space over the years to exist in whatever frustrations, triumphs, joys, and sorrows I had. Grateful for Joel Hatungimana who seemed to have a better idea of my progress than me. To this day I'm not sure how. Thank you for encouraging me and reminding me to take care of myself and smothering me in your astonishing optimism. You always expected my best to come back around in moments I wasn't sure that was. Thank you.

I would be remiss if I did not thank the Madison & Lila Self Graduate Fellowship and the Fellows I had the good fortune to interact with over the four years of the program. I'm forever indebted to the Board of Trustees, the SGF staff, and my fellow Fellows. To Madison & Lila Self, I hope to one day pay your gift to me forward.

A special thank you to my home away from home: Bridges International at KU. Specifically: Cliff and Connie Harder, Josh and Kristin Lee, Katie Clemens and her family, Margarita Pavlova, Jonathan Crookham, Rute Muniz, Yuri Lee, Tianlu Wang, Chen Liang, Ayotunde Ikujuni, Jeremy Ensz, Matheus Oliveira DeSouza, Kali Hinmann, and Gregory Leung.

Thank you to my committee: Dr. Sara Wilson (Chair), Dr. Carl Luchies, Dr. Neena Sharma, Dr. Adam Rouse, and Dr. Eduardo Rosa-Molinar for their support and assistance. A

special thank you to Dr. Randolph Nudo, Dr. Jacob Sosnoff, Dr. Linda D'Silva, Dr. Chun-Kai Huang, James Fang, and Lingjun Chen for inviting me into your work, for letting me learn with you, and helping me see possibilities beyond my dissertation.

Table of Contents

Table of Figures

Table of Tables

Chapter 1 Development of the problem

1.1 Background

In the United States, an estimated 150,000 people undergo lower limb amputation (LLA) for reasons ranging from cancer to complications of diabetes and vascular disease, severe malfunction necessitating amputation, or trauma [1]. LLA on its own, regardless of etiology, is a traumatic and life-altering event. The accompanying musculoskeletal complications are of particular concern because of their long-term impacts on amputees' activities and quality of daily life. These complications include but are on limited to: ankle, knee, hip and back pain, osteoarthritis in the residual and intact limb, phantom limb sensations and pain, pain in the non-amputated limb and increased fall risk [2–6]. Of the LLAs surveyed by Smith and colleagues, 63.3% of them reported experiencing phantom limb pain, 76.1% residual limb pain, and 70.8% back pain in the past 4-weeks. These problems are often comorbid with nearly half (41.7%) experiencing all three [4]. These LLAs and others surveyed report that their back pain is more bothersome than phantom limb pain and some more bothersome than residual limb pain [2,4].

There have been efforts in both the general and amputee population to map back pain, especially back pain that presents without a physiological origin, to biopsychosocial parameters [1,3]. These parameters include psychosocial parameters such as depression, anxiety, kinesiophobia, and catastrophizing, and social parameters such as employment [7]. Butowicz and colleagues found no differences between amputees with and without chronic low-back pain (cLBP) in psychosocial parameters. They did find differences in kinesiophobia, where amputees intentionally avoid activities because they fear being in pain. These psychosocial parameters have been linked to bothersomeness in both upper and lower-extremity amputees. Ephraim et.al

found that amputees with a depressed mood were 3.9 times more likely to rate their back pain as "extremely bothersome" than not bothersome [8].

The loss of lower extremity musculature, as well as somatosensory feedback, has led to characteristic asymmetries in gait kinematics and kinetics, as well as thorax/trunk, lumbar, pelvic, and hip rotations. [9–17]. Studies that have evaluated gait kinematics have found an overall decrease in preferred walking velocity, longer intact side stance times, shorter swing and step times, and longer step widths [10,11,13–15]. As walking velocity increases, intact and amputated side temporal asymmetries decrease particularly in unilateral trans-tibial amputees (TTA) [13]. As for gait kinetics, amputees exhibit greater vertical ground reaction forces, which increase as walking velocity increases [13]. Studies evaluating postural changes during gait initiation in unilateral TTAs have found that changes in gait kinematics are largely due to longer stance times, especially when gait is initiated with the intact limb [18].

Studies evaluating changes in gait kinematics, and thorax, trunk, pelvis, and hip rotations in non-amputees with low-back pain (LBP) have found similar changes [19–23]. Mainly decreases in preferred walking velocity, an increase in stride-to-stride variability in pelvis and thorax transverse and sagittal rotations [21,23]. Results from some studies suggest that spinal segment rotations may not capture the full extent of the effects of LBP. Vogt reported seeing no differences in frontal, sagittal, and transverse plane pelvis, and thorax rotations between controls and those with idiopathic chronic LBP. However, they did report significant differences in coefficients of variation between groups in all three planes of motion [23]. In response to the lack of sensitivity in traditional rotation measures like range of motion, ensemble average calculations, and timing of peaks, other measures have come to the fore. Namely, those that characterize relative phasing and coupling between adjacent segments like Continuous Relative

Phase (CRP), Continuous Relative Phase using the Hilbert Transform (CRP_{HT}), and Relative Fourier Phase (CRP). Studies conducted by Lamoth and Seay have used them to identify changes in pelvis-trunk or pelvis-thorax coordination patterns in those with LBP, those whose back pain has resolved and controls [20,24–27].

In healthy adults, as walking speed increases, coordination patterns of the thorax/torso and pelvis generally transition from an in-phase pattern in the frontal and transverse planes – where the pelvis and thorax/torso rotate together; to an out-of-phase or anti-phase pattern where the pelvis and torso/thorax counter-rotate [28–30]. In those with LBP, this transition is either delayed non-existent [20,21,25,27]. During running, those without LBP exhibit a variety of pelvis-thorax coordination patterns [31]. In the sagittal and transverse planes, the pelvis and thorax adopt an out-of-phase coordination pattern, while in the frontal plane the coordination patterns remain in-phase with the thorax preceding the pelvis. Preece et al. hypothesized that these changes are to minimize center of pressure (COP) movement [31]. Like in walking, these pelvis-thorax coordination patterns remain largely in-phase in those with LBP [27,27]. Moreover, Seay et al. have found that those with resolved back pain have coordination patterns that are reminiscent of their pained counterparts. This leads them to conclude that those with resolved LBP represent a transition group and could help us better understand the biomechanical etiology of LBP.

To the author's knowledge, there is only one study that evaluates these coordination patterns in unilateral LLAs [10]. The aim of that study was to investigate the effects of walking velocity on pelvis-thorax coordination patterns in unliteral transfemoral amputees (TFAs). Goujon-Pillet et.al, reported that like those LBP, unilateral TFAs exhibited a guarded gait pattern characterized by a more in-phase trunk-pelvis axial coordination pattern [10]. They also reported

an effect of residual limb length and walking velocity on pelvis rotations. Together, walking velocity and residual limb length explained 40% of the variation in pelvic frontal plane range of motion [10].

1.2 Significance

Current literature shows surprising similarities in the gait kinematics and kinetics, and thorax, trunk, pelvis, and hip rotations of LLAs and those with LBP [32]. Therefore, it is likely that parallels may also be present in their coordination patterns. A deeper understanding of the effects of unilateral LLA on coordination patterns could lend insight into the etiology of LBP in both amputee and non-amputee populations. The overall goal of this study is in two parts: firstly, to understand the effects of unilateral LLA on coordination patterns. Secondly, to provide a comprehensive comparison of continuous methods used to calculate them.

In summary, this study will contribute to the knowledge of how unilateral lower-limb amputation affects coordination patterns during running in UTAs and walking, how different analysis methodologies affect these calculations, and how changes to coordination patterns could be correlated with the development of LBP. This knowledge can be combined with current physical and rehabilitation therapies to create interventions that directly target maladaptive coordination patterns. The work proposed here is expected to lead to improvements in physical and rehabilitation therapies.

In the short term, understanding coordination patterns between body segments could lead to a better understanding of other types of joint pain and musculoskeletal disorders including those with a neurological origin. Furthermore, this work will create a firm basis for choosing the proper methodology for characterizing coordination patterns, and adequate interpretation of results based on the chosen methodology. This work is also expected to solidify the importance

of coordination patterns in Biomechanics. Long-term this work and others building on it will improve prosthetic design and physical therapy interventions which will improve the quality of life, and reduce the long-term costs associated with lower limb amputation and LBP.

1.3 Specific Aims & Hypotheses

Specific Aim 1: Characterize gait parameters, segment rotations, coordination patterns of unilateral lower limb amputees (ULLAs), and controls during walking and running. We hypothesize that unilateral transtibial amputees (UTAs) during running will show gait asymmetries such as shorter stride lengths, longer contact times, and increased pelvic obliquity on the amputated sides. We also expect to see more in-phase coordination patterns between segments during running. Results of this study will be evaluated in chapter 4 of this dissertation titled "Evaluation of upper-torso, torso, and pelvic coordination patterns in runners with unilateral-transtibial amputation".

To characterize early adaptations to prosthetic use in amputees during walking, we will test controls with and without a handless crutch – iWalk 2.0. The iWalk will function as a surrogate for a prosthetic which will allow us to compare gait adaptations with and without the crutch. We expect to see gait asymmetries as well as a reduction in preferred walking velocity with the iWalk 2.0. Without the iWalk, we expect to see a transition from in-phase to out-of-phase coordination patterns as walking velocity increases. With the iWalk, we expect subjects to maintain an in-phase coordination pattern even as walking velocity increases. This study and it's results will be described in chapter 5 titled "Changes to upper-torso, torso, and pelvic coordination patterns in healthy controls with and without a handless crutch".

Specific Aim 2: Compare the effects of sinusoidal and non-sinusoidal signals on the interpretation of coordination patterns using standard CRP, CRP using the Hilbert Transform

(CRP_{HT}), and RFP. We expect CRP, CRP_{HT}, and RFP methodologies to accurately measure phase differences of 18º and 126º between sinusoidal signals regardless of frequency. We expect RFP and CRP_{HT} to better detect phase shifts in non-sinusoidal signals. For RFP this is because it does not rely on the oscillator assumption and does not normalize frequencies [33–35].
For CRP_{HT} because it transforms signals into a complex analytical signal it, therefore, does not rely on the identification of a fundamental frequency like RFP, and does not require normalization like traditional CRP [36,37]. Results from this aim will be discussed in chapter 6 titled "A comparison of continuous methods for calculating coordination patterns: a review of current approaches".

Accomplishing these specific aims will allow us to understand how coordination patterns change with lower limb amputation and determine whether these changes represent adaptations that could lead to the development of low back pain in general and lower limb amputee populations.

1.4 Summary

In recent years, relative phasing analysis that characterizes coordination patterns between torso/thorax and pelvis coordination patterns have shown to be more sensitive than traditional measures of range of motion and peak time in differentiating controls from pathological populations. This has been particularly true when evaluating the effects of LBP status on coordination patterns during walking and running. Surprisingly, unilateral LLAs present with similar spatiotemporal changes to gait as those with LBP. Namely a slower preferred running and walking velocity, and gait asymmetries in stance times, stride time and lengths, and swing times. Given the prevalence of LBP in unilateral LLAs, and how bothersome and persistent it is, characterizing changes to coordination patterns along with spatiotemporal gait parameters could

lend insight into the etiology of LBP in both amputee and non-amputee populations. Additionally, there are currently three ways to characterize coordination patterns: CRP, CRP_{HT}, and RFP. Understanding how each impacts the interpretation of coordination patterns would help inform best practices for their use in analysis.

1.5 References

[1] C.S. Molina, J. Faulk, Lower Extremity Amputation, in: StatPearls, StatPearls Publishing, Treasure Island (FL), 2021. http://www.ncbi.nlm.nih.gov/books/NBK546594/ (accessed November 13, 2021).

[2] D.M. Ehde, D.G. Smith, J.M. Czerniecki, K.M. Campbell, D.M. Malchow, L.R. Robinson, Back pain as a secondary disability in persons with lower limb amputations, Archives of Physical Medicine and Rehabilitation. 82 (2001) 731–734. https://doi.org/10.1053/apmr.2001.21962.

[3] W.C. Miller, M. Speechley, B. Deathe, The prevalence and risk factors of falling and fear of falling among lower extremity amputees, Archives of Physical Medicine and Rehabilitation. 82 (2001) 1031–1037. https://doi.org/10.1053/apmr.2001.24295.

[4] D.G. Smith, D.M. Ehde, M.W. Legro, G.E. Reiber, M. del Aguila, D.A. Boone, Phantom Limb, Residual Limb, and Back Pain After Lower Extremity Amputations, Clinical Orthopaedics and Related Research®. 361 (1999) 29–38.

[5] R. Gailey, K. Allen, J. Castles, J. Kucharik, M. Roeder, Review of secondary physical conditions associated with lower-limb amputation and long-term prosthesis use, Journal of Rehabilitation Research and Development. 45 (2008) 15–29.

[6] L.L. McNealy, S. A. Gard, Effect of prosthetic ankle units on the gait of persons with bilateral trans-femoral amputations, Prosthet Orthot Int. 32 (2008) 111–126. https://doi.org/10.1080/02699200701847244.

[7] C.M. Butowicz, J.C. Acasio, C.L. Dearth, B.D. Hendershot, Trunk muscle activation patterns during walking among persons with lower limb loss: Influences of walking speed, Journal of Electromyography and Kinesiology. 40 (2018) 48–55. https://doi.org/10.1016/j.jelekin.2018.03.006.

[8] P.L. Ephraim, S.T. Wegener, E.J. MacKenzie, T.R. Dillingham, L.E. Pezzin, Phantom Pain, Residual Limb Pain, and Back Pain in Amputees: Results of a National Survey, Archives of Physical Medicine and Rehabilitation. 86 (2005) 1910–1919. https://doi.org/10.1016/j.apmr.2005.03.031.

[9] B.S. Baum, B.L. Schnall, J.E. Tis, J.S. Lipton, Correlation of residual limb length and gait parameters in amputees, Injury. 39 (2008) 728–733. https://doi.org/10.1016/j.injury.2007.11.021.

[10] H. Goujon-Pillet, E. Sapin, P. Fodé, F. Lavaste, Three-Dimensional Motions of Trunk and Pelvis During Transfemoral Amputee Gait, Archives of Physical Medicine and Rehabilitation. 89 (2008) 87–94. https://doi.org/10.1016/j.apmr.2007.08.136.

[11] S.M.H.J. Jaegers, Prosthetic gait of unilateral transfemoral amputees: A kinematic study, Archives of Physical Medicine and Rehabilitation. 76 (1995) 736–743. https://doi.org/10.1016/S0003-9993(95)80528-1.

[12] S.B. Michaud, S.A. Gard, D.S. Childress, A preliminary investigation of pelvic obliquity patterns during gait in persons with transtibial and transfemoral amputation., Journal of Rehabilitation Research and Development. 37 (2000) 1–10.

[13] L. Nolan, A. Lees, The functional demands on the intact limb during walking for active trans□femoral and trans□tibial amputees, Prosthet Orthot Int. 24 (2000) 117–125. https://doi.org/10.1080/03093640008726534.

[14] Y. Sagawa Jr, K. Turcot, S. Armand, A. Thevenon, N. Vuillerme, E. Watelain, Biomechanics and physiological parameters during gait in lower-limb amputees: A

systematic review, Gait & Posture. 33 (2011) 511–526. https://doi.org/10.1016/j.gaitpost.2011.02.003.
[15] G.R.B. Hurley, R. McKenney, M. Robinson, M. Zadravec, M.R. Pierrynowski, The role of the contralateral limb in below-knee amputee gait, Prosthet Orthot Int. 14 (1990) 33–42. https://doi.org/10.3109/03093649009080314.
[16] H. Nadollek, S. Brauer, R. Isles, Outcomes after trans-tibial amputation: the relationship between quiet stance ability, strength of hip abductor muscles and gait, Physiotherapy Research International. 7 (2002) 203. https://doi.org/10.1002/pri.260.
[17] C. Sjödahl, G.-B. Jarnlo, B. Söderberg, B.M. Persson, Pelvic motion in trans-femoral amputees in the frontal and transverse plane before and after special gait re-education, Prosthetics and Orthotics International. 27 (2003) 227–237. https://doi.org/10.1080/03093640308726686.
[18] C.D. Tokuno, D.J. Sanderson, J.T. Inglis, R. Chua, Postural and movement adaptations by individuals with a unilateral below-knee amputation during gait initiation, Gait & Posture. 18 (2003) 158–169. https://doi.org/10.1016/S0966-6362(03)00004-3.
[19] C.J.C. Lamoth, A. Daffertshofer, O.G. Meijer, G. Lorimer Moseley, P.I.J.M. Wuisman, P.J. Beek, Effects of experimentally induced pain and fear of pain on trunk coordination and back muscle activity during walking, Clinical Biomechanics. 19 (2004) 551–563. https://doi.org/10.1016/j.clinbiomech.2003.10.006.
[20] C.J.C. Lamoth, O.G. Meijer, A. Daffertshofer, P.I.J.M. Wuisman, P.J. Beek, Effects of chronic low back pain on trunk coordinations and back muscle activity during walking: changes in motor control, European Spine Journal. 15 (2006) 23–40. https://doi.org/10.1007/s00586-004-0825-y.
[21] R.W. Selles, R.C. Wagenaar, T.H. Smit, P.I.J.M. Wuisman, Disorders in trunk rotation during walking in patients with low back pain: a dynamical systems approach, Clinical Biomechanics. 16 (2001) 175–181. https://doi.org/10.1016/S0268-0033(00)00080-2.
[22] J. Steele, S. Bruce-Low, D. Smith, D. Jessop, N. Osborne, Lumbar kinematic variability during gait in chronic low back pain and associations with pain, disability and isolated lumbar extension strength, Clinical Biomechanics. 29 (2014) 1131–1138. https://doi.org/10.1016/j.clinbiomech.2014.09.013.
[23] L. Vogt, K. Pfeifer, M. Portscher, W. Banzer, Influences of Nonspecific Low Back Pain on Three- Dimensional Lumbar Spine Kinematics in Locomotion, Spine. 26 (2001) 1910–1919.
[24] C.J.C. Lamoth, Pelvis-Thorax Coordination in the Transverse Plane During Walking in Persons With Nonspecific Low Back Pain, Spine (Philadelphia, Pa. 1976). 27 (2002) E92–E99. https://doi.org/10.1097/00007632-200202150-00016.
[25] J.F. Seay, Influence of Low Back Pain Status on Pelvis-Trunk Coordination During Walking and Running, Spine (Philadelphia, Pa. 1976). 36 (2011) E1070–E1079. https://doi.org/10.1097/BRS.0b013e3182015f7c.
[26] J.F. Seay, R.E.A. Van Emmerik, J. Hamill, Trunk bend and twist coordination is affected by low back pain status during running, European Journal of Sport Science. 14 (2014) 563–568. https://doi.org/10.1080/17461391.2013.866167.
[27] J.F. Seay, R.E.A. Van Emmerik, J. Hamill, Low back pain status affects pelvis-trunk coordination and variability during walking and running, Clinical Biomechanics. 26 (2011) 572–578. https://doi.org/10.1016/j.clinbiomech.2010.11.012.

[28] J.R. Franz, K.W. Paylo, J. Dicharry, P.O. Riley, D.C. Kerrigan, Changes in the coordination of hip and pelvis kinematics with mode of locomotion, Gait & Posture. 29 (2009) 494–498. https://doi.org/10.1016/j.gaitpost.2008.11.011.
[29] Y.-T. Yang, Y. Yoshida, T. Hortobágyi, S. Suzuki, Interaction Between Thorax, Lumbar, and Pelvis Movements in the Transverse Plane During Gait at Three Velocities, Journal of Applied Biomechanics. 29 (2013) 261–269. https://doi.org/10.1123/jab.29.3.261.
[30] R.E.A. van Emmerik, R.C. Wagenaar, Effects of walking velocity on relative phase dynamics in the trunk in human walking, Journal of Biomechanics. 29 (1996) 1175–1184. https://doi.org/10.1016/0021-9290(95)00128-X.
[31] S.J. Preece, D. Mason, C. Bramah, The coordinated movement of the spine and pelvis during running, Human Movement Science. 45 (2016) 110–118. https://doi.org/10.1016/j.humov.2015.11.014.
[32] H. Devan, P.A. Hendrick, D.C. Riberio, L.A. Hale, A. Carman, Asymmetrical movements of the lumbopelvic region: Is this a potential mechanism for low back pain in people with lower limb amputation?, Medical Hypotheses. 82 (2014) 77–85. https://doi.org/10.1016/j.mehy.2013.11.012.
[33] Y. Li, R.S. Kakar, M.A. Walker, L. Guan, K.J. Simpson, Upper Trunk-Pelvis Coordination During Running Using the Continuous Relative Fourier Phase Method, J Appl Biomech. 34 (2018) 312–319. https://doi.org/10.1123/jab.2017-0250.
[34] B.T. Peters, J.M. Haddad, B.C. Heiderscheit, R.E.A. Van Emmerik, J. Hamill, Limitations in the use and interpretation of continuous relative phase, Journal of Biomechanics. 36 (2003) 271–274. https://doi.org/10.1016/S0021-9290(02)00341-X.
[35] G.E. Robertson, G.E. Caldwell, J. Hamill, G. Kamen, S. Whittlesey, Research Methods in Biomechanics, Human Kinetics, 2013.
[36] P.F. Lamb, M. Stöckl, On the use of continuous relative phase: Review of current approaches and outline for a new standard, Clinical Biomechanics. 29 (2014) 484–493. https://doi.org/10.1016/j.clinbiomech.2014.03.008.
[37] M. Varlet, M.J. Richardson, Computation of continuous relative phase and modulation of frequency of human movement, Journal of Biomechanics. 44 (2011) 1200–1204. https://doi.org/10.1016/j.jbiomech.2011.02.001.

Chapter 2 Literature Review

2.1 Introduction

In the United States, it is estimated that 150,000 people lower extremity amputation each year [1]. While amputation of any limb can significantly impact activities and quality of daily life, lower limb amputation (LLA) has been associated with residual limb pain, phantom limb pain and sensations, non-amputated side pain, and back pain. Various surveys have found that 52% - 68.7% of LLA report experiencing low back pain (LBP) [2,3]. Approximately 17% of amputees report that their back pain is their most debilitating and persistent problem [3].

Within the non-amputee population, gait parameters and segment rotations have primarily been used to quantify the effects of LBP. However, findings from different studies are contradictory. Vogt and others reported changes to traditional gait parameters where those with LBP take smaller steps and have a reduced stride length. However, they only reported seeing increased pelvis thorax variability but not in the rotations [4–6]. A study conducted by Barzilay which characterized the effects of physical therapy to treat LBP on traditional gait parameters found that these measures return to normal after pain has resolved [4]. However, LBP is also a recurrent problem, suggesting that therapeutic interventions do not correct maladaptive movement patterns, and gait parameters do not capture underlying changes to gait that may predispose LBP sufferers to recurrent bouts.

Measures that characterize the coordination or coupling between rotating segments have shown to be more sensitive to the effects of LBP [5,7–9]. Additionally, changes in coordination patterns have been identified in those with resolved LBP in both walking and running [7,8]. These studies have generally found that those with LBP or a history of LBP have a delayed or

non-existent transition from an in-phase to an out-of-phase pelvis-thorax/trunk coordination pattern in frontal and transverse plane rotations [5,8,10].

Little is currently known about the effects of LLA on these coordination patterns. A study conducted by Goujon-Pillet found that those with unilateral transfemoral amputees (TFAs) presented with coordination pattern changes that mimic those seen in LBP populations [11]. Namely, a delay in the transition from an in-phase to out-of-phase coordination pattern between the pelvis and trunk. Given the prevalence of LBP among LLA, and the sensitivity of relative phasing and coupling in differentiating LBP, resolved and control populations, understanding how LLA impacts these coordination patterns could lend valuable insight into LBP etiology in both non-amputees and amputees.

2.2 Characteristics of amputee movements: postural sway, trunk stability, and walking and running gait

2.2.1 Postural sway and balance in amputees during standing

A significant characteristic of amputee gait is asymmetry. These are most apparent during intact and amputated side swing and stance timing and duration. Nadolleck and colleagues hypothesized these asymmetries are due to weak hip abductor musculature in TTAs [12]. To determine whether their hypothesis was valid, they evaluated quiet standing in unilateral TTAs under four conditions: quiet stance and even stance with eyes open and closed. They used correlation analysis to quantify the relationship between stance asymmetry, gait, and hip abductor strength measures. They discovered that TTAs increased weight-bearing on their intact limb compared to the amputated limb. This increase in weight-bearing was correlated with stronger hip abductor musculature on the intact side. As a result, amputees took longer steps and strides, had a lower stance to swing time ratio on the intact limb, and faster comfortable walking

velocities. In addition, a decrease in mediolateral center of pressure (COP) was correlated with decreased hip abductor muscle strength on the amputated side when standing with eyes closed. Increases in anterior-posterior COP accompanied decreases in amputated side mediolateral COP. Nadolleck et al. hypothesized that this increase is indicative of greater dependence on the sound limb for balance. Since COP exertion was associated with a longer time since amputation, it is possible that lack of confidence in the prosthetic, decreases in proprioceptive feedback, and weak hip abductor musculature all contribute to changes in COP.

Given the changes in standing sway and gait parameters in LLAs, other authors have been interested in characterizing mediolateral balance during gait and gait initiation [13,14]. Hof et al. conducted a study to evaluate mediolateral balance in unilateral TFAs during gait [13]. They evaluated traditional gait parameters and balance during support phases at three walking velocities: 0.75 m/s, 1.00 m/s, and 1.25 m/s, as well as during a visual Stroop test. Measures of interest included amputated and prosthetic side stride times, single and double limb stance as a percentage of stride, and the minimal distance at foot contact of the center of pressure and extrapolated center of mass (b_{min}). They hypothesized that amputees use a "stepping strategy" to maintain balance by dropping the center of mass (COM) towards the swing limb. Like previous studies, they found asymmetries during stance time. Interestingly, these authors did not see any amputated and intact side asymmetries in stride or double-stance times. However, there were differences between amputees and controls in all other parameters. These asymmetries in stance time did not decrease as walking velocity increased. Lateral b_{min} distance was greater on the prosthetic side when compared to the intact side and controls. This lateral displacement was like controls at all walking velocities on the intact side. They believe that this increase in lateral displacement on the amputated side showed an increase in step width. They hypothesize that the

lack of ankle on the prosthetic side reduces the ability of amputees to adjust foot placement, impacting stability. Therefore, amputees adopt a wider step width to maintain stability.

Tokuno et al. were interested in balance control in unilateral TTAs during gait initiation [14]. They hypothesized that there would be temporal, kinematic, and kinetic adaptations due to the limitations of the prosthetic. These limitations included decreased propulsive force generated by the prosthetic and the lack of proprioceptive feedback. Gait initiation begins with a limb beginning the swing phase of the gait cycle. During this portion, the swing limb exerts a lateral force that shifts the center of mass towards the stance limb. This frees the swing limb to generate a forward propulsive force with a peak of approximately 7% of body weight. At the same time, the stance limb generates a posterior force with a peak of approximately 14% of body weight. After finishing its swing phase, the heel of the leading limb contacts the ground. The trailing limb ends its stance phase and begins the swing phase, generating a posterior force. The leading limb, which is now at stance, acts as a shock absorber. These researchers found that COP measures were like controls on the intact side. However, the COP displacement on the prosthetic side was smaller than on the intact side. Moreover, when the intact limb was the leading limb, the COP was placed more anteriorly than when the prosthetic was leading. The sum of the COP under each foot was of a greater magnitude when leading with the intact limb than with the prosthetic. Given the changes to gait parameters, it is reasonable to hypothesize that unilateral LLAs rely heavily on their intact limbs. Tokundo and colleagues found that unilateral TTAs compensate entirely for the lack of propulsive forces generated by the prosthetic with the intact limb during forward propulsion [14]. When leading with the intact limb, the impulse was two times greater than controls, and when leading with the prosthetic, it was 1.5 times greater. They

hypothesize that longer intact side stance times are used to generate these propulsive forces and help counteract the instability of the prosthetic limb.

2.2.2 Trunk stability in amputees during sitting and implications for stability during walking

The effects of LLA go far beyond changes to standing balance because of the loss of lower-limb musculature and the need to compensate for that loss further upstream. A study conducted by Hendershot et al. evaluated trunk stability in LLAs [15]. To eliminate the contribution of the intact side ankle, knee, and hip on balance, they opted for a seated sway protocol. Along with traditional measures of postural sway (95% ellipse area, RMS distance, mean sway velocity), they also reported the short-term scaling exponent (H_s) calculated from the stabilogram-diffusion plots.

Stabilograms are created by plotting the averaged squared distance traveled by the COP against corresponding time intervals [16]. These graphs have two distinct regions – a short and long-term region representing open-loop and closed-loop postural control. From stabilograms, the scaling exponents for the short-term (H_s) and long-term (H_L) regions which describe the correlations between step increments are calculated, as well as the critical point (C_p), which represents the point of transition from short-term to long-term to control [17]. Interpretation of H is as follows: an $H > 0.5$ indicates a persistent system indicating that past and future displacements are positively correlated. Therefore, a system that is increasing in the past will continue to increase in the future. An $H < 0.5$ indicates an anti-persistent system where past and future displacements are negatively correlated.

Hendershot et al. found that traditional postural sway measures were larger in LLAs than in controls [15]. H_s was greater in the anterior-posterior direction for LLAs than controls but similar

in the mediolateral direction, indicating a level of persistence. While both groups showed H_s > 0.5, the level of persistence among LLAs was less than for controls. Hendershot and colleagues hypothesized that coupled with the increases in COP sway measures, the reduction in persistence indicated a less healthy system. Furthermore, they found that for LLAs, the anterior-posterior C_p amplitude was nearly twice that of controls, meaning that LLAs likely have a significant delay when adjusting to perturbations. According to Radebold, the increase in C_p amplitude may indicate a proprioceptive "dead zone" that can predispose LLAs to additional injury because deviations in trunk position and orientation that would normally be corrected in non-amputees are left uncorrected in LLAs [18].

Changes to seated trunk stability can have implications for stability during gait. Mahon et al. evaluated trunk motion as a measure of stability in unilateral TFAs [19]. They characterize the effects of unilateral TFA on a broad range of measures that fell into four broad categories: biomechanical, physiological, functional, and subjective. Parameters that fell under the biomechanical category included stability (fall risk), overuse, and efficiency. Among changes found in gait kinematics described previously, they also saw increases in peak trunk velocity and lateral flexion towards the amputated limb. They hypothesized that increases in peak trunk velocity and step width variability are compensations for increased instability during gait in amputees. Evidence suggests that step width variability decreases with time since amputation [13]. However, no such evidence exists for trunk stability measures. The increase in trunk lateral flexion towards the prosthetic side may help stabilize the prosthetic limb during gait. However, it reduces efficiency and increases bending moments between L5 and S1. The increase in bending moments could lead to overuse injuries and contribute to LBP development in LLAs.

2.2.3 Gait kinematics of amputees during walking

The gait of LLAs, particularly unilateral LLAs, is often characterized by asymmetries in gait kinematics, kinetics, and trunk or thorax, pelvis, and hip rotations. Generally, those with LLA have slower self-selected walking velocities, and present with asymmetries in stance and swing times when intact and prosthetic sides are compared [11,12,20,21]. One such study was conducted by Nolan and colleagues [22]. They characterized sagittal plane kinematics, joint movements, and power dynamics of the intact limb in both unilateral TTAs and TFAs. Both amputee types compensate by increasing intact side ankle range of motion. This results in increased knee extensor moments and power absorption during push-of and power absorption, and greater hip flexor moments and power generation during push-off. Nolan et al. found that these results were impacted by prosthetic type however, none was able to mimic the joint kinematics and kinetics of controls.

A similar study also by Nolan and colleagues investigated the effects of increased walking velocity on vertical Ground Reaction Forces (vGRF), vertical impulse during stance, duration of stance, swing, step, and magnitude of asymmetry during gait in both unilateral TTAs and TFAs [23]. They tested participants walking at 0.5, 0.9, and 1.2 m/s. Initial analysis revealed that there were no significant correlations between intact and amputated limbs for any of these variables therefore, each limb was treated as a separate variable. Both groups showed stance and swing time asymmetries where the intact side had longer stance times, and shorter swing and step times. As walking velocity increased, amputated side swing and step time duration increased. In addition, amputated side swing and step time durations increased with increasing walking velocity. Nolan et al. hypothesized that this may be an adaptation to allow amputees to walk faster.

Some studies have evaluated the effects of stump length on gait parameters [20]. This is particularly important because those with TFA lose ankle and knee joints and a portion of their thigh and hip musculature depending on residual limb length. It is thought that atrophy of thigh and hip musculature caused by long-term adaptations to amputation and prosthetic use can impact gait kinematics and kinetics. Jaegers et al. conducted a study whose aim was to evaluate gait kinematics and trunk, hip, and knee rotations in those with unilateral TFA. Their findings were like those mentioned previously. In addition, they also found wider step lengths on the prosthetic side in TFAs at comfortable walking velocity and that amputees compensate for higher walking velocities by increasing stride length rather than cadence. As for the effect of stump length, they found that stance times increased with increasing stump length. They hypothesized that this was due to the absence of a propulsive mechanism in the prosthetic leg.

2.2.4 Hip, pelvis, lumbar, and trunk rotations during walking in amputees

The effects of LLA are not limited to changes to gait, and seated trunk stability. In fact, the impact of LLA on seated trunk stability implies that rotations of spinal segments may also be affected. Studies that have characterized how LLA influences upper body rotations have found differences between LLA and control populations [11,12,19–22,24–26].

A study conducted by Jaegers and colleagues found no significant differences in hip flexion on the amputees' intact sides and healthy controls during walking [20]. However, there is greater overall hip flexion/extension range of motion on the amputated side during walking, which increases with velocity. Evidence suggests that this is correlated with stride length [20]. Sagawa et al. believe that this is used to maintain adequate speed and increase functional step length [21]. As walking velocity increases, timing differences in intact and prosthetic side flexion and extension become more apparent [20]. At fast walking velocities, maximum hip

extension occurs earlier, likely due to the shortened stance time on the prosthetic side. After prosthetic side heel strike, amputees also show a rapid transition from flexion to extension. Some studies suggest that prosthetic foot type does not influence the hip motion of TTA or TFAs [27]. In the long-term, increases in hip sagittal range of motion could lead to LBP development in this population.

Changes in pelvis rotations have also been reported in LLAs, and asymmetries between the pelvis and lumbar region during walking have been implicated in LBP development in this population [11,25,26,28,29]. In normal gait, the pelvis is neutral at initial contact with pelvic drop occurring at the loading response [25]. Pelvis obliquity generally reaches its greatest amplitude at toe-off, returning to its neutral position as the trailing leg begins its swing phase. At a self-selected speed, healthy pelvic obliquity is usually 5-7º and increases with increasing walking velocity.

Unilateral TTAs displayed a smaller magnitude of pelvic obliquity from amputated side initial contact to intact side toe-off. Unilateral TFAs specifically show a smaller pelvic drop than controls [11,25,26]. Michaud et al. hypothesize that this may be due to prosthetic fit or inability to flex the knee, which allows the pelvis to drop [30]. Both TFAs and TTAs exhibit the hip hike characteristic of amputee gait. However, they exhibit pelvic drop at different points of the gait cycle. TTAs demonstrate pelvic drop during intact side single-limb-stance and TFAs during intact and prosthetic side single-limb stance. Hip hike is thought to help amputees clear the swing limb and reduce the reliance on the weak hip abductor musculature for lateral stability. Amputees instead increase trunk lateral flexion to assist with lateral stability. Peak-to-peak pelvic obliquity in TTAs and controls was similar. However, TFAs present with significantly less peak-to-peak pelvic obliquity. Additionally, Goujon-Pillet et al. found that unilateral TFAs

have significantly less pelvic rotation in anterior-posterior tilt, obliquity, and rotation [11]. Pelvic tilt, walking velocity, and limb length were correlated with stump length. For every additional meter/second increase in walking velocity, there was an 8.4º increase in pelvic tilt. For every millimeter decrease in stump length, there was a 0.02º decrease in pelvic tilt.

Morgenroth et al. designed a study whose aim was to identify differences in the lumbar spine kinematics of unilateral TFAs with and without LBP and controls [30]. They hypothesized that TFAs with LBP would exhibit greater lumbar excursions in all planes of rotations. To tease out the effects of lower-limb amputation and LBP on lumbar spine kinematics, they collected data on a cohort of unilateral TFAs with and without LBP walking at their preferred velocity. Their control population walked at a pace that matched the self-selected speed of the amputees. The authors reported no statistically significant differences in the lumbar spine excursions in the frontal and sagittal planes of TFAs with and without LBP. However, those with LBP showed more significant lumbar spine rotation. This was driven by changes in trunk kinematics more than pelvic kinematics. In cadaveric studies, transverse plane rotations, or complex rotations that include rotations in the transverse plane, have been shown to increase annulus fiber strain [31]. This increase in strain and shear stress on the discs could be a factor in disc degeneration that leads to the development of LBP [28].

Several studies have evaluated the effects of LLA on thorax/trunk rotations [11,15,20,32]. LLAs show greater trunk lateral flexion towards the amputated limb during the swing phase. Jaegers and Baum hypothesize that LLAs follow through the hip hike to clear the swing limb by increasing trunk lateral flexion [20,32]. Goujon-Pillet et al. reported a greater range of motion in all planes in the trunk in TFAs [11]. Baum conducted a study whose aim was to understand the impact of TFA and knee-disarticulation (KA) on gait kinematics and kinetics

and its effects on trunk and hip rotations [32]. Their findings on gait kinematics and pelvic rotations are like those expressed earlier. However, like Jaegers, they found no impact of stump length on trunk rotations, particularly trunk lateral-flexion [20,32].

2.2.5 Gait kinematics, and hip, pelvic, and trunk rotations in amputees during running

While evaluation of amputee walking gait and spinal segment rotations is common in the literature, there are several studies explore running gait in LLAs as well. These studies focus on joint reaction forces, running kinetics, ankle, knee, and hip kinematics, and the energy cost of running in LLAs [33–35]. Running gait is critical to evaluate for two reasons. Firstly, the effects of walking cannot be extrapolated to running because of the replacement of the double-stance phase with the double float phase as one transitions from walking to running. Unilateral TFAs show increased interlimb asymmetries during running. More specifically, unilateral TFAs present with increased prosthetic side hip hike during swing [33]. This phenomenon is more significant during running than walking due to the need to compensate for the prosthetic knee, which remains straighter for longer than the intact side.

Like Burkett, Sanderson and Martin conducted a study to evaluate running in unilateral TTAs rather than unilateral TFAs [35]. They found that TTAs also increase running velocity by increasing stride length like controls. However, this increase is significantly less than in controls. To accommodate, amputees adjust the stance to swing ratio and maintain their stride velocity on their amputated sides. The stride frequency of controls was like the intact side in amputees. These TTAs, like Burkett's TFAs, also showed an overall straighter amputated limb. Sanderson and Martin hypothesize that this compensation is used to reduce knee collapse and reduce braking and propulsive forces.

Studies that evaluate energy costs associated with walking and running in amputees have been used to determine whether different prosthetic types, mainly those that differ in foot and ankle architecture, give LLAs an unfair advantage in sports compared to controls [34]. Mengelkoch and colleagues conducted a study to evaluate energy costs of unilateral TTAs using three types of prosthetics: the solid joint ankle cushioned heel (SACH), and two energy storing and return prosthetics (ESAR) meant for general use (Renegade foot) and specifically for running (Nitro foot). They measured both self-selected walking and running velocities (SSWS & SSRS) and tested subjects at various prescribed walking and running velocities. TTAs had slower SSWS and SSRS than controls with all prosthetic types but ambulated significantly slower with the SACH foot and fastest with the Nitro foot. TTAs in this study had shorter aerial and swing times, which the authors hypothesized increased ground contact times, resulting in more time to apply a propulsive force. TTAs also exhibited a decrease in ground reaction forces indicative of a force impairment. As for energy expenditure during walking and running, TTAs had higher VO_2 and lower gait efficiency scores than controls with all prosthetics. However, there was a prosthetic foot type effect. The SACH foot had the greatest VO_2 and lowest gait efficiency score, while the Nitro foot had the greatest efficiency score. They also reported that at similar peak VO_2, amputees had a lower running velocity when compared to controls. Studies that evaluate the energy costs of various prosthetics are essential for understanding the implications of LLA and prosthetic type on sports performance. However, these studies do not answer questions related to the long-term effects of prosthetic use and the ways in which adaptation could lead to the development of LBP in this population.

2.3 Low back pain in the general population

Little is known about the development of LBP in amputee populations. However, it has been well studied in the general population, where studies suggest that 17.6% of the population experience a bout of back pain lasting a week or more in a year [36]. This results in 149 million workdays lost. Like those with LLA, those with LBP also present with changes to stability, gait, and segment rotations. Whether these changes are caused by the onset of LBP or can cause LBP is unknown. An understanding of the effects of LBP in the general population could inform our understanding of LBP in LLAs.

2.3.1 Postural sway and balance during sitting and standing in those with LBP

Like amputees, those with LBP also present with changes to standing and seated sway measures [15,18,37–39]. Like amputees, both measures are of interest because they show a full range of effects of LBP. Seated sway isolates postural control of the lumbar spine, which is vital for stability, balance recovery, and injury avoidance [18].

A study conducted by Radebold characterized postural control in the lumbar spine and muscle response latencies during loading in a seated position in those with LBP [18]. They hypothesized that those with LBP would perform more poorly than controls during the unstable sitting test, that there would be correlations between trunk muscle response and balance performance, and that average muscle response times, age, and body weight will have stronger correlations with balance performance when the task was performed with eyes opened than with eyes closed. They tested 16 subjects with chronic idiopathic LBP, and 14 matched healthy controls to test the hypotheses. Each sat on hemispheric seats with four different diameters representing four levels of instability (flat surface, 50, 44, and 22 cm) with eyes open and eyes closed. They also calculated muscle response times to the quick release test. To evaluate

differences in seated postural control they used stabilogram plots [16]. Overall, both H_s and H_L increased with increasing instability and when the task was performed with eyes closed. However, the LBP group had greater diffusion coefficients under all conditions. This indicates that they moved their COP more than controls. Overall, H_s was less in those with LBP than controls. While both groups had short-term scaling exponents greater than 0.5 indicating persistent short-term movements, persistence was less in those with LBP. Radebold and colleagues hypothesize that this may be due to proprioceptive "dead zones" resulting from damage to the lumbar spine's proprioceptive tissue. To overcome these "dead zones", those with LBP generate larger COP movements in the short-term, leading to decreased short-term persistence.

A similar study conducted by Reeves measured the impact of LBP on trunk neuromuscular control on stability thresholds [38]. Their research aimed to identify a critical seat stiffness at which subjects could no longer maintain their balance. They hypothesized that critical seat stiffness is more sensitive than standing postural sway to deficits in neuromuscular control since it is more sensitive to visual feedback. They recruited 79 subjects with non-specific LBP who performed a stability threshold test during seated balancing. They conducted correlation analysis to determine whether there was a significant relationship between the seat stiffness at which subjects lost their balance, current pain levels, 7-day average pain score, and disability level as measured by Oswestry Disability Index. Reeves and colleagues found a significant correlation between the 7-day average pain score and seat stiffness such that a one-unit increase in pain score resulted in a 2.6 Nm/rad increase in the seat stiffness at which seated balance could no longer be maintained. This indicates that those with LBP had decreased trunk neuromuscular control.

A study conducted by della Volpe et al. characterized the effects of chronic LBP on COP measures during quiet standing [39]. These authors believe that changes to postural sway in those with LBP are not an adaption to pain but rather is indicative of an underlying dysfunction in proprioception or the processing of proprioceptive information. This is similar to the proprioceptive "dead zone" that Radebold discussed during seated sway tasks [18]. Subjects were tested under two support conditions and three visual conditions. The support conditions were fixed, and sway referenced where the platform would move in proportion to anterior/posterior sway. The visual conditions were fixed, eyes closed, and sway referenced where their visual field was moved in proportion to anterior/posterior sway. They found that the LBP group increased COP velocity and root mean square (RMS) COP in the anterior/posterior direction. There were no statistically significant differences in velocity or RMS of the COP in the mediolateral direction. The most significant changes to the COP occurred when eyes were closed, and both the visual field and platform were moving in proportion to anterior/posterior sway. Those with LBP tended to sway more, indicating a greater reliance on optical inputs for maintaining balance. Furthermore, to ensure that these changes were not because of pain, they tested controls before and after experimentally inducing arm pain. They found no changes in this population. Like Radebold, della Volpe and colleagues concluded that the increase in anterior/posterior sway in those with LBP is indicative of a proprioceptive "dead zone". Due to changes in proprioception, those with LBP cannot detect small changes in postural sway; therefore, larger deviations in postural sway are needed for adjustments to be made.

Lafond and colleagues were interested in the effects of chronic LBP on postural way measures during short and long periods of quiet stance [37]. Their study consisted of a 32-minute trial with two 60-second intervals of quiet standing tested before and after a 30-minute prolonged

standing period. During short period standing trials, subjects were instructed to stand with their feet approximately pelvis width apart and stand as still as possible. During prolonged standing, subjects were allowed to shift as needed. They found that those with LBP had fewer postural changes during prolonged stance and tended to sway less than controls. During short quiet stance periods, those with LBP showed increased postural sway in the anterior/posterior direction, and RMS COP and sway velocity were greater than in controls. There was a significant increase in postural sway during the short quiet stance period after prolonged stance than before. This indicates the possibility of neuromuscular fatigability in both groups, which is exacerbated by LBP. The reduced postural sway during prolonged stance in those with LBP may indicate a lack of mobility in these subjects. Lafond et al. hypothesize that this is due to the impact of LBP on hip balance strategy, which results in a stiffer posture in this population. Like Radebold and della Volpe, they also came to conclude that those with LBP have a proprioceptive "dead zone" which was exemplified by fewer postural changes during prolonged stance in LBP subjects, likely due to the inability to sense musculoskeletal discomfort. Adaptations to these proprioceptive "dead zones" could include changes to gait kinematics, as well as trunk, lumbar and pelvic rotations.

2.3.2 Effects of LBP on gait kinematics, and trunk, lumbar, and pelvic rotations during walking

A study conducted by Vogt and colleagues compared the gait parameters and thoracolumbar and pelvis three-dimensional kinematics of subjects with and without chronic idiopathic LBP and controls [6]. Those with LBP had significantly shorter stride times due to shorter step lengths than controls. These results are in line with other studies which have found that those with LBP increase walking velocity by increasing cadence rather than stride length [4]. In addition, they found that those with LBP showed more significant upper lumbar movement

variability in the sagittal and transverse planes and higher coefficients of variation in the pelvis in all three planes of motion. No statistically significant differences were reported between groups in the range of motion or rotational amplitudes of thoracolumbar or pelvis segments in any plane. Vogt and colleagues initially assumed that changes in stride times and step lengths were due to an adoption of a guarded gait pattern in those with LBP. However, the lack of statistically significant differences in thoracolumbar and pelvis range of motion and rotational amplitudes does not support this hypothesis. Moreover, they concluded that variability measures captured general variability in human movement, not distinct changes to variability induced by LBP. They did not identify significant group differences in range of motion because they tested at one prescribed walking velocity that had no relation to the preferred walking velocity. Since prescribed walking velocity may be too fast for some participants and too slow for others, LBP-induced changes to average range of motion would be similar between groups.

In a similar vein, Steele conducted a study to find correlations between lumbar kinematic variability and isolated lumbar extension strength in those with and without chronic LBP [40]. They hypothesized that those with chronic LBP had motor control deficiencies which placed stress on the lumbar spine resulting in pain. Additionally, they seemed less capable of repeating lumbar spine movement patterns than controls. They also found correlations between lumbar spine extension strength and transverse plane kinematics that were more rigid in those with LBP. Like Vogt, Steele found that healthy controls show a mostly sinusoidal, repeatable kinematic pattern indicating decreased variability and fine control of the lumbar spine musculature. In contrast, those with chronic LBP show more significant variability and a loss of fine motor control of the lumbar spine. Steele et al. hypothesize that the increase in variability seen in LBP

populations is due to lumbar extensor deconditioning. This would also explain the high correlation between lumbar extensor strength and transverse plane kinematics.

Studies that have evaluated changes to gait kinematics and trunk, lumbar, and pelvic rotations in those with LBP report that after back pain has resolved these parameters return to normal [4,41]. However, the high recurrence rate of LBP suggests that current methods are not sensitive to the long-term adaptations to LBP that could explain high recurrence. One measure that has shown some promise evaluates relative phasing or coordination patterns between the pelvis and trunk.

2.4 Relative Phase Analysis

Relative phase analysis is used to characterize the relationship between two signals. In Biomechanics, it is often used to describe inter-joint, intra-joint, or segment coordination during tasks that have a repetitive motion such as walking, running, lifting, or balance [5,7–9,24,42–54]. Four primary methods appear in the literature for calculating coordination patterns. These are discrete relative phase (DRP), continuous relative phase, also known as portrait analysis (CRP), continuous relative Fourier phase (RFP), and continuous relative phase using the Hilbert transform (CRP_{HT}). In this section, these methods will be described briefly along with their underlying assumptions, implications on interpretations, and a summary of the existing comparative literature. For details on how to calculate coordination patterns using each method, see Chapter 3.

2.4.1 Discrete relative phase (DRP)

DRP is a method for calculating the difference in the relative timing of events [44,55]. For instance, McClay and Manal used DRP to calculate the differences in the relative timing of tibial internal rotation and foot eversion, knee flexion, and foot eversion, and knee internal

rotation and foot eversion in runners with and without excessive pronation [55]. The disadvantage of DRP is that it is a point estimate and therefore only reveals the coupling of the joints or segments of interest at a particular time. In the case of McClay and Manal, these were peak tibial eversion, maximum knee flexion, and internal rotation. However, the advantage of DRP is that it only requires calculating joint or segment rotations as normal [44].

2.4.2 Continuous relative phase (CRP)

As the name suggests, CRP is a method that continuously estimates the relative phasing between two signals. This method involves calculating the angular velocities from angular positions and normalizing them so that the signals for each segment are nearly circular in the phase plane and lie between ±1. CRP is then calculated as the difference between distal and proximal phase angles [44]. The advantage of CRP lies in that it is a continuous calculation. This enables researchers to track coordination patterns throughout the cycle of interest (ex: walking). The absolute value of the CRP gives the overall coordination patterns where 0˚ indicates an in-phase pattern and 180º indicates an out-of-phase (or anti-phase) coordination pattern [49]. A negative CRP would indicate that the proximal segment is lagging, while a positive CRP would indicate that the distal segment is lagging.

There are two primary limitations to CRP. Firstly, the methodology assumes perfectly sinusoidal (or harmonic) signals. Human motion is typically non-sinusoidal, consisting of signals with multiple frequencies that may not be harmonic. Peters et al. and Lamb et al. showed the effects of sinusoidal waves with frequencies deviating from $0.5/\pi$ Hz and non-sinusoidal signals on the position-velocity phase planes [Figure 2.2]. Signals with frequencies not equal to $0.5/\pi$ Hz are elliptical along the velocity axis (plotted on the y-axis) on the position-velocity phase plane graphs, and non-sinusoidal signals usually have non-circular phase-plane graphs. To impose a circular shape these signals often need to be normalized [Figure 2.1]. It also functions to eliminate low-frequency oscillations that appear in the non-normalized CRP signal. Peters and Haddad, Hamill and

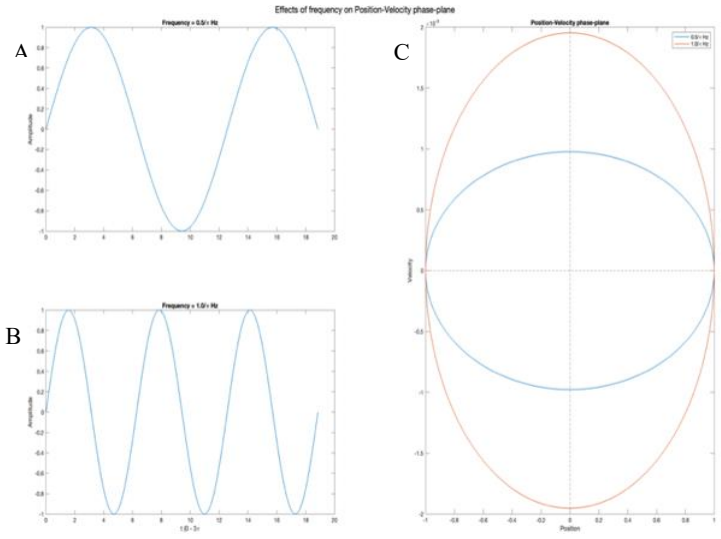

Figure 2.2: the effects of sinusoidal signals of different frequencies on position-velocity phase planes. A) Sinusoidal signal with an amplitude of 1, and frequency of 0.5/π Hz. B) Sinusoidal signal with amplitude of 1 and frequency of 1/π Hz. C) Position-velocity phase plane graphs for both signals. Velocity was calculated using the central difference method of vector used to

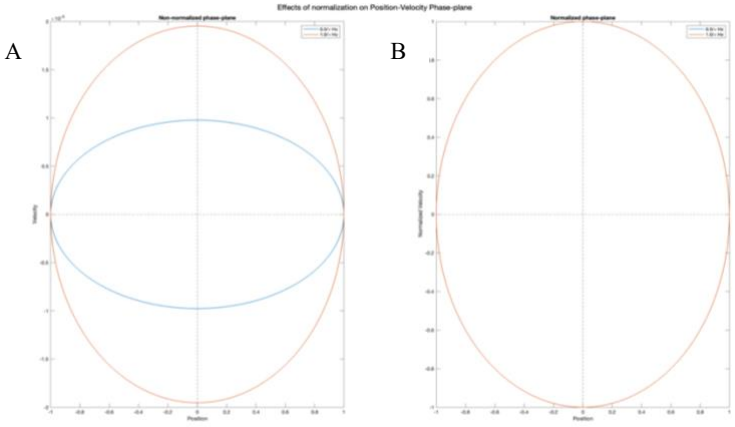

Figure 2.1: Effects of frequency normalization on the position-velocity phase-plane. A) 0.5/π Hz and 1/π Hz phase-plane graphs showing the distortion of the 1/π Hz signal phase-plane in the velocity axis prior to normalization. B) After normalization of the velocity vector, 0.5/π Hz and 1/π Hz signals overlap, and the 1/π Hz signal is circular.

Haddad, and z normalization methods and characterize their effects on CRP calculations and interpretations [44,45,56,57].

2.4.3 Continuous relative Fourier phase (RFP)

RFP is also a continuous method used to calculate coordination patterns between joints and segments. Instead of normalizing angular position and/or velocity to approximate a circular phase plane, RFP removes the higher frequencies of the signal by calculating the phase angles using the fundamental frequency of the segment with the greatest index of harmonicity. This method was preferred by Li and Kakar and Lamoth et al. to calculate trunk-pelvis coordination in all planes during walking and running [5,24,47,58]. The advantage of RFP is that its application to non-sinusoidal signals does not require normalizing like CRP. Like CRP, RFP is also calculated as the difference between distal and proximal phase angles and interpreted in the same way where 0˚ indicates an in-phase pattern and 180˚ is indicative of an out-of-phase pattern.

There are two primary limitations associated with RFP: when using the fundamental frequency of the segment with the highest index of harmonicity, all other frequencies are discarded. Therefore, if the signal does not have a dominant frequency, valuable information about the signal may be lost. Secondly, it is inappropriate for signals with significant differences in fundamental frequency. Li et al. recommend against using it to describe locomotor-respiratory coordination because of the large differences in the fundamental frequencies of these signals [58]. Significant differences in the fundamental frequencies may misrepresent the actual coordination patterns.

2.4.4 Continuous relative phase using the Hilbert Transform (CRP_{HT})

The CRP_{HT} has been described in detail by Lamb and Stöckl and used to calculate coordination patterns during lifting in those with acute LBP and walking in elderly adults

[43,46,52]. Like RFP referenced above, it does not require phase-plane normalization. This is primarily because it transforms the signal into a complex analytical signal and is therefore not bound by the sinusoidal oscillator assumption. The CRP_{HT} works by taking the Hilbert transform of the angular positions which provides the real and analytical portions of it. The phase is calculated using the arctangent of the real and imaginary outputs from the Hilbert transform. As in all other cases, CRP_{HT} is calculated as the difference between proximal and distal segment phases. CRP_{HT}, RFP, and CRP are all interpreted similarly.

A study conducted by Varlet and Richardson highlighted potential limitations of CRP_{HT} and posited half-phase normalization for CRP as an alternative [59]. They tested three different signals: a sinusoidal signal without additional frequency modulations, a sinusoidal signal with modulation frequency between cycles, and a sinusoidal signal with modulation frequency within cycles. Along with the Hilbert transform, they also tested three normalization techniques: no-normalization, mean period normalization, and half period normalization. They found that the mean period normalization technique presented unexpected oscillations like non-normalized CRP in frequency-modulated signals. The Hilbert transform over-estimated the CRP indicating that modulated frequencies impact it. The half-period normalization technique showed the most accurate results in all three signals. While Varlet makes a compelling argument, their analysis fails to consider that human motion is frequency modulated and non-sinusoidal. From other studies of human motion, non-sinusoidal signals seem to present a more significant challenge than frequency modulated signals. Since half-period normalization is based on the CRP analysis method, it is also tied by the sinusoidal oscillator assumption. It would likely require additional normalization to account for the other frequencies in non-sinusoidal signals.

2.4.5 Relative phase methods – a summarization of strengths and limitations

As noted, DRP, CRP, $CRP_{HT,}$ and RFP have their strengths and limitations. DRP is advantageous when the goal is to determine the relative timing of joint or segment during a movement event. For example, McClay and Manal used DRP to calculate the timing of maximum knee flexion and foot eversion during the stance period of the gait cycle [55]. Limiting the calculation to specific movement events and rotations of interest removes the challenges of analyzing non-sinusoidal signals and therefore does not require normalization. The constraint also requires a researcher to consider which events are important and why. However, if the researcher's primary interest is in characterizing relative movements over time, DRP is no longer applicable and must instead choose a continuous method.

CRP, CRP_{HT}, or RFP are all advantageous for continuously calculating relative movements of joints and segments. For instance, one can track the relative motion of the knee and hip throughout a gait cycle, which may lend insight into how diseases like osteoarthritis, pain, or surgical interventions the relative movements of these joints. This is insightful in the long term because patients rarely show changes to joint kinematics and kinetics years after intervention. Still, compensatory changes that appear in relative timing can persist long after intervention. Since these changes can be subtle, choosing the proper method to capture the changes to relative timing is essential. The main differences between these methods lie in how they manage non-sinusoidal signals. CRP normalizes the angular position and velocity to make the phase plane as close to circular as possible. Many authors have explored the impacts of these normalization techniques on the coordination calculations [44,57,59,60]. RFP and CRP_{HT} are advantageous because they do not require normalization of the phase planes. Theoretically, this means their calculations and interpretation of coordination patterns should be more accurate.

While there are studies that compare CRP and CRP_{HT}, and CRP and DRP, none compare CRP or CRP_{HT} and RFP [46,60].

2.4.6 Relative phase in the general population

Several studies have evaluated coordination patterns between hip, knee, and ankle rotations during lifting and walking, and trunk/thorax, lumbar, and pelvis rotations during walking and running [5,7,8,24,42,43,47,50,52–54,58,61,62]. Studies evaluating coordination patterns and their variability during walking and running in healthy controls will be reviewed in this section.

Studies that have evaluated the effect of walking velocity on trunk/thorax and pelvis coordination patterns and variability in the general population have found velocity effects these measures [24,53,54]. With increasing walking velocity there is a transition from an in-phase pelvis-thorax coordination pattern to an out-of-phase pattern in the transverse plane. Yang et al. hypothesized that this change in coordination was driven by the pelvis, whose transverse plane rotation increased with increasing walking velocity to increase strides length [54]. Studies that evaluate coordination variability do so as a proxy for stability [53]. Van Emmerik et al. found that pelvis-thorax coordination variability increased and then decreased as walking velocity increased [53]. The Yang and van Emmerik studies mentioned above used CRP to calculate coordination patterns. Other studies like those conducted by Lamoth used RFP [47]. Despite the different methods, the three authors identified velocity-dependent changes in coordination. Lamoth evaluated pelvis and thorax indexes of harmonicity instead of the individual pelvis and thorax rotations to see which segment contributed to the changes in coordination. They found additional peaks between 2 and 3 Hz in pelvic power spectrums as walking velocity increased. Meanwhile, the thoracic segment consisted of a single harmonic at all walking velocities. Like

Yang, they concluded that this change in the pelvis index of harmonicity drove the velocity-dependent changes in coordination.

Few studies use the Hilbert Transform to evaluate coordination patterns in any population to the author's knowledge. One such study was conducted by Choi who evaluated ankle, knee, and hip coordination in older adults using both CRP_{HT} and CRP . Generally, they found that hip-knee and knee-ankle coordination was out-of-phase during swing and in-phase during stance. Choi and colleagues concluded that there was little difference between these methods. This was supported by a high cross-correlation coefficient (≥ 0.9). The main difference between these methods is that CRP_{HT} signals were the inverse of the CRP signal. This is likely because CRP is calculated as the absolute value differences of the segments or joints of interest.

Studies that have evaluated coordination patterns during running have also found unique patterns [7,8,62]. A study by Preece et al. aimed to explore coordination patterns between the pelvis and spine in all three planes during running and map it back to the motion of the center of mass [62]. In the sagittal and frontal planes, the pelvis and thorax exhibited an out-of-phase coordination pattern. In the frontal plane at stance, there was a pelvis-only coordination pattern. Pelvis-only coordination occurred when the resulting coupling vector between the pelvis and thorax was more vertically aligned because of a more significant increase in pelvis rotation when compared to the thorax. In the transverse plane, subjects exhibited a more in-phase pelvis-thorax coordination pattern, where the pelvis motion preceded the pelvis in most subjects. Preece and colleagues hypothesized that the anti-phase coordination in the frontal plane was used to minimize mediolateral movement of the COM during running, elevate the swing leg to ensure foot clearance, and increase the stride length.

2.4.7 Effects of LBP on relative phase

A study conducted by Seay and colleagues provides a comprehensive exploration of the effects of LBP status on pelvis-thorax coordination patterns and variability as a function of walking and running velocity [7,8]. Their study consisted of three groups: an LBP group experiencing pain, a resolved group (RES) who had experienced LBP that impacted their running but had been running pain-free for at least six months before testing, and a control group who had not experienced LBP. Trials were collected while walking/running on a treadmill whose speed was increased from 0.8m/s to 3.8m/s in increments of 0.5m/s. Seay reported that their subjects naturally began to run at 2.3m/s. Therefore, there were three walking speeds of 0.8, 1.3, and 1.8 m/s, and four running speeds of 2.3, 2.8, 3.3, 3.8 m/s. Seay used CRP to calculate pelvis-trunk coordination patterns.

In both populations, they found that as walking velocity increased, CRP also increased. In the frontal plane, those with LBP had significantly more in-phase coordination. LBP group showed more in-phase coordination than the RES group, however, this result did not reach statistical significance. In addition, the LBP group spent more time in-phase in the frontal and transverse planes than controls. These more in-phase coordination patterns were seen in those with LBP despite increases in walking velocity. Therefore, at no walking velocity tested were the coordination patterns of those with LBP and controls similar.

As running speed increased, CRP decreased in the sagittal plane and increased in the frontal plane. CRP in the transverse plane showed a preference effect. At running velocities close to preferred, CRP was low. As running velocity deviated from preferred CRP increased. All subjects spent a higher percentage of the gait cycle out-of-phase in the frontal plane during running. Controls spent significantly more time out-of-phase than both RES and LBP subjects. In

the sagittal and transverse planes, all three groups spent equal time in both in-phase and out-of-phase coordination patterns. The LBP and RES groups spent significantly more time in-phase than controls, and the control groups spent considerably more time in-phase than the LBP group in the transverse plane. Seay hypothesized that the double stance period during walking presents a convenient way for subjects to adjust pelvic gait mechanics in the frontal plane and pelvic axial rotation. Changes in the frontal and transverse planes in those with LBP indicate a guarded gait pattern which reduces frontal and transverse plane rotations. The statistically significant difference in pelvis-trunk coordination patterns in the RES and LBP and RES and control groups suggests that the RES group presents a transition group between those with LBP and controls.

All three groups presented with approximately equal CRP variability during walking in all three planes. Variability during running in all three groups was smaller than during running. Only in pelvis-trunk transverse plane coordination was there a statistically significant difference. Those with LBP showed significantly less variability than controls. Seay hypothesized that this decrease in CRP variability in the transverse plane during running indicates a guarded gait pattern. Those with LBP maintain more control over the movement of their pelvis and trunk, decreasing relative motion between the segments likely to reduce pain incidence. The result is a decrease in the variability. Additionally, the reduction in CRP variability shows that those with LBP cannot adjust to external perturbations. This could increase their risk of injury.

In addition to pelvis-trunk coordination in all three planes, Seay also evaluated the effects of LBP status and running velocity on trunk bend-and-twist coordination [10]. They argue that looking at relative motions within a segment allows for a better understanding of how LBP status impacts functional movements. This is particularly applicable to athletes who often engage in complex motions as a part of their sport, and because cadaveric show that complex rotations that

include twist studies increase annulus fiber strain which can lead to the development of LBP [31]. As for trunk bend-and-twist coordination, Seay found statistically significant differences in the CRP of controls and those with LBP. Post-hoc analysis revealed that those with LBP had significantly more in-phase trunk bend-and-twist coordination than controls. There were no statistically significant differences between RES and control, and RES and LBP groups. However, large effect sizes indicated clinically substantial differences between these groups. Unlike other coordination pattern analyses, trunk bend-and-twist coordination showed no velocity effects.

With all studies summarized above, the primary limitation is that it is unknown whether the presence of LBP caused the changes in coordination or whether changes in coordination lead to the development of LBP. To answer this, Lamoth conducted a study whose aim was to characterize the effects of experimentally induced pain and fear of pain on the trunk and pelvis coordination during walking [47]. Lamoth recruited healthy subjects for a four-minute treadmill walk at four velocities: 2.2, 3.8, 4.6, and 5.5 km/h. For the pain tasks, Lamoth administered a hypertonic saline solution intramuscularly. For the fear of pain condition, Lamoth injected an isotonic saline solution. Finally, subjects walked while expecting electrical shocks in the low back for fear of impending pain and no pain tasks.

Lamoth reported no statistically significant differences in the coordination patterns during any conditions. While they reported a velocity effect for coordination patterns, there was no velocity by condition interaction. There are three primary limitations of this study. Firstly, subjects may not have experienced pain for long enough to induce changes in coordination patterns. Secondly, the location and intensity of the pain may have been below the threshold at which changes would be observed. Lastly, experimentally induced pain is not associated with

movement. Those with LBP experience varying pain levels depending on the activities they are engaged in. Since no such correlation exists for those experiencing experimentally induced pain, changes to coordination patterns may have been dampened.

2.4.8 Relative phase in amputees

To the author's knowledge, only one study evaluated the impacts of LLA on the relative phase between the trunk and pelvis [11]. It has been documented in other studies that there is an effect of walking velocity on pelvis-trunk coordination patterns [53]. In healthy controls, as walking velocity increases, there is a linear increase in the relative phase between the pelvis and thorax from approximately 25º at 0.3 m/s to 110º at 1.3 m/s. These changes are characterized as a transition from an in-phase pelvis-thorax coordination pattern to an out-of-phase pattern. The study conducted by Goujon-Pillet aimed to evaluate the pelvis-thorax relative phasing of unilateral TFAs at a self-selected speed. They hypothesized that there would be a decrease in the pelvis-thorax counter-rotation in amputees. In other words, TFAs would maintain a more in-phase coordination pattern when compared to their non-amputated counterparts. As expected, they found a significant decrease in the pelvis-thorax relative phase in the transverse plane in TFAs who had a CRP of 76º and controls who had a CRP mean of 105º. Goujon-Pillet and colleagues hypothesized that this more in-phase coordination pattern seen in TFAs was indicative of a guarded gait pattern. Additionally, their results show the ineffectiveness of range of motion measures in capturing differences between populations. They reported seeing similar pelvis axial range of motion measures between TFAs and controls. While they did not report seeing changes in sagittal plane relative phasing, they did see greater angular pelvis and trunk range of motion. It is possible that while the range of motion was greater, the coordination patterns between these segments remained the same during walking.

2.5 Conclusions

Studies that characterize how LLA impacts human movement are critical because of the long-term impacts of amputation. It is well documented that those with LLA suffer from other musculoskeletal injuries. Back pain is among the most common and bothersome of these injuries [2,3]. Studies that evaluate LBP effects have found changes to traditional gait parameters, trunk stability, and segment and joint rotations [4,6,18,37,39,40]. Since these measures return to normal after back pain has resolved, the etiology of LBP remains unknown [4]. Interestingly, those with LBP and unilateral LLA present with similar changes to gait parameters, trunk stability, and segment and joint coordination patterns. Both groups have slower preferred walking velocities, spend less time during the stance phases of the gait cycle, which are also the most unstable, have decreased trunk stability, and adopt a guarded gait pattern which reduces the amount and variability in pelvic rotations [11,12,20,21]. Studies that evaluate the effects of LBP in unilateral LLA show that changes to these parameters are exacerbated by LBP [30]. While these studies have helped develop our understanding of the effects of LBP and LLA on activities of daily living, high occurrence and recurrence rates of LBP suggest that current analysis methods are not sensitive enough to identify changes to movement that increase the likelihood of developing LBP in the general population. This, in turn, reduces the ability of researchers and rehabilitation specialists to identify adaptations to LLA that predispose this population to LBP.

In recent years, coordination patterns have come to the fore as a potentially sensitive measure for identifying changes to movement in a pained state that persist when pain has resolved [5,7,8,10]. These persistent adaptations could predispose non-amputee populations to recurrent LBP. To the author's knowledge, three continuous methods are used to characterize coordination patterns, each with its strengths, weaknesses, and limitations [46,56,57,59]. CRP

and RFP have been used successfully to identify changes in coordination in those with and without LBP [7,8,10]. CRP has been used to identify changes in those with and without LBP and those with resolved LBP. While CRP has shown to be sensitive to persistent changes in coordination, the use of this method and interpretation of results is often challenged by the need for normalization. Peters and Haddad performed a thorough comparison of DRP and CRP. They explored the impacts of one normalization technique on the interpretation of signals with known phase shifts [57]. In another work, Kurz and Stergiou compared the effects of different normalization techniques on calculating coordination patterns [46]. Lamb and Colleagues compared CRP and CRP_{HT}. A comprehensive comparison of continuous methods for calculating coordination patterns has not been done to the author's knowledge. Conducting a systematic evaluation of these methods within the same context will give researchers much-needed guidance when choosing the proper method for analysis given the type of data they wish to analyze, present their strengths, weaknesses, and limitations clearly, and inform the interpretation of results using each method.

2.5.1 Project goals

This project has two primary aims. Firstly, this project will characterize coordination patterns of unilateral LLAs during walking and running. Doing so will give a more comprehensive understanding of the effects of LLA on walking. Data on unilateral LLAs performing overground running tasks at various velocities and healthy controls walking with and without the iWalk 2.0 at multiple speeds will be used to accomplish these aims. Testing overground walking and running at speeds that deviate from comfortable is important because studies have shown that walking and running velocity can impact coordination patterns. The iWalk 2.0 will be used to mimic knee-disarticulation in LLAs. Data from controls wearing the

device will uncover early adaptations made by LLAs that could increase their likelihood of developing LBP in the future. Secondly, this project will meticulously compare existing methods for calculating coordination patterns. Sinusoidal and non-sinusoidal signals with known phase shifts and human subjects' data will be used to compare these methods. Using known signals will allow for testing of the accuracy of the results and the development of a set of best practices. Recommendations concerning the use, interpretations, strengths, weaknesses, and limitations will be given from this data. Human subjects' data will be used to better understand how these methods impact the interpretation of this data.

2.5.2 Future applications

Coordination patterns have been used to evaluate the effects of various disorders that impact movements such as Parkinson's Disease, stroke, and Diabetic Peripheral Neuropathy [44,63,64]. These studies suggest that coordination patterns may be sensitive to changes in proprioception, vestibular function, and visual-motor impairment. However, the evaluation of coordination patterns in rehabilitation settings is limited. For instance, it is well documented that patients who suffer a mild Traumatic Brain Injury (mTBI) present with reduced neck range of motion. Guidelines for treatment and evaluation of this population encourage rehabilitation specialists to measure these decrements and include interventions that address reduced neck range of motion [65]. Incidentally, rehabilitation specialists also observe that those with mTBI have trouble independently moving the neck and upper torso. This inability to de-couple neck and upper torso movement can change coordination patterns. It is currently unknown whether coordination patterns of segments and joints below the upper torso impact mTBI.

A thorough understanding of how various pathologies impact coordination patterns and methods to measure them in clinical settings could provide clinicians with more detailed

knowledge of how pathology affects human movement. In turn, they can adapt interventions to address the most pressing needs of patients and improve outcomes.

Table 2.1: Summary of studies which evaluate the effects of LBP and lower-limb amputation on various aspects of human movement. List of abbreviations used in the table: low-back pain (LBP), unilateral transfemoral amputees (UTFA), unilateral knee disarticulation (UKA), unilateral transfemoral amputees (UTTA), lower-limb amputees (LLA), root mean square (RMS), L/R (left/right), % gait cycle (%GC), center of pressure (COP), anterior/posterior (A/P), mediolateral (M/L), vertical ground reaction forces (vGRF), continuous relative phase (CRP), relative Fourier phase (RFP)

Study	Population	Activity	Measures	Objective	Outcomes
Barzilay et al, 2015 [4]	LBP & controls	Walking	Spatiotemporal gait parameters - walking velocity, cadence (steps/m), L/R step length, L/R stance (%GC), L/R single-limb support (%GC)	Measures the effects on spatiotemporal gait parameters 3 and 6 months after treatment	At baseline (prior to intervention), LBP impacted all spatiotemporal parameters. A statistically significant decrease in step length was found in LBP subjects when compared to controls
Baum et al., 2008 [32]	UTFA/UKA	Walking	Spatiotemporal gait parameters - walking velocity, intact/prosthetic step length and stance time Hip, pelvis, and trunk kinematics	Characterize the effect of residual limb ratio in UTFAs and UKAs on spatiotemporal gait parameters, and hip, pelvis, and trunk kinematics	No correlation was found between limb ratio and walking velocity, intact/prosthetic step length or stance time, hip flexion, or trunk lateral and forward flexion Correlations were found between limb ratio and pelvic tilt excursion
Buckley et al., 2002 [66]	UTTA, UTFA, controls	Standing postural sway and active balance	Quiet standing balance strategy - ankle vs. hip Postural sway measures - COP, RMS COP Dynamic balance measures vision/no vision - board angular displacement and contact duration	Measure dynamic and static postural sway and balance control ins amputees	<u>During static balance</u> the COP range, variability and RMS were greater in amputees in all directions when compared to controls <u>During dynamic</u> balance tasks amputees spent significantly less time in balance when compared to controls. In addition, there was a significant increase in board contacts on the prosthetic side in the M/L direction during no vision condition. However, there were no overall group differences in board contacts

Burkett et al., 2007 [33]	UTFA & controls	Walking and running	Hip and knee kinematics and kinetics (Kinematic results reported)	Compare control and amputee hip and knee kinematics and kinetics during walking and running	As tasks transitioned from walking to running inter-limb hip asymmetries increased. More specifically, amputees displaced reduced hip flexion which resulted in smaller steps Overall asymmetry decreased with the transition from walking to running Angular velocity of the prosthetic hip was greater than in the intact hip Increased hip hike on the prosthetic side during swing Prosthetic knee extends 1.6 times faster than the intact knee. While this is dependent on the prosthetic type, Burkett hypothesized that was a strategy adopted to lock the knee in preparation for the stance phase
della Volpe et al., 2006 [39]	LBP & controls	Standing postural sway	COP, RMS COP and COP velocity in the M/L and A/P directions	Characterize the effects of chronic LBP on postural sway during quiet under two platform conditions and three visual conditions: - Platform conditions: fixed platform and platform way referenced (platform moves in proportion to A/P sway) - Visual conditions: fixed, eyes closed, sway referenced	Subjects with LBP presented with increased A/P COP velocity and RMS COP when compared to controls. No statistically significant differences were found between groups in the M/L direction Authors hypothesize that these changes are due to a proprioceptive "dead zone" which dampens the ability of those with LBP to detect small changes to A/P sway

				(proportion to A/P sway)	
Fatone et al., 2016 [67]	UTFAs w/ & w/o LBP, controls	Walking	Pelvic, lumbar, and thoracic kinematics	Measure the effects of LBP on pelvic, lumbar, and thoracic kinematics and determine if any differences between groups could be attributed to LBP	Rotations of the thoracic, lumbar, and pelvis were similar between groups in all planes There were no significant differences in the proportion of each group that exhibited a flexion or extension pattern of the lumbar spine in the sagittal plane In the transverse plane, 75% of amputees with LBP adopted a lumbar spine rotation away from the prosthesis while 50% of amputees without LBP adopted a similar pattern
Goujon-Pillet et al., 2008 [11]	UTFA & controls	Walking	Temporal gait parameters Trunk and pelvis range of motion and CRP	Investigate the effects of walking velocity on pelvis and thoracic kinematics in UTFAs	Statistically significant differences were found between amputees and controls in pelvic range of motion. Amputees had greater standing pelvic obliquity. Authors hypothesize that this is due to weak hip abductor musculature At single limb support, UTFAs had significantly less pelvic tilt in the frontal plane Pelvis and trunk ROM was greater in amputees in sagittal and frontal planes for the pelvis and in all planes for the trunk

Hendershot et al., 2013 [15]	UTFA, UTTA		Seated sway parameters - 95% Ellipse area (cm^2), RMS distance - A/P (cm), RMS distance - ML (cm), Mean velocity - A/P (cm/s), Mean velocity - ML (cm/s) Stabilogram plot analysis - short term scaling exponents (H_s), Critical point time (C_pT) Critical point amplitude (C_pA), and COP	Isolate the effects of LLA on trunk stability	Statistically significant effects of LLA were found in all seated sway parameters when compared to controls. Stabilogram analysis revealed statistically significant differences between LLA and controls in all A/P measures and in no M/L measures. More specifically: - H_s was larger for both UTTAs and UTFAs when compared to controls indicating they had less persistence than controls. $H_s > 0.5$ indicates a persistent direction of the COP. This persistence was significantly less in LLAs - C_pT and C_pA was nearly twice as long in LLAs as in controls. This indicates amputees have a significant delay in corrective responses to postural perturbations
Isakov et al., 1996 [68]	UTTA	Walking	Spatiotemporal gait parameters - number of steps, stride time (s), stride length (cm), cadence (steps/min), walking velocity Gait events for intact and amputated sides - stance (s), swing (s), double-limb-support (s), step time(s), step length (cm) Hip joint angles measured at - heel-strike, stance extension (max), toe-off, swing flexion (max) Knee joint angles measured at - loading response, toe-off, swing flexion (max) Two walking velocities tested - self-selected & fast (faster than self-selected)	Determine the effects of walking velocity on gait spatiotemporal parameters and hip, and knee kinematics	There were significant asymmetries between intact and prosthetic sides in all spatio-temporal parameters that were maintained as walking velocity increased Walking velocity also increased knee interlimb asymmetries during loading response and toe-off Walking velocity did not affect intact and amputated side hip asymmetries There were no significant effects of timing of knee loading response, maximum hip extension at stance, toe-off, maximum knee flexion at swing, and maximum hip flexion at swing

Jaegers 1995 [52]	UTFA, controls		Temporal gait parameters Trunk and hip range of motion	Study the effects of UTFA on spatiotemporal gait parameters, and trunk, hip, and knee kinematics as walking velocity increases	Spatiotemporal gait parameters: UTFAs generally increase walking velocity by increasing stride length and decreased step rate. At comfortable walking velocities they show wider step widths. The double-limb support phase of the gait cycle is 10-30% longer on the prosthetic side than on the intact side. Prosthetic/intact side asymmetries increase with increasing walking velocity. As stump length decreases there is an increase in the stance time of the gait cycle Trunk rotations: amputees show greater lateral rotation of the trunk towards the prosthetic side at prosthetic sie stance. Hip rotations: there were no statistically significant differences between control and amputee intact side hip flexion. however, on the prosthetic side there was an increase in hip flexion which increased with increasing walking velocity. IN the sagittal plane, amputees showed greater hip range of motion on the amputated side when compared to the intact side. Timing of hip rotation: maximum hip extension occurred earlier during the fast walking velocities due to the shortening of the stance time. This was accompanied by a rapid transition from flexion to extension on the prosthetic side after intact side heel strike

Khodadadeh et al., 1993 [69]	LBP & controls	Walking	Spatiotemporal gait parameters - walking velocity, cadence, L/R stance, L/R swing, LR double-limb support, force-time curves	Characterize the effects of spinal fusion on spatiotemporal gait parameters	Prior to surgery, those with LBP walked 50% slower than controls, their cadence was 75% slower, and they showed L/R asymmetries in stance, swing and double-limb support phases. Stance, swing, and double-limb support phases were also longer in those with LBP 6 months after surgery there were minor changes to spatiotemporal gait parameters 2 years after surgery, changes to gait parameters were mixed While the majority of spinal fusion surgeries were considered successful, this was not often accompanied by an improvement in gait parameters
Lafond et al., 2014 [37]	LBP & controls	Standing postural sway Prolonged standing	COP	Characterize the effects of chronic LBP on prolonged stance (30min) and quiet standing (60s)	During prolonged stance subjects with LBP showed fewer postural changes and decreased sway when compared to control. This could be indicative of a lack of mobility in these subjects. In addition, fewer postural changes suggests that those with LBP have a decreased ability to sense musculoskeletal discomfort which could be due to decreased proprioception. During quiet stance those with LBP showed increased postural sway particularly in the A/P direction. COP RMS and COP velocity were greater in those with LBP than in controls Those with LBP showed increased postural sway during quiet stance after prolonged stance indicating neuromuscular fatiguability

Lamoth et al, 2004 [47]	Controls & controls w/ experimentally induced pain	Walking	Pelvis, lumbar, and thorax relative phase (RFP)	Determine whether experimentally induced pain or fear of pain impacts lumbar erector spinae activity, or pelvis-thorax coordination patterns as walking velocity increases (relative phase results discussed)	As walking velocity increases there is an increase in transverse plane relative phasing of the pelvis and thorax, lumbar and thorax, and pelvis and lumbar Pelvis-thorax relative phase transitions from an in-phase pattern to an out-of-phase pattern in the transverse plane as walking velocity increases Experimentally induced pain and fear of pain do not significantly impact segment relative phasing
Lamoth et al., 2002 [24]	LBP & controls	Walking	Pelvis and thorax range of motion, relative phase (RFP)	Characterize the effects of LBP on transverse plane pelvis-thorax relative phasing at various walking velocities	There were no statistically significant differences between groups in pelvis or thorax range of motion At the highest walking velocity (5.4 km/hr) there were statistically significant differences in pelvis range of motion Statistically significant differences between controls and those with LBP were found at higher walking velocities (>3.0 km/hr) Pelvis-thorax mean relative phasing was greater in controls than in those with LBP
Michaud et al., 2000 [25]	UTFA, UTTA, controls	Walking	Pelvis range of motion in the frontal plane (L/R tilt)	Characterize the differences between UTTA and UTFA pelvic frontal plane rotations at four walking velocities (Self-selected speed (SSS), Slow - SSS - 20%, Fast + 20%, maximum(	In UTTAs, pelvic frontal plane rotations were asymmetric around neutral. Pelvic drop at prosthetic loading response was significantly less than sound side. UTTAs showed prosthetic side hip hike during the swing phase while UTFAs showed hip hike during single-limb-support on both prosthetic and intact

					sides and decreased pelvic drop at loading response on prosthetic side. Increased hip hike is assumed to help clear the swing limb The linear relationship between peak-to-peak pelvic obliquity and walking speed was similar between UTTAs and controls. UTFAs and controls had similar intercepts but a lower slope
Morgenroth 2010 [30]	UTFAs w/ & w/o LBP, controls	Walking	Lumbar range of motion	Study the differences in lumbar spine kinematics between UTFAs with and without LBP and controls	UTFAs showed greater lumbar spine rotation. Authors hypothesized this was influenced more by trunk kinematics than by the pelvis No significant differences between UTFAs with and without LBP in sagittal or frontal plane lumbar excursion Pooled UTFAs showed greater lumbar sagittal plane range of motion than controls
Müller et al., 2015 [70]	LBP & controls	Walking and running on even and uneven surfaces	Spatiotemporal gait parameters - walking velocity, step length (m) Transverse plane rotations of the trunk, pelvis and thorax Sagittal plane rotations of the ankle, knee and trunk Ground reaction forces	Characterize the effects of chronic LBP on trunk and pelvis rotations while walking and running on even and uneven surfaces	LBP subjects showed decreased pelvic rotational amplitudes when compared co controls during walking Trunk inclination at touchdown was significantly higher in those with LBP There were no statistically significant differences between groups during running in thorax or trunk inclination at touchdown. However, there was a decrease in pelvis and trunk rotational amplitudes in those with LBP on even ground
Nadollek et al., 2002 [12]	UTTA	Walking	Temporal gait parameters Hip range of motion COP	To measure the effects of hip abductor musculature strength on gait parameters and standing sway measures in UTTAs	Strong hip abductor musculature is correlated with larger step and stride lengths and faster walking velocities Strong hip abductor musculature also lowers stance and swing time rations in the intact limb

Nolan et al., 2000 [23]	UTTA, UTFA	Walking	Temporal gait parameters	Determine the effects of increased walking velocity on vGRFs, and various spatiotemporal gait parameters	Temporal gait asymmetries decrease with increasing walking velocity Amputees generally have greater vGRFs
Nolan et al., 2003 [23]	UTTA, UTFA	Walking	Temporal gait parameters Ankle, knee, and hip range of motion, kinetics, and kinematics	Measure sagittal plane kinematics, and joint moment and power dynamics in the intact limb of UTTAs and UTFAs	Amputees compensate by increasing intact side ankle range of motion which increase: knee extensor moments power generation during weight acceptance knee extensor moments and power absorption during push-off hip extensor moments and power absorption during weight acceptance hip flexor moments and power generation during push-off
Pelegrinelli et al., 2020 [50]	LBP	Walking and running	Pelvis, lumbar, and thorax relative phase (vector coding)	Measures the effects of LBP on thorax, lumbar, and pelvis coordination and coordination pattern variability during running	Lumbar-thorax frontal plane coordination is most impacted by LBP status Inability to adopt an out-of-phase lumbar-pelvis coordination pattern may be indicative of a guarded gait pattern that is used to reduce stress on soft tissues and avoid pain While distinct differences appeared in coordination patterns, there were no statistically significant differences in the variability of these patterns
Radebold et al., 2001	LBP	Seated sway	Stabilogram plot analysis COP - A/P Path - COP path lengths RMS	Characterize the effects of LBP on postural control of the lumbar spine	Those with LBP had poorer lumbar spine postural control which had correlations with delayed trunk muscle response. Authors hypothesize that poor trunk muscle response and postural control suggests reduced proprioceptive feedback
Reeves et al., 2008 [38]	LBP & controls	Seated way	Stability thresholds	To determine the effects of LBP on trunk neuromuscular control and how it impacts stability thresholds	Stability thresholds are sensitive to current pain, changes in average pain and disability

Russel Esposito et al., 2014 [71]	UTFAs w/ & w/o LBP, controls	Walking	Pelvis and trunk relative phase (CRP)	Determine the effects of LBP on UTFA pelvic-trunk transverse plane coordination and variability at various walking velocities	LBP did not seem to significantly impact coordination pattern or variability in the transverse plane in UTFAs There were no differences in coordination pattern variability between groups
Sanderson et al., 1997 [35]	UTTA & controls	Running	Ankle, knee, and hip kinematics	Characterize the effects of UTTA on ankle, knee, and hip kinematics at two running speeds	As running velocity increases, both amputees and controls increase stride length, although the magnitude of this increase in amputees is lower Overall prosthetic side ankle, knee, and hips remain less flexed/extended resulting in an overall straighter limb when compared to the intact side and to controls
Seay et al., 2011 (a,b) [7,8]	LBP, resolved LBP & controls	Walking and running	Trunk and pelvis CRP & vector coding	Characterize the effects of LBP and history of LBP on pelvic and trunk coordination patterns in all planes during walking and running	Overall, those with LBP or history of LBP maintained ore in-phase pelvis-trunk coordination particularly in the transverse plane during walking, and in the frontal plane during running As walking velocity deviated from comfortable, there was an increase in coordination pattern variability. However, magnitude of this increase was less in those with LBP or history of LBP
Selles et.al., 2001 [9]	LBP	Walking	Thorax and pelvis relative phase (CRP)	Characterize the effects of LBP on thorax and pelvis coordination patterns	In controls, as walking velocity increases, there is a transition from an in-phase pelvis-thorax coordination pattern to an out of-phase one.2/3 of the LBP subjects tested were unable to transition to this out-of-phase pattern
Steele et al., 2014 [40]	LBP & controls	Walking	Lumbar kinematics & range of motion	Examine the correlations between lumbar kinematic variability, pain, and isolated lumbar extension strength	While subjects without LBP show high intra-stride reproducibility in lumbar spine kinematics, those with LBP seem less able to repeat these movement patterns

Taylor et al., 2003 [41]	LBP & controls	Walking	Pelvis and lumbar spine kinematics	To determine whether a period of treadmill walking at different velocities is a valid way to manage acute LBP	When in pain, subjects with LBP use a unique set of strategies to adapt to increased walking velocities. These include changes to pelvic and lumbar rotations, and a tendency to increase walking velocity by increasing stride length rather than cadence. After pain had resolved, subjects used strategies to increase walking velocity that

2.6 References

[1] C.S. Molina, J. Faulk, Lower Extremity Amputation, in: StatPearls, StatPearls Publishing, Treasure Island (FL), 2021. http://www.ncbi.nlm.nih.gov/books/NBK546594/ (accessed November 13, 2021).

[2] P.L. Ephraim, S.T. Wegener, E.J. MacKenzie, T.R. Dillingham, L.E. Pezzin, Phantom Pain, Residual Limb Pain, and Back Pain in Amputees: Results of a National Survey, Archives of Physical Medicine and Rehabilitation. 86 (2005) 1910–1919. https://doi.org/10.1016/j.apmr.2005.03.031.

[3] D.M. Ehde, D.G. Smith, J.M. Czerniecki, K.M. Campbell, D.M. Malchow, L.R. Robinson, Back pain as a secondary disability in persons with lower limb amputations, Archives of Physical Medicine and Rehabilitation. 82 (2001) 731–734. https://doi.org/10.1053/apmr.2001.21962.

[4] Y. Barzilay, B.S. Lonner, B. Amit Mor, B. Avi Elbaz, Patients with chronic non-specific low back pain who reported reduction in pain and improvement in function also demonstrated an improvement in gait pattern, European Spine Journal. 25 (2015) 2761–2766. https://doi.org/10.1007/s00586-015-4004-0.

[5] C.J.C. Lamoth, Pelvis-Thorax Coordination in the Transverse Plane During Walking in Persons With Nonspecific Low Back Pain, Spine (Philadelphia, Pa. 1976). 27 (2002) E92–E99. https://doi.org/10.1097/00007632-200202150-00016.

[6] L. Vogt, K. Pfeifer, M. Portscher, W. Banzer, Influences of Nonspecific Low Back Pain on Three- Dimensional Lumbar Spine Kinematics in Locomotion, Spine. 26 (2001) 1910–1919.

[7] J.F. Seay, Influence of Low Back Pain Status on Pelvis-Trunk Coordination During Walking and Running, Spine (Philadelphia, Pa. 1976). 36 (2011) E1070–E1079. https://doi.org/10.1097/BRS.0b013e3182015f7c.

[8] J.F. Seay, R.E.A. Van Emmerik, J. Hamill, Low back pain status affects pelvis-trunk coordination and variability during walking and running, Clinical Biomechanics. 26 (2011) 572–578. https://doi.org/10.1016/j.clinbiomech.2010.11.012.

[9] R.W. Selles, R.C. Wagenaar, T.H. Smit, P.I.J.M. Wuisman, Disorders in trunk rotation during walking in patients with low back pain: a dynamical systems approach, Clinical Biomechanics. 16 (2001) 175–181. https://doi.org/10.1016/S0268-0033(00)00080-2.

[10] J.F. Seay, R.E.A. Van Emmerik, J. Hamill, Trunk bend and twist coordination is affected by low back pain status during running, European Journal of Sport Science. 14 (2014) 563–568. https://doi.org/10.1080/17461391.2013.866167.

[11] H. Goujon-Pillet, E. Sapin, P. Fodé, F. Lavaste, Three-Dimensional Motions of Trunk and Pelvis During Transfemoral Amputee Gait, Archives of Physical Medicine and Rehabilitation. 89 (2008) 87–94. https://doi.org/10.1016/j.apmr.2007.08.136.

[12] H. Nadollek, S. Brauer, R. Isles, Outcomes after trans-tibial amputation: the relationship between quiet stance ability, strength of hip abductor muscles and gait, Physiotherapy Research International. 7 (2002) 203. https://doi.org/10.1002/pri.260.

[13] A.L. Hof, EMG and muscle force: An introduction, Human Movement Science. 3 (1984) 119–153. https://doi.org/10.1016/0167-9457(84)90008-3.

[14] C.D. Tokuno, D.J. Sanderson, J.T. Inglis, R. Chua, Postural and movement adaptations by individuals with a unilateral below-knee amputation during gait initiation, Gait & Posture. 18 (2003) 158–169. https://doi.org/10.1016/S0966-6362(03)00004-3.

[15] B.D. Hendershot, M.A. Nussbaum, Persons with lower-limb amputation have impaired trunk postural control while maintaining seated balance, Gait & Posture. 38 (2013) 438–442. https://doi.org/10.1016/j.gaitpost.2013.01.008.
[16] J.J. Collins, C.J. De Luca, A. Burrows, L.A. Lipsitz, Age-related changes in open-loop and closed-loop postural control mechanisms, Exp Brain Res. 104 (1995) 480–492. https://doi.org/10.1007/BF00231982.
[17] J.J. Collins, C.J. DeLuca, The effects of visual input on open-loop and closed-loop postural control mechanisms, Journal of Rehabilitation Research and Development. 30–31 (1994) 49.
[18] A. Radebold, J. Cholewicki, G.K. Polzhofer, H.S. Greene, Impaired postural control of the lumbar spine is associated with delayed muscle response times in patients with chronic idiopathic low back pain, Spine (Philadelphia, Pa. 1976). 26 (2001) 724–730. https://doi.org/10.1097/00007632-200104010-00004.
[19] C.E. Mahon, A.L. Pruziner, B.D. Hendershot, E.J. Wolf, B.J. Darter, K.B. Foreman, J.B. Webster, Gait and Functional Outcomes for Young, Active Males With Traumatic Unilateral Transfemoral Limb Loss, Military Medicine. 182 (2017) e1913–e1923. https://doi.org/10.7205/MILMED-D-16-00356.
[20] S.M.H.J. Jaegers, Prosthetic gait of unilateral transfemoral amputees: A kinematic study, Archives of Physical Medicine and Rehabilitation. 76 (1995) 736–743. https://doi.org/10.1016/S0003-9993(95)80528-1.
[21] Y. Sagawa Jr, K. Turcot, S. Armand, A. Thevenon, N. Vuillerme, E. Watelain, Biomechanics and physiological parameters during gait in lower-limb amputees: A systematic review, Gait & Posture. 33 (2011) 511–526. https://doi.org/10.1016/j.gaitpost.2011.02.003.
[22] L. Nolan, A. Lees, The functional demands on the intact limb during walking for active transfemoral and transtibial amputees, Prosthet Orthot Int. 24 (2000) 117–125. https://doi.org/10.1080/03093640008726534.
[23] L. Nolan, A. Wit, K. Dudziñski, A. Lees, M. Lake, M. Wychowañski, Adjustments in gait symmetry with walking speed in trans-femoral and trans-tibial amputees, Gait & Posture. 17 (2003) 142–151. https://doi.org/10.1016/S0966-6362(02)00066-8.
[24] C.J.C. Lamoth, P.J. Beek, O.G. Meijer, Pelvis–thorax coordination in the transverse plane during gait, Gait & Posture. 16 (2002) 101–114. https://doi.org/10.1016/S0966-6362(01)00146-1.
[25] S.B. Michaud, S.A. Gard, D.S. Childress, A preliminary investigation of pelvic obliquity patterns during gait in persons with transtibial and transfemoral amputation., Journal of Rehabilitation Research and Development. 37 (2000) 1–10.
[26] C. Sjödahl, G.-B. Jarnlo, B. Söderberg, B.M. Persson, Pelvic motion in trans-femoral amputees in the frontal and transverse plane before and after special gait re-education, Prosthetics and Orthotics International. 27 (2003) 227–237. https://doi.org/10.1080/03093640308726686.
[27] L.L. McNealy, S. A. Gard, Effect of prosthetic ankle units on the gait of persons with bilateral trans-femoral amputations, Prosthet Orthot Int. 32 (2008) 111–126. https://doi.org/10.1080/02699200701847244.
[28] H. Devan, P.A. Hendrick, D.C. Riberio, L.A. Hale, A. Carman, Asymmetrical movements of the lumbopelvic region: Is this a potential mechanism for low back pain in people with

lower limb amputation?, Medical Hypotheses. 82 (2014) 77–85. https://doi.org/10.1016/j.mehy.2013.11.012.
[29] A.G. Schache, P. Blanch, D. Rath, T. Wrigley, K. Bennell, Three-dimensional angular kinematics of the lumbar spine and pelvis during running, Human Movement Science. 21 (2002) 273–293.
[30] D.C. Morgenroth, The Relationship Between Lumbar Spine Kinematics during Gait and Low-Back Pain in Transfemoral Amputees, American Journal of Physical Medicine & Rehabilitation. 89 (2010) 635–643. https://doi.org/10.1097/PHM.0b013e3181e71d90.
[31] H. Schmidt, A. Kettler, F. Heuer, U. Simon, L. Claes, H.-J. Wilke, Intradiscal pressure, shear strain and fiber strain in the intervertebral disc under combined loading, Journal of Biomechanics. 39 (2006) S29–S29. https://doi.org/10.1016/S0021-9290(06)82983-0.
[32] B.S. Baum, B.L. Schnall, J.E. Tis, J.S. Lipton, Correlation of residual limb length and gait parameters in amputees, Injury. 39 (2008) 728–733. https://doi.org/10.1016/j.injury.2007.11.021.
[33] B. Burkett, J. Smeathers, T. Barker, Walking and running inter-limb asymmetry for Paralympic trans-femoral amputees, a biomechanical analysis, Prosthet Orthot Int. 27 (2003) 36–47. https://doi.org/10.3109/03093640309167975.
[34] L. Mengelkoch, J. Kahle, M. Highsmith, Energy Costs & Performance of Transtibial Amputees & Non-amputees during Walking & Running, Int J Sports Med. 35 (2014) 1223–1228. https://doi.org/10.1055/s-0034-1382056.
[35] D.J. Sanderson, P.E. Martin, Joint kinetics in unilateral below-knee amputee patients during running, Archives of Physical Medicine and Rehabilitation. 77 (1996) 1279–1285. https://doi.org/10.1016/S0003-9993(96)90193-8.
[36] H.R. Guo, S. Tanaka, W.E. Halperin, L.L. Cameron, Back pain prevalence in US industry and estimates of lost workdays., Am J Public Health. 89 (1999) 1029–1035. https://doi.org/10.2105/AJPH.89.7.1029.
[37] D. Lafond, A. Champagne, M. Descarreaux, J.-D. Dubois, J.M. Prado, M. Duarte, Postural control during prolonged standing in persons with chronic low back pain, Gait & Posture. 29 (2009) 421–427. https://doi.org/10.1016/j.gaitpost.2008.10.064.
[38] N.P. Reeves, V.G.S. y R. Celi, A. Ramadan, J.M. Popovich, L.L. Prokop, M.A. Zatkin, L.A. DeStefano, T.J. Francisco, J.J. Rowan, C.J. Radcliffe, J. Choi, N.D. Cowdin, J. Cholewicki, Stability threshold during seated balancing is sensitive to low back pain and safe to assess, Journal of Biomechanics. 125 (2021). http://dx.doi.org/10.1016/j.jbiomech.2021.110541.
[39] R. della Volpe, T. Popa, F. Ginanneschi, R. Spidalieri, R. Mazzocchio, A. Rossi, Changes in coordination of postural control during dynamic stance in chronic low back pain patients, Gait & Posture. 24 (2006) 349–355. https://doi.org/10.1016/j.gaitpost.2005.10.009.
[40] J. Steele, S. Bruce-Low, D. Smith, D. Jessop, N. Osborne, Lumbar kinematic variability during gait in chronic low back pain and associations with pain, disability and isolated lumbar extension strength, Clinical Biomechanics. 29 (2014) 1131–1138. https://doi.org/10.1016/j.clinbiomech.2014.09.013.
[41] N.F. Taylor, O.M. Evans, P.A. Goldie, The effect of walking faster on people with acute low back pain, European Spine Journal. 12 (2003) 166–172. https://doi.org/10.1007/s00586-002-0498-3.

[42] R. Burgess-Limerick, B. Abernethy, R.J. Neal, Relative phase quantifies interjoint coordination, Journal of Biomechanics. 26 (1993) 91–94. https://doi.org/10.1016/0021-9290(93)90617-N.
[43] S. Choi, S.-K. Kim, G.-J. Lee, H.-K. Park, Paper-based 3D microfluidic device for multiple bioassays, Sensors and Actuators B: Chemical. 219 (2015) 245–250. https://doi.org/10.1016/j.snb.2015.05.035.
[44] J. Hamill, J.M. Haddad, W.J. McDermott, Issues in Quantifying Variability From a Dynamical Systems Perspective, Journal of Applied Biomechanics. 16 (2000) 407.
[45] J. Hamill, R.E.A. van Emmerik, B.C. Heiderscheit, L. Li, A dynamical systems approach to lower extremity running injuries, Clinical Biomechanics. 14 (1999) 297–308. https://doi.org/10.1016/S0268-0033(98)90092-4.
[46] P.F. Lamb, M. Stöckl, On the use of continuous relative phase: Review of current approaches and outline for a new standard, Clinical Biomechanics. 29 (2014) 484–493. https://doi.org/10.1016/j.clinbiomech.2014.03.008.
[47] C.J.C. Lamoth, A. Daffertshofer, O.G. Meijer, G. Lorimer Moseley, P.I.J.M. Wuisman, P.J. Beek, Effects of experimentally induced pain and fear of pain on trunk coordination and back muscle activity during walking, Clinical Biomechanics. 19 (2004) 551–563. https://doi.org/10.1016/j.clinbiomech.2003.10.006.
[48] S. Mehdizadeh, A.R. Arshi, K. Davids, Quantifying coordination and coordination variability in backward versus forward running: Implications for control of motion, Gait & Posture. 42 (2015) 172–177. https://doi.org/10.1016/j.gaitpost.2015.05.006.
[49] S. Mehdizadeh, P.S. Glazier, Order error in the calculation of continuous relative phase, Journal of Biomechanics. 73 (2018) 243–248. https://doi.org/10.1016/j.jbiomech.2018.03.032.
[50] A.R.M. Pelegrinelli, M.F. Silva, L.C. Guenka, A.C. Carrasco, F.A. Moura, J.R. Cardoso, Low back pain affects coordination between the trunk segments but not variability during running, Journal of Biomechanics. 101 (2020) 109605. https://doi.org/10.1016/j.jbiomech.2020.109605.
[51] Z. Sawacha, C.D. Sartor, L.C. Yi, A. Guiotto, F. Spolaor, I.C.N. Sacco, Clustering classification of diabetic walking abnormalities: a new approach taking into account intralimb coordination patterns, Gait & Posture. 79 (2020) 33–40. https://doi.org/10.1016/j.gaitpost.2020.03.016.
[52] I. Shojaei, M. Vazirian, E.G. Salt, L.R. Van Dillen, B. Bazrgari, Timing and magnitude of lumbar spine contribution to trunk forward bending and backward return in patients with acute low back pain, Journal of Biomechanics. 53 (2017) 71–77. https://doi.org/10.1016/j.jbiomech.2016.12.039.
[53] R.E.A. van Emmerik, R.C. Wagenaar, Effects of walking velocity on relative phase dynamics in the trunk in human walking, Journal of Biomechanics. 29 (1996) 1175–1184. https://doi.org/10.1016/0021-9290(95)00128-X.
[54] Y.-T. Yang, Y. Yoshida, T. Hortobágyi, S. Suzuki, Interaction Between Thorax, Lumbar, and Pelvis Movements in the Transverse Plane During Gait at Three Velocities, Journal of Applied Biomechanics. 29 (2013) 261–269. https://doi.org/10.1123/jab.29.3.261.
[55] I. McClay, K. Manal, Coupling Parameters in Runners with Normal and Excessive Pronation, Journal of Applied Biomechanics. 13 (1997) 109–124. https://doi.org/10.1123/jab.13.1.109.

[56] M.J. Kurz, N. Stergiou, Effect of normalization and phase angle calculations on continuous relative phase, Journal of Biomechanics. 35 (2002) 369–374. https://doi.org/10.1016/S0021-9290(01)00211-1.
[57] B.T. Peters, J.M. Haddad, B.C. Heiderscheit, R.E.A. Van Emmerik, J. Hamill, Limitations in the use and interpretation of continuous relative phase, Journal of Biomechanics. 36 (2003) 271–274. https://doi.org/10.1016/S0021-9290(02)00341-X.
[58] Y. Li, R.S. Kakar, M.A. Walker, L. Guan, K.J. Simpson, Upper Trunk-Pelvis Coordination During Running Using the Continuous Relative Fourier Phase Method, J Appl Biomech. 34 (2018) 312–319. https://doi.org/10.1123/jab.2017-0250.
[59] M. Varlet, M.J. Richardson, Computation of continuous relative phase and modulation of frequency of human movement, Journal of Biomechanics. 44 (2011) 1200–1204. https://doi.org/10.1016/j.jbiomech.2011.02.001.
[60] N. Stergiou, J.L. Jensen, B.T. Bates, S.D. Scholten, G. Tzetzis, A dynamical systems investigation of lower extremity coordination during running over obstacles, Clinical Biomechanics. 16 (2001) 213–221. https://doi.org/10.1016/S0268-0033(00)00090-5.
[61] J.R. Franz, K.W. Paylo, J. Dicharry, P.O. Riley, D.C. Kerrigan, Changes in the coordination of hip and pelvis kinematics with mode of locomotion, Gait & Posture. 29 (2009) 494–498. https://doi.org/10.1016/j.gaitpost.2008.11.011.
[62] S.J. Preece, D. Mason, C. Bramah, The coordinated movement of the spine and pelvis during running, Human Movement Science. 45 (2016) 110–118. https://doi.org/10.1016/j.humov.2015.11.014.
[63] R.E.A. van Emmerik, R.C. Wagenaar, Dynamics of movement coordination and tremor during gait in Parkinson's disease, Human Movement Science. 15 (1996) 203–235. https://doi.org/10.1016/0167-9457(95)00044-5.
[64] M. Shafizadeh, R. Crowther, A. Ali, K. Davids, Effects of dual task constraints on intra-limb coordination during treadmill walking in people with chronic stroke, Clinical Kinesiology. 71 (2017) 8–18.
[65] C.C. Quatman-Yates, A. Hunter-Giordano, K.K. Shimamura, R. Landel, B.A. Alsalaheen, T.A. Hanke, K.L. McCulloch, R.D. Altman, P. Beattie, K.E. Berz, B. Bley, A. Cecchini, J. Dewitt, A. Ferland, I. Gagnon, K. Gill-Body, S. Kaplan, J.J. Leddy, S. McGrath, G.L. Pagnotta, J. Reneker, J. Schwertfeger, N. Silverberg, Physical Therapy Evaluation and Treatment After Concussion/Mild Traumatic Brain Injury: Clinical Practice Guidelines Linked to the International Classification of Functioning, Disability and Health From the Academy of Orthopaedic Physical Therapy of the American Physical Therapy Association, J Orthop Sports Phys Ther. 50 (2020) CPG1–CPG73. https://doi.org/10.2519/jospt.2020.0301.
[66] J.G. Buckley, D. O'Driscoll, S.J. Bennett, Postural sway and active balance performance in highly active lower-limb amputees, American Journal of Physical Medicine & Rehabilitation. 81 (2002) 13–20. https://doi.org/10.1097/00002060-200201000-00004.
[67] S. Fatone, R. Stine, P. Gottipati, M. Dillon, Pelvic and Spinal Motion During Walking in Persons With Transfemoral Amputation With and Without Low Back Pain, American Journal of Physical Medicine & Rehabilitation. 95 (2016) 438–447. https://doi.org/10.1097/PHM.0000000000000405.
[68] E. Isakov, H. Burger, J. Krajnik, M. Gregoric, C. Marincek, Influence of speed on gait parameters and on symmetry in transtibial amputees, Prosthet Orthot Int. 20 (1996) 153–158. https://doi.org/10.3109/03093649609164437.

[69] S. Khodadadeh, S.M. Eisenstein, Gait analysis of patients with low back pain before and after surgery., Spine. 18 (1993) 1451–5.
[70] R. Müller, T. Ertlet, R. Blickhan, Low back pain affects trunk as well as lower limb movements during walking and running, Journal of Biomechanics. 48 (2015) 1009–1014. https://doi.org/10.1016/j.jbiomech.2015.01.042.
[71] E. Russell Esposito, J.M. Wilken, The relationship between pelvis–trunk coordination and low back pain in individuals with transfemoral amputations, Gait & Posture. 40 (2014) 640–646. https://doi.org/10.1016/j.gaitpost.2014.07.019.

Chapter 3 Characterization of upper torso, torso, pelvis, and hip segment rotations and coordination patterns in unilateral transtibial amputees during running

3.1 Abstract

In recent years, Continuous Relative Phase (CRP) has been used to identify subtle changes to relative phasing in various low-back pain groups (LBP). Lower-limb amputees are a population who experience frequent and bothersome LBP. Therefore, the aim of this study is to characterize upper-torso, torso, and pelvis coordination patterns in all planes of this population. We compared data from a cohort of unilateral transtibial amputee (TTA) runners at two velocities. Subjects performed overground walking trials at a prescribed speed of 3.5 m/s (PS), and a self-selected speed (SSS) while kinematics (300Hz) and kinetics (1800Hz) were collected. Evaluation of traditional gait parameters and upper-torso, torso, pelvis, and hip rotational amplitudes showed few velocity dependent changes. While the PS was significantly lower than the SSS, the only statistically significant measure was stride length which was also shorter for the PS. Analysis of CRP mean, and proportion of the gait cycle spent out-of-phase revealed both increases and decreases in pelvis/upper-torso and pelvis/torso axial coordination with increasing walking velocity. There were no statistically significant differences in CRP variability. These findings align in some respects with others that have reported velocity dependent changes to CRP mean. Fewer or lack of change to CRP variability with increased running velocity has been reported by some authors in populations with LBP. This study adds to the growing body of literature characterizing the full effects of lower-limb amputation and how it leads to increased risk of other musculoskeletal injuries.

3.1 Background

In the United States, an estimated 150,000 people undergo lower limb amputation (LLA) each year for reasons ranging from cancer to complications of diabetes and vascular disease, severe malfunction necessitating amputation, or trauma [1]. LLA on its own, regardless of etiology, is a traumatic and life-altering event. The accompanying musculoskeletal complications are of particular concern because of their long-term impacts on amputees' activities and quality of daily life. These complications include but are not limited to ankle, knee, hip, and back pain, osteoarthritis in the residual and intact limb, phantom limb sensations and pain, and increased fall risk. Surveyed LLAs report that their back pain is more bothersome than phantom limb pain and residual limb pain [2,3].

3.1.1 Amputee Gait

Gait kinematics: The loss of lower extremity musculature, as well as somatosensory feedback, leads to characteristic asymmetries in amputee gait [4–9]. Several have found an overall decrease in preferred walking velocity, longer intact side stance times, shorter swing and step times, and longer step widths [5,6,8,10,11]. As walking velocity increases, intact and amputated side temporal asymmetries decrease particularly in unilateral trans-tibial amputees (TTA) [8]. As for gait kinetics, amputees exhibit greater vertical ground reaction forces, which increase as walking velocity increases [8]. Studies evaluating postural changes during gait initiation in unilateral TTAs have found that changes in gait kinematics are largely due to longer stance times, especially when gait is initiated with the intact limb [12].

Trunk/thorax, and hip segment rotations: LLA impacts more than gait parameters and lower-limb kinematics and kinetics. It can also affect hip, pelvis, and thorax/trunk rotations. When evaluating hip flexion in unilateral trans-femoral amputees (TFAs) studies have found that

this population has greater hip flexion than controls [6,7,11]. The magnitude of this difference in hip flexion extension between amputees and controls increases with increasing walking velocity suggesting that this is an attempt at lengthening the stride [6,11]. Both unilateral TFAs and TTAs exhibit hip hike in the frontal plane, which is thought to help amputees clear the swing limb and reduce the reliance on the weak hip abductor musculature for lateral stability [13]. This is also accompanied by increased pelvic drop which occurs during intact side single-limb stance in unilateral TTA and during both intact and prosthetic side single-limb stance in unilateral TFAs [14].

Studies that evaluate the effects of LLA on thorax/trunk rotations report that LLAs show greater trunk lateral flexion towards the amputated limb during the swing phase [4–6,15]. It is hypothesized this is a follow-through of the hip hike used to clear the swing limb [4,6]. Goujon-Pillet et al. reported a greater range of motion in all planes in the trunk in TFAs [5]. Baum conducted a study whose aim was to understand the impact of TFA and knee-disarticulation (KA) on gait kinematics and kinetics and its effects on trunk and hip rotations [4]. Their findings on gait kinematics and pelvic rotations are like those discussed earlier. However, like Jaegers, they found no impact of stump length on trunk rotations, particularly trunk lateral-flexion [4].

Few studies have evaluated the effects of LBP on trunk, lumbar and pelvic rotations in unilateral LLAs. One study that did reported no statistically significant differences in the lumbar spine excursions in the frontal and sagittal planes of TFAs with and without LBP. However, those with LBP showed more significant lumbar spine rotation. This was driven by changes in trunk kinematics more than pelvic kinematics. In cadaveric studies, transverse plane rotations, or complex rotations that include rotations in the transverse plane, have been shown to increase

strain in annulus fibers [16]. This increase in strain and shear stress on the discs could be a factor in disc degeneration that leads to the development of LBP [17].

3.1.2 Relative phase analysis

In response to the lack of sensitivity in traditional measures like gait parameters, segment rotations, and range of motion, measures that characterize the relative rotations between segments have come to the fore. In healthy adults, as walking speed increases, coordination patterns of the thorax/torso and pelvis generally transition from an in-phase pattern in the frontal and transverse planes – where the pelvis and thorax/torso rotate together; to an out-of-phase or anti-phase pattern where the pelvis and torso/thorax counter-rotate [18–20]. During running, controls display an out-of-phase pattern in the sagittal and transverse planes, while in the frontal plane the coordination patterns remain in-phase [21]. Those with LBP tend to maintain an in-phase coordination pattern during walking. Interestingly, studies evaluating coordination patterns in those with resolved LBP have found that they have coordination patterns that are reminiscent of their pained counterparts [22,23]. This led the authors to conclude that those with resolved LBP represent a transition group and could help improve the current understanding of the biomechanical etiology of LBP.

To the author's knowledge, there is only one study that evaluates these coordination patterns in unilateral LLAs which is done during walking [5]. They found that unilateral TFAs like those with LBP demonstrate a guarded walking gait pattern characterized by a more in-phase trunk/pelvis axial coordination pattern. They also reported an effect of residual limb length and walking velocity on pelvis rotations. Together, walking velocity and residual limb length explained 40% of the variation in pelvic frontal plane range of motion during walking.

The first aim (Aim 1.1) of this study was to first calculate the standard gait parameters, and rotational amplitudes of the upper-torso, torso, pelvis, and intact and amputated side hips in unilateral TTAs during running at two velocities. We hypothesized that there will be no statistically significant differences in the rotational amplitudes of these segments at these running velocities. The second aim (Aim 2.2) of this study is to characterize upper-torso, torso, and pelvis coordination patterns in all planes of this population using Continuous Relative Phase (CRP). As walking velocity increases, an increase in average relative phase in the transverse plane (axial coordination) is expected. An increase in the proportion of the gait cycle spent in an out-of-phase pattern is also expected.

3.2 Methods

This study was approved by the Naval Medical Center – San Diego Institutional Review Board (NMCSD.2013.0109). All subjects gave consent to have their data collected. Data was shared with the University of Kansas through the Freedom of Information Act.

Participants: 9 UTAs (8 - male, 1 - female, average age: 26 y/o, age range: 21 – 41 y/o, 6 with left side amputation) with an Ossur C-shaped running blade were recruited for this study. Each participant performed 3-6 trials of over ground running at a self-selected speed (SSS, 4.1 m/s ± 0.73), and at a prescribed speed of 3.5m/s (PS, 3.5 m/s ± 0.12). SSS data for subject 3 was missing, a type 3 repeated measures ANOVA was used for statistical analysis because it accounts for unbalanced data. Therefore, subject 3's data was maintained. Data was capture over a 9-meter portion of a walkway with approximately 15-meters on either side to allow for acceleration and deceleration. For the prescribed speed trials, only the trials that fell within 3.3-3.7 m/s were kept. For most subjects, the SSS was faster than the PS. PS and SSS designations were maintained for all subjects regardless of which running velocity was faster During these

trials kinematic data was collected using a modified 6 degree of freedom marker set without head and arm sensors. A 16 camera Motion Analysis (Motion Analysis Corporation, Santa Rosa, CA) and 4 force plates (Kistler Inc., Novi, MI) were used to collect running data on a 40-meter runway at 300 Hz and 1800 Hz respectively, using Cortex Software (Motion Analysis Corporation, Santa Rosa, CA).

Analysis: Running velocity was calculated by taking the derivative of the position of the sensor placed on the seventh cervical vertebrae (C7) in the direction of movement. Gait parameters stride length and single-limb stance time in seconds were also calculated. A stride was defined as the distance from heel strike to heel strike on the same side. Type 3 repeated measures ANOVA was used to determine the effects of running velocity (PS or SSS) on stride length and stance times of the intact and amputated sides.

Axes for the upper-torso, torso, pelvis, and intact and amputated sides were created and tracked throughout the gait cycle. For example, to draw the upper-torso axis, a vector was first drawn between the C7 and left acromion process sensors (C7 → LSHO = $\vec{a}$), Another vector was drawn between LSHO and RSHO (LSHO → RSHO = $\vec{b}$). Lastly, these two vectors were crossed to produce a vector that would represent the z-axis or the transverse plane. Rotations about this axis represent axial rotation. Lastly, the $\vec{a}$ and $\vec{z}$ were crossed to produce the x-axis or the frontal plane. Rotations about this axis represent lateral bend. Lastly, the $\vec{b}$ became the y-axis or the sagittal plane. Rotations about this axis represent flexion/extension. The torso axis consisted of sensors placed on C7, the manubrium and a virtual sensor on the sacrum which was calculated as the mean of sensors on the left and right posterior superior iliac spine. The axis for the pelvis was created from the virtual sacral sensors, and sensors placed on left and right anterior superior iliac spine. Lastly, hip axes were created from sensors on the anterior and posterior superior iliac

spine, and a sensor placed on the lateral thigh sensor placed on the greater trochanter. Intact side strides were used to divide the data which was then interpolated to 100 data points such that each data point represented an event during the gait cycle. Intact side strides were used to divide the data which was then interpolated to 100 data points such that each data point represented an event during the gait cycle. A similar method was used to create axes for the torso, pelvis, and hips.

Rotational Amplitude Calculations: Individual subject and task rotational amplitudes were calculated by taking the absolute value of the difference between the maximum and minimum rotations (Equation 3.1). Type 3 repeated measures ANOVA was used to determine the effects of running velocity on segment rotational amplitudes in all planes. Pairwise comparisons using a Tukey correction were used to compare intact and amputated side hip rotational amplitudes at both running velocities.

$$Rotational\ Amplitude = |Max_{rot} - Min_{rot}|$$

Equation 3.1

CRP: Coordination patterns between upper torso, torso and pelvic segments were calculated using the Continuous Relative Phase methodology described by Hamill [24]. To begin, angular velocity was calculated by taking the derivative of the angular position using the central difference method. Then angular position (θ) and velocity (ω) were normalized using Equation 3.2 and Equation 3.3. Phase angle (ϕ) was calculated using a four-quadrant, unit-circle normalization of the arctangent of angular velocity and angular position (Figure 3.1). CRP was then calculated as the absolute value difference between proximal and distal segment (Equation 3.4). In other studies, CRP is usually calculated as the difference between proximal and distal segments resulting in CRP ranges of -180º to 180º, or 0º to 360º. Values of -180º to 180º typically indicate that the signals of interest are completely out-of-phase, and values of 0º or 360º

indicate completely in-phase coordination patterns [22,23,25–27]. It is important to note that while CRP range was 0º to 180º, the range for -180º to 180º as output for ϕ by the arctangent was maintained. Since the signals are periodic, descriptive statistics for CRP are often calculated using circular statistics to avoid redundancies. In addition, Hamill has suggested that a CRP range of 180º to 180º allows researchers to identify which segment is responsible for the shift in coordination patterns [29]. However, Mehdizadeh and colleagues have shown that calculating ϕ as $\arctan\frac{\omega}{\theta}$ or CRP using Equation 3.4 it results in a non-intuitive interpretation of CRP [30]. When calculating CRP, it is expected to be positive when the distal segment is lagging, and negative when it is leading. However, Mehdizadeh showed that mathematically the results are the opposite. Since leading and lagging segments were not the focus of this study CRP was calculated using the absolute value difference between signal phase angles. This also has the effect of removing the redundancy at ±180º allowing descriptive statistics for CRP such as average (CRP mean) and standard deviation (CRP variability) to be calculated using linear methods. CRP mean was calculated as the average CRP for each stride. To calculate CRP variability, CRP signals for each stride were aligned and the standard deviation of datapoints at the same time point were calculated, the average of these standard deviations was taken as the CRP variability.

Proportion of the gait cycle spent out-of-phase was also calculated for each stride for each subject. A study by van Emmerik and Wagnaar which evaluated the effects of increasing walking velocity on thorax pelvic coordination patterns considered phase angles greater than 110º out-of-phase [20]. To calculate the proportion of the gait cycle spent out-of-phase, the number of datapoints in the CRP vector greater than 110º was divided by the length of the vector (100 data points). Linear mixed model analysis was used to fit a model to the data, and a type 3

repeated ANOVA was used to determine the significance of running velocity on CRP mean, CRP variability, and proportion of the cycle spent out-of-phase. Pairwise comparisons and calculation of differences in PS and SSS estimated marginal means (PS EMM – SSS EMM = ΔEMM) were used to determine the effects of running velocity on CRP mean, CRP variability, and proportion of the gait cycle spent out-of-phase. For example, positive differences in estimated marginal means indicates that as running velocity increases there is an increase in the CRP mean while negative values indicate that there is a decrease in CRP mean.

$$\theta_i = \frac{2 * [\theta_i - min\ (\theta_i)]}{max(\theta_i) - min\ (\theta_i)}$$

Equation 3.2

$$\omega_i{}' = \frac{\omega_i}{max\ \{max(\omega_i)\,, max(-\omega_i)\}}$$

Equation 3.3

$$CRP_{torso-pelvis} = |\varphi_{pelvis} - \varphi_{torso}|$$

Equation 3.4

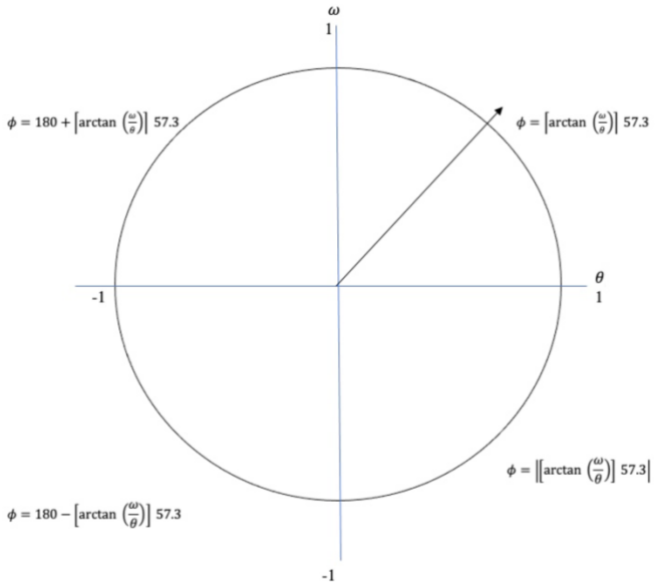

Figure 3.1: normalization of position-velocity phase angles (ϕ)

3.3 Results

3.3.1 Gait parameters

Repeated measures ANOVA found statistically significant differences between PS and SSS running velocities, where SSS (EMM = 4.10 m/s) was higher than PS (EMM = 3.46 m/s). Therefore, SSS and PS groups were maintained. Repeated measures ANOVA with intact/amputated side and running velocity as factors reported statistically significant interaction effects between task and gait parameters (i.e.: stride length and stance time). Main effects of running velocity on gait parameters was found. Pairwise comparisons revealed statistically significant differences between walking velocities in stride length ($p < 0.05$). Differences in estimated marginal means indicate that on average the PS stride length was 17cm shorter than the SSS ($\Delta EMM = 0.17$). There were no significant differences between intact and amputated side gait parameters or effects of running velocity on stance times (

Table 3.1).

Gait parameters				
Running Velocity	**Stride Length (m)**		**Stance time (s)**	
	Intact	**Amputated**	**Intact**	**Amputated**
PS	2.44 ± 0.17	2.43 ± 0.18	0.70 ± 0.04	0.13 ± 0.02
SSS	2.55 ± 0.38	2.63 ± 0.41	0.13 ± 0.04	0.12 ± 0.03

Gait parameters				
Running Velocity	**Stride Length (m)**		**Stance time (s)**	
	Intact	**Amputated**	**Intact**	**Amputated**
PS	2.44 ± 0.17	2.43 ± 0.18	0.70 ± 0.04	0.13 ± 0.02
SSS	2.55 ± 0.38	2.63 ± 0.41	0.13 ± 0.04	0.12 ± 0.03

Table 3.1: Mean ± standard deviations for gait parameters (stride length and stance times) for intact and amputated sides. No statistically significant side effects were found in stride length or stance time. Pairwise comparisons revealed statistically significant effects of running velocity on stride length where the PS stride length was on average 17cm shorter than SSS stride lengt

3.3.2 Rotational Amplitudes

Repeated measures ANOVA reported a significant main effect of segment ($p < 0.05$). That is there were statistically significant differences in the rotational amplitudes of each segment. Insignificant interaction of running velocity and segment ($p = 0.14$) indicate that running velocity did not significantly impact upper-torso, torso, pelvis, or hip rotational amplitudes. Pairwise comparisons with a Tukey correction found no statistically significant differences in the rotational amplitudes of the intact and amputated hips in any plane.

3.3.3 CRP

A statistically significant interaction effect between coordination pattern and task was identified indicating that running velocity significantly affected coordination patterns. CRP mean averages and average standard deviations are reported in

Table 3.1. Pairwise comparisons were used to determine which coordination patterns changed

Gait parameters				
Running Velocity	**Stride Length (m)**		**Stance time (s)**	
	Intact	**Amputated**	**Intact**	**Amputated**
PS	2.44 ± 0.17	2.43 ± 0.18	0.70 ± 0.04	0.13 ± 0.02
SSS	2.55 ± 0.38	2.63 ± 0.41	0.13 ± 0.04	0.12 ± 0.03

with running velocity and how, starting with CRP mean (

Proportion of gait cycle spent	Upper-Torso / Torso	Pelvis/Upper-Torso	Pelvis/Torso

out-of-phase	Lat Bend	Flex/Ext	Ax.Rot	Lat Bend	Flex/Ext	Ax.Rot	Lat Bend	Flex/Ext	Ax.Rot
ΔEMM	0.04	-0.04	0.03	0.01	0.03	0.12	-0.01	0.05	-0.09
P-Value	0.27	0.35	0.38	0.84	0.48	***< 0.05***	0.88	0.20	***< 0.05***

Table 3.6). Statistically significant differences were found in CRP means of axial coordination patterns between the pelvis and upper-torso, and the pelvis and torso. ΔEMM indicate that average pelvis/upper-torso axial relative phase was higher during the PS (PS EMM = 76.8º, SSS EMM = 59.9º, ΔEMM = 16.91º). However, pelvis-torso axial relative phase during PS was lower (PS EMM = 98.4º, SSS EMM = 108.7º, ΔEMM = -10.26º).

Table 3.2: Average and average standard deviations for CRP mean.

CRP mean descriptive statistics									
	Torso/Upper-Torso			**Pelvis/Upper-Torso**			**Pelvis/Torso**		
	Lat Bend	**Flex/Ext**	**Ax.Rot**	**Lat Bend**	**Flex/Ext**	**Ax.Rot**	**Lat Bend**	**Flex/Ext**	**Ax.Rot**
PS avg ± std (º)	106.08 ± 11.79	83.86 ± 22.00	132.66 ± 19.63	103.82 ± 13.30	90.32 ± 21.53	77.17 ± 17.97	25.06 ± 7.95	85.95 ± 25.37	98.81 ± 23.31
SSS avg ± std (º)	100.16 ± 14.81	87.12 ± 29.66	126.35 ± 24.09	103.11 ± 16.98	84.89 ± 21.56	59.19 ± 20.10	23.82 ± 9.87	81.14 ± 15.75	108.00 ± 22.37

Table 3.3: PS and SSS pairwise comparisons for CRP mean. Statistically significant differences were found in axial rotation CRP mean between the pelvis and upper-torso, and the pelvis and torso. Difference in PS and SSS ΔEMM indicate that average pelvis/upper-torso axial relative phase was higher during the PS. However, pelvis-torso axial relative phase during PS was lower.

CRP mean	**Torso/Upper-Torso**			**Pelvis/Upper-Torso**			**Pelvis/Torso**		
	Lat Bend	**Flex/Ext**	**Ax.Rot**	**Lat Bend**	**Flex/Ext**	**Ax.Rot**	**Lat Bend**	**Flex/Ext**	**Ax.Rot**
PS-SSS ΔEMM (º)	4.86	-4.33	5.23	-0.35	4.36	16.91	0.17	3.74	-10.26
P-Value	0.31	0.36	0.27	0.94	0.36	***< 0.05***	0.97	0.43	***< 0.05***

CRP variability descriptive statistics									
	Torso/Upper-Torso			**Pelvis/Upper-Torso**			**Pelvis/Torso**		
	Lat Bend	**Flex/Ext**	**Ax.Rot**	**Lat Bend**	**Flex/Ext**	**Ax.Rot**	**Lat Bend**	**Flex/Ext**	**Ax.Rot**

PS avg ± std (°)	48.59 ± 5.36	39.35 ± 9.15	34.32 ± 14.63	48.43 ± 5.50	39.15 ± 9.70	41.09 ± 7.74	17.06 ± 6.30	46.18 ± 6.10	44.37 ± 8.21
SSS avg ± std (°)	47.50 ± 6.08	37.05 ± 9.22	37.20 ± 13.69	46.65 ± 6.50	40.88 ± 11.17	39.57 ± 9.04	17.27 ± 6.03	49.44 ± 7.29	44.84 ± 7.97

Table 3.4: Average and standard deviations for CRP variability.

Average and standard deviations for CRP variability are reported in Table **3.4**. Repeated measures ANOVA showed no effect of running velocity on coordination pattern variability ($p = 0.41$). There was however a significant main effect of segment indicating that there were differences in the variability of the relative phasing for each segment.

Proportion of the gait cycle spent in phase was calculated to determine whether changes to CRP mean indicate a transition from an in-phase coordination pattern to an out-of-phase pattern with increasing running velocity. Descriptive statistics for proportion of the gait cycle spent out of phase are reported in Table **3.4**. Repeated measures ANOVA revealed a statistically significant interaction between the proportion of the gait cycle spent out-of-phase and running velocity. Descriptive statistics are reported in Table **3.5**. Pairwise comparisons were carried out to determine whether proportion of the gait cycle spent out-of-phase was impacted by running velocity (Table **3.6**).

The simultaneous increase in proportion of the gait cycle spent out-of-phase in pelvis/upper-torso axial coordination patterns and decrease in pelvis/torso coordination patterns in the same plane is an interesting phenomenon to note. Studies that evaluate coordination patterns in those with LBP or resolved LBP have reported a decreased ability or inability to adopt out-of-phase coordination patterns between the pelvis and torso with increasing walking and running velocities [22,23,25,26,31]. Results from this study would seem to suggest that decreased counterrotation of between the pelvis and torso is accompanied by increased counterrotation between the pelvis and upper-torso.

Table 3.5: Descriptive statistics for proportion of the gait cycle spent out-of-phase.

Proportion spent out-of-phase descriptive statistics									
Avg ± std	**Torso/Upper-Torso**			**Pelvis/Upper-Torso**			**Pelvis/Torso**		
	Lat Bend	**Flex/Ext**	**Ax.Rot**	**Lat Bend**	**Flex/Ext**	**Ax.Rot**	**Lat Bend**	**Flex/Ext**	**Ax.Rot**
PS avg ± std	0.54 ± 0.10	0.33 ± 0.17	0.78 ± 0.16	0.51 ± 0.10	0.39 ± 0.19	0.30 ± 0.14	0.00 ± 0.01	0.38 ± 0.20	0.47 ± 0.19
SSS avg ± std	0.48 ± 0.14	0.36 ± 0.24	0.74 ± 0.21	0.50 ± 0.16	0.35 ± 0.19	0.18 ± 0.13	0.00 ± 0.00	0.33 ± 0.13	0.55 ± 0.19

Table 3.6: Difference in PS and SSS Estimated Marginal Means (EMM) and pairwise-comparison p-values for proportion of the gait cycle spent out-of-phase as running velocity changes. Results indicate subjects typically show a 12% increase in out-of-phase patterning in pelvis/upper-torso axial rotation as running velocity increases. This is accompanied by a nearly10% decrease in out-of-phase patterning in pelvis/torso axial rotation.

Proportion of gait cycle spent out-of-phase	**Upper-Torso / Torso**			**Pelvis/Upper-Torso**			**Pelvis/Torso**		
	Lat Bend	**Flex/Ext**	**Ax.Rot**	**Lat Bend**	**Flex/Ext**	**Ax.Rot**	**Lat Bend**	**Flex/Ext**	**Ax.Rot**
ΔEMM	0.04	-0.04	0.03	0.01	0.03	0.12	-0.01	0.05	-0.09
P-Value	0.27	0.35	0.38	0.84	0.48	***< 0.05***	0.88	0.20	***< 0.05***

3.4 Discussion

Previous studies that have evaluated running in healthy controls have found that running velocity increases there is an increase in stride length [32,33]. This study found similar results in lower-limb amputees. The lack of asymmetry between intact and prosthetic sides, and insignificant changes in other gait parameters may be due to the high activity level of this population (servicemembers), and the availability of well fitted and running specific prostheses.

There was no significant effect of running velocity on upper-torso, torso, pelvis, or intact and amputated hip rotational amplitudes. In addition, there were not statistically significant differences in intact and amputated side hip rotations. This was slightly contradictory to results reported by Sanderson who reported finding greater hip extension on the prosthetic side in amputees at stance indicating that the prosthetic limb was held in a more vertical orientation than

the intact limb [33]. However, rotational amplitudes are a crude measure because they measure differences between the largest and smallest rotation in the gait cycle. Therefore, they would be unable to identify changes at specific gait event. Furthermore, adaptations by amputees could easily be averaged out.

In this analysis, coordination patterns identified more changes due to running velocity than traditional gait parameters and rotational amplitude calculations. As running velocity increased there were no changes to coordination patterns in flexion/extension or lateral bend. This is in contrast to studies conducted by Seay who found that as running velocity increased there were accompanying changes in flexion/extension and lateral bend coordination [23]. However, results from axial coordination in this study agree with those seen by Seay. In this study as running velocity increased, there was an increase in pelvis/upper-torso axial, and a decrease in pelvis/torso axial coordination patterns. This was accompanied by changes in the proportion of the gait cycle spent out-of-phase. In pelvis and upper-torso axial coordination patterns as running velocity increased there was an increase in the proportion of the gait cycle these segments adopted an out-of-phase pattern. In pelvis and torso axial coordination patterns there was a decrease in the proportion of the gait cycle these segments adopted an out-of-phase coordination patterns as running velocity increased. Seay and colleagues identified a similar pattern in their populations, however the magnitude of the increase in CRP mean with increasing running velocity was much less in their LBP and resolved LBP groups [22,23]. Insignificant velocity dependent changes to coordination patterns in lateral bend and flexion/extension may be because only two running velocities were tested. In their study, Seay tested three prescribed running velocities.

Seay also reported increases in pelvis-trunk CRP variability as running deviated from comfortable in their control population [22,23]. Like CRP mean, the magnitude of this increase in CRP variability was significantly less in LBP and resolved LBP populations. It is unclear whether the amputees in this study had a history of LBP which could influence these results. This amputee population shows no changes to coordination pattern variability that could be like what Seay has reported in LBP and resolved LBP populations. However, analysis of a larger cohort of amputees is needed to validate whether this is a common pattern among amputees during running.

Another measure of interest in this study was whether there were running velocity dependent changes to the proportion of the gait cycle spent adopting an out-of-phase coordination pattern. This measure was chosen because it is more descriptive than CRP mean. Clinical implications of changes to CRP mean and variability are difficult to elucidate. Proportion of the gait cycle spent out-of-phase presents a diagnostic and therapeutic target. In this study a 12% increase in pelvis/upper-torso axial coordination was accompanied by a 10% decrease in pelvis/torso coordination. Previous authors have hypothesized that excessive axial rotations of the spine could cause strain and lead to the development of LBP [34]. The decrease in pelvis/torso axial counter rotation is accompanied by an increase in the pelvis/upper-torso counter rotation. Increased counterrotation further upstream could be made to compensate for the lack of counterrotation between the pelvis and torso.

Various authors have identified velocity dependent changes to CRP in healthy controls [20,22,23]. In walking, these authors have found that as running velocity increases there is a transition from in-phase pelvis-trunk coordination patterns to out-of-phase. This is also accompanied by an increase in CRP variability. Flexion/extension and lateral bend relative

phasing remains largely unchanged because the pelvis does not need to rotate as much in the frontal plane to clear the swing limb [23]. The need for increased stability, and the replacement of the double-stance phase with the double-float phase is likely why authors like Seay saw greater changes in CRP during walking than during running. Their study illustrates why it is important to characterize coordination patterns in amputee populations during running. When compared to controls, changes to these patterns may lend greater insight into gait adaptations than traditional measures.

3.5 Conclusions

This paper adds to the growing body of literature which aims to characterize gait changes in LLAs. This paper identified changes to coordination patterns that are in-line with results reported by other authors. For instance, amputees in this study maintained more in-phase pelvis/trunk axial coordination patterns as running velocity increased. Moreover, amputees show compensations further upstream that were characterized by more out-of-phase pelvis/upper-torso axial coordination pattern. This paper concludes that like HCs, amputees exhibit velocity dependent changes to coordination patterns that are also seen in non-amputee populations. However, because this data did not include a cohort of non-amputees for comparison therefore, the degree of similarity cannot be ascertained.

This amputee populations, however, did not exhibit velocity dependent changes to coordination variability that are reported in non-amputee populations. In fact, this maintenance of variability despite increases in running velocity is seen in populations with LBP [23]. While the LBP status of this population is unknown because similar invariance is seen in populations with a history of LBP, it is possible that an inability to increase coordination variability could lead to the development of LBP in this population. Further studies would be needed to assess

whether static coordination variability is an adaptation to lower-limb amputation or previous LBP. Seay and colleagues believe that coordination patterns could be a target for clinical interventions that target segment position and velocity [23]. The inclusion of the proportion of the gait cycle spent out-of-phase could be a target measure. Additional studies would need to be conducted to determine the optimal range for this measure.

3.7 References

[1] C.S. Molina, J. Faulk, Lower Extremity Amputation, in: StatPearls, StatPearls Publishing, Treasure Island (FL), 2021. http://www.ncbi.nlm.nih.gov/books/NBK546594/ (accessed November 13, 2021).

[2] D.M. Ehde, D.G. Smith, J.M. Czerniecki, K.M. Campbell, D.M. Malchow, L.R. Robinson, Back pain as a secondary disability in persons with lower limb amputations, Archives of Physical Medicine and Rehabilitation. 82 (2001) 731–734. https://doi.org/10.1053/apmr.2001.21962.

[3] D.G. Smith, D.M. Ehde, M.W. Legro, G.E. Reiber, M. del Aguila, D.A. Boone, Phantom Limb, Residual Limb, and Back Pain After Lower Extremity Amputations, Clinical Orthopaedics and Related Research®. 361 (1999) 29–38.

[4] B.S. Baum, B.L. Schnall, J.E. Tis, J.S. Lipton, Correlation of residual limb length and gait parameters in amputees, Injury. 39 (2008) 728–733. https://doi.org/10.1016/j.injury.2007.11.021.

[5] H. Goujon-Pillet, E. Sapin, P. Fodé, F. Lavaste, Three-Dimensional Motions of Trunk and Pelvis During Transfemoral Amputee Gait, Archives of Physical Medicine and Rehabilitation. 89 (2008) 87–94. https://doi.org/10.1016/j.apmr.2007.08.136.

[6] S.M.H.J. Jaegers, Prosthetic gait of unilateral transfemoral amputees: A kinematic study, Archives of Physical Medicine and Rehabilitation. 76 (1995) 736–743. https://doi.org/10.1016/S0003-9993(95)80528-1.

[7] H. Nadollek, S. Brauer, R. Isles, Outcomes after trans-tibial amputation: the relationship between quiet stance ability, strength of hip abductor muscles and gait, Physiotherapy Research International. 7 (2002) 203. https://doi.org/10.1002/pri.260.

[8] L. Nolan, A. Lees, The functional demands on the intact limb during walking for active transfemoral and transtibial amputees, Prosthet Orthot Int. 24 (2000) 117–125. https://doi.org/10.1080/03093640008726534.

[9] L. Nolan, A. Wit, K. Dudziñski, A. Lees, M. Lake, M. Wychowañski, Adjustments in gait symmetry with walking speed in trans-femoral and trans-tibial amputees, Gait & Posture. 17 (2003) 142–151. https://doi.org/10.1016/S0966-6362(02)00066-8.

[10] G.R.B. Hurley, R. McKenney, M. Robinson, M. Zadravec, M.R. Pierrynowski, The role of the contralateral limb in below-knee amputee gait, Prosthet Orthot Int. 14 (1990) 33–42. https://doi.org/10.3109/03093649009080314.

[11] Y. Sagawa Jr, K. Turcot, S. Armand, A. Thevenon, N. Vuillerme, E. Watelain, Biomechanics and physiological parameters during gait in lower-limb amputees: A systematic review, Gait & Posture. 33 (2011) 511–526. https://doi.org/10.1016/j.gaitpost.2011.02.003.

[12] C.D. Tokuno, D.J. Sanderson, J.T. Inglis, R. Chua, Postural and movement adaptations by individuals with a unilateral below-knee amputation during gait initiation, Gait & Posture. 18 (2003) 158–169. https://doi.org/10.1016/S0966-6362(03)00004-3.

[13] D.C. Morgenroth, The Relationship Between Lumbar Spine Kinematics during Gait and Low-Back Pain in Transfemoral Amputees, American Journal of Physical Medicine & Rehabilitation. 89 (2010) 635–643. https://doi.org/10.1097/PHM.0b013e3181e71d90.

[14] S.B. Michaud, S.A. Gard, D.S. Childress, A preliminary investigation of pelvic obliquity patterns during gait in persons with transtibial and transfemoral amputation., Journal of Rehabilitation Research and Development. 37 (2000) 1–10.

[15] B.D. Hendershot, M.A. Nussbaum, Persons with lower-limb amputation have impaired trunk postural control while maintaining seated balance, Gait & Posture. 38 (2013) 438–442. https://doi.org/10.1016/j.gaitpost.2013.01.008.
[16] H. Schmidt, A. Kettler, F. Heuer, U. Simon, L. Claes, H.-J. Wilke, Intradiscal pressure, shear strain and fiber strain in the intervertebral disc under combined loading, Journal of Biomechanics. 39 (2006) S29–S29. https://doi.org/10.1016/S0021-9290(06)82983-0.
[17] H. Devan, P.A. Hendrick, D.C. Riberio, L.A. Hale, A. Carman, Asymmetrical movements of the lumbopelvic region: Is this a potential mechanism for low back pain in people with lower limb amputation?, Medical Hypotheses. 82 (2014) 77–85. https://doi.org/10.1016/j.mehy.2013.11.012.
[18] J.R. Franz, K.W. Paylo, J. Dicharry, P.O. Riley, D.C. Kerrigan, Changes in the coordination of hip and pelvis kinematics with mode of locomotion, Gait & Posture. 29 (2009) 494–498. https://doi.org/10.1016/j.gaitpost.2008.11.011.
[19] Y.-T. Yang, Y. Yoshida, T. Hortobágyi, S. Suzuki, Interaction Between Thorax, Lumbar, and Pelvis Movements in the Transverse Plane During Gait at Three Velocities, Journal of Applied Biomechanics. 29 (2013) 261–269. https://doi.org/10.1123/jab.29.3.261.
[20] R.E.A. van Emmerik, R.C. Wagenaar, Effects of walking velocity on relative phase dynamics in the trunk in human walking, Journal of Biomechanics. 29 (1996) 1175–1184. https://doi.org/10.1016/0021-9290(95)00128-X.
[21] S.J. Preece, D. Mason, C. Bramah, The coordinated movement of the spine and pelvis during running, Human Movement Science. 45 (2016) 110–118. https://doi.org/10.1016/j.humov.2015.11.014.
[22] J.F. Seay, Influence of Low Back Pain Status on Pelvis-Trunk Coordination During Walking and Running, Spine (Philadelphia, Pa. 1976). 36 (2011) E1070–E1079. https://doi.org/10.1097/BRS.0b013e3182015f7c.
[23] J.F. Seay, R.E.A. Van Emmerik, J. Hamill, Low back pain status affects pelvis-trunk coordination and variability during walking and running, Clinical Biomechanics. 26 (2011) 572–578. https://doi.org/10.1016/j.clinbiomech.2010.11.012.
[24] J. Hamill, R.E.A. van Emmerik, B.C. Heiderscheit, L. Li, A dynamical systems approach to lower extremity running injuries, Clinical Biomechanics. 14 (1999) 297–308. https://doi.org/10.1016/S0268-0033(98)90092-4.
[25] C.J.C. Lamoth, Pelvis-Thorax Coordination in the Transverse Plane During Walking in Persons With Nonspecific Low Back Pain, Spine (Philadelphia, Pa. 1976). 27 (2002) E92–E99. https://doi.org/10.1097/00007632-200202150-00016.
[26] C.J.C. Lamoth, P.J. Beek, O.G. Meijer, Pelvis–thorax coordination in the transverse plane during gait, Gait & Posture. 16 (2002) 101–114. https://doi.org/10.1016/S0966-6362(01)00146-1.
[27] P.F. Lamb, M. Stöckl, On the use of continuous relative phase: Review of current approaches and outline for a new standard, Clinical Biomechanics. 29 (2014) 484–493. https://doi.org/10.1016/j.clinbiomech.2014.03.008.
[28] J.S. Wheat, P.S. Glazier, Measuring Coordination and Variability in Coordination, (n.d.) 16.
[29] J. Hamill, J.M. Haddad, W.J. McDermott, Issues in Quantifying Variability From a Dynamical Systems Perspective, Journal of Applied Biomechanics. 16 (2000) 407.
[30] S. Mehdizadeh, P.S. Glazier, Order error in the calculation of continuous relative phase, Journal of Biomechanics. 73 (2018) 243–248. https://doi.org/10.1016/j.jbiomech.2018.03.032.

[31] N.F. Taylor, O.M. Evans, P.A. Goldie, The effect of walking faster on people with acute low back pain, European Spine Journal. 12 (2003) 166–172. https://doi.org/10.1007/s00586-002-0498-3.
[32] R.M. Enoka, D.I. Miller, E.M. Burgess, Below-knee amputee running gait, Am J Phys Med. 61 (1982) 66–84.
[33] D.J. Sanderson, P.E. Martin, Lower extremity kinematic and kinetic adaptations in unilateral below-knee amputees during walking, Gait & Posture. 6 (1997) 126–136. https://doi.org/10.1016/S0966-6362(97)01112-0.
[34] X. Shan, X. Ning, Z. Chen, M. Ding, W. Shi, S. Yang, Low back pain development response to sustained trunk axial twisting, Eur Spine J. 22 (2013) 1972–1978. https://doi.org/10.1007/s00586-013-2784-7.

Chapter 4 Characterization of upper torso, torso, pelvis, and hip segment rotations and coordination patterns in healthy controls with and without a handless crutch

4.1 Abstract

Low back pain (LBP) is a common and bothersome problem among lower-limb amputees. Previous studies have identified changes to pelvis and trunk coordination patterns after back pain has resolved that could explain the high recurrence of LBP. It remains unknown how adaptation to prosthetic use changes coordination patterns, and how these changes could lead to the development of LBP in lower-limb amputees. Therefore, the aim of this study was to isolate the effects of wearing lower-limb prostheses (LLP) on one side on coordination patterns. Eighteen subjects were recruited to perform over-ground walking tasks under two conditions, with and without the iWalk 2.0 (Norm & iWalk) at four walking velocities, Slow20, Slow10, SSS, Fast (Sampling rate = 60Hz). When walking with the iWalk, subjects showed no intact and iWalk side stride length asymmetry. However, subjects did increase stance times on the intact side. Upper-torso, torso, pelvis, and hip rotational amplitudes were larger during the Norm tasks. However, the difference in Estimated Marginal Means was less than 5º. During iWalk tasks CRP mean results showed that subjects maintained a more in-phase coordination pattern. These results were confirmed by results from proportion of the gait cycle spent out-of-phase. Subjects also exhibited greater CRP variability during Norm tasks in lateral bend. Both CRPmean and CRP variability showed walking velocity effects. Overall results from this study aligned well with others which evaluated amputees. In addition, this study showed that wearing a LLP causes changes to coordination patterns that are similar to ones seen in people with LBP.

4.2 Background

Common complaints among lower limb amputees (LLAs) include residual limb pain, phantom limb pain and sensation, non-amputated side pain and back pain [1]. It is estimated that 52% - 68.7% of LLAs report experiencing low back pain (LBP). For 17% of amputees LBP is debilitating and persistent [2,3].

Within the non-amputee population, gait parameters and segment rotations have primarily been used to quantify the effects of LBP. In fact, the effects of LBP and LLA on gait mechanics are quite similar. Amputees and those with LBP take smaller steps and have a reduced stride length [4–9]. Some studies have reported changes to pelvis and thorax rotation variability in those with LBP while amputees show changes to both range of motion and variability [4,10]. A study conducted by Barzilay which characterized the effects of physical therapy to treat LBP in non-amputee populations on traditional gait parameters found that these measures return to normal after pain has resolved [5]. However, the recurrent nature of LBP suggests that therapeutic interventions do not always correct maladaptive movement patterns, and gait parameters do not capture underlying changes to gait that predispose LBP sufferers to recurrent bouts [5,11].

In recent years, methods that quantify coordination patterns between the trunk and pelvis have proven to be more sensitive to a history of LBP than gait parameters. Studies conducted by Seay et al. and Lamoth et al. found that those with LBP or a history of LBP adopted or maintained coordination patterns that are different from their non-pained counterparts [12–15]. For instance, studies that assess coordination patterns in healthy controls have found that as walking velocity increases there is a transition from an in-phase pelvic/thorax coordination in the frontal and transverse planes, to an out-of-phase pattern [16,17]. As for variability, as walking

velocity deviates from a comfortable speed, variability of coordination patterns increase. In those with LBP or a history of LBP, the transition to an out-of-phase pattern at higher velocities is either delayed or non-existent and there are smaller changes to coordination variability. While these methods have shown promise in non-amputee population, there is only one study that similarly evaluated coordination patterns in lower-limb amputees [6].

Understanding the biomechanical etiology of non-specific LBP is often challenged by a lack of detectable changes to spinal structures when imaged, comorbidities, and the high recurrence of pain. These challenges are often exacerbated when studying LLAs because of changes to lower-limb structure and musculature, development of osteoarthritis in the lower limb, and design, quality, and fit of a prosthetic. Each of these factors can add variability to studies that evaluate the gait in amputees. To the author's knowledge, such a study has yet to be undertaken. Therefore, the aim of this study was to understand how adaptation to prosthetic use impacts coordination patterns. Understanding the effects of prosthetic use on coordination patterns can help researchers better understand the overall effects of amputation on gait and movement. Coupled with current literature on non-amputees with LBP, results from this study could help uncover specific ways in which adaptation to prosthetic use increases likelihood of developing LBP.

4.3 Methods

4.3.1 Participants

Eighteen subjects between 18 and 64 were recruited (Avg: 28.2yr, Range: 22 – 34, Males: 12). All subjects had no history of LBP within the past year. All subjects were healthy and had no history of musculoskeletal injury or physiological conditions that would prevent participation in this study. In accordance with university policies, all subjects consented by

signing an IRB-approved consent form. In addition, they completed a general health questionnaire that determined eligibility and weekly physical activity.

4.3.2 Experimental set-up

During a single visit to the Human Performance Laboratory (HPL) at the University of Kansas Medical Center's Landon Center on Aging, each subject completed the health questionnaire and IRB-approved consent form. Thirty-three reflective markers were placed according to a Helen Hayes configuration on the lower limbs, along with sensors on the acromioclavicular processes, seventh cervical, and tenth thoracic vertebrae, on the manubrium below the jugular notch, on the xiphoid process, and on the sacrum (Figure 4.1) [18]. Kinematic data were collected using six Kestral and two RaptorE cameras (MotionAnalysis Corporation, Santa Rosa, CA) sampling at 60Hz. After static data was collected, medal sensors (six) were removed and the remaining 27 were used for dynamic data collection.

This marker set also included three bilateral sensors placed on the medial knee, medial ankle, and medial foot between the first proximal phalange and metatarsal. Subjects then stood on the calibration platform in the middle of the capture volume. Facing in the position of progression (+ X) (**Figure 4.2**a), with their right leg pressed against the circular discs with their hands their stomachs between ASIS and xiphoid sensors, feet shoulder-width apart. They then repeated this process for their left leg. Afterward, medial sensors were removed, and subjects were asked to stand in the middle of the capture volume while not on the platform. This static position was considered anatomically neutral. All other motions collected during these trials were described relative to this position. Sensors for this trial were identified in the software, and a wireframe model was generated (Cortex, MotionAnalysis, **Figure 4.2**b).

After calibration, subjects were asked to walk at a comfortable pace, the number of steps taken per minute was used to calibrate a metronome. This comfortable walking velocity was taken as their preferred walking velocity and all other velocities were calculated relative to it. Subjects then performed six trials of overground walking at four randomly selected velocities: self-selected speed (SSS), SSS– 20% (Slow20), SSS – 10% (Slow10), and SSS + 10% (Fast). The metronome was used to help subjects maintain a consistent walking velocity throughout the trial. Subjects were instructed to walk to the metronome's beat without ramp-up or slow-down from one end of the capture volume to the other. A successful trial was when the wireframe was present during collection within the capture volume (**Figure 4.2**b). Each subject then performed each walking velocity with and without the iWalk (iWalk/Norm).

Figure 3.2: sensor placement for iWalk study. A) Frontal view. B) posterior view. C) Left lateral view

Measurements were taken of each subjects' shin from the lateral patella to the ground. This was used to adjust the length of the iWalk. The iWalk was then fitted to the dominant leg which was identified by asking each subject which leg they kicked or dribbled a ball with. Subjects were given time to acclimate to the iWalk and allow for fine adjustments to the length and height of the thigh attachment as requested by subjects. Each subject was given as much time as they needed to practice and testing only resumed after they indicated they were ready to proceed. Sensors were removed from dominant leg's ankle and foot and placed on the iWalk in positions that would approximate the native ankle and foot. A new static posture was captured along with new preferred walking velocities. They then performed six trials of the randomly selected walking velocities.

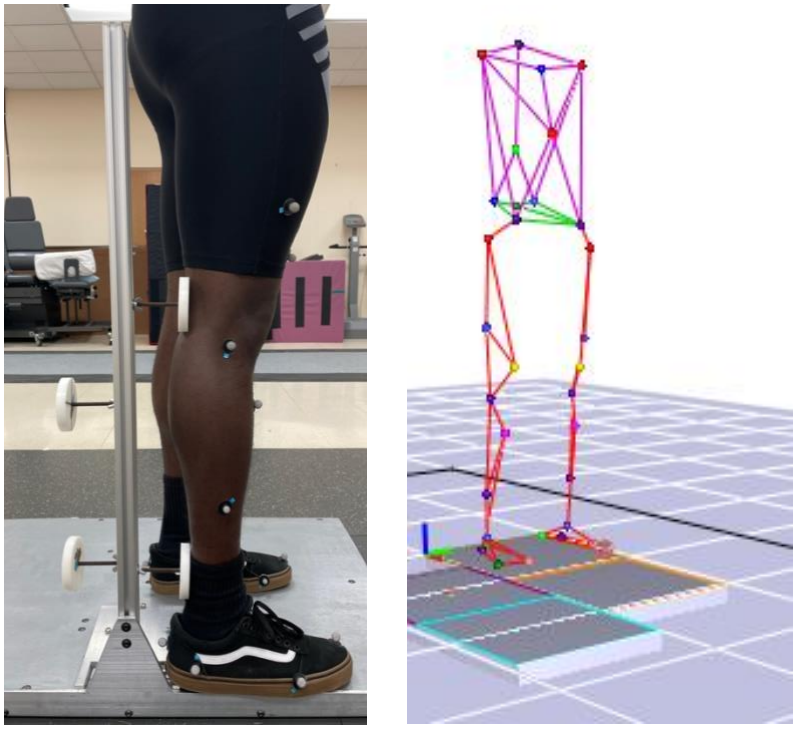

Figure 3.3: a) calibration pose for right leg, b) wireframe model

Data Processing

Each subject performed six trials under each condition and walking velocity. Kinematic data was first processed in Cortex. Missing marker trajectories were filled using a cubic spline or virtual joined using nearby sensors. For example, missing sacral trajectories were virtual joined using sensors on the right and left acromioclavicular joints and the manubrium. Data was then low-pass filtered using a 6Hz fourth order Butterworth filter which is the default filter in Cortex. Common filters for human movement range between 3Hz and 10Hz [19]. Data was then exported to MATLAB where gait parameters, segment rotations, and coordination patterns were calculated (MathWorks, Natick, MA). These measures were then exported to R/RStudio for statistical analysis (RStudio, Boston, MA).

4.3.3 Analysis

Walking velocity was calculated by taking the derivative of the sensor placed on the seventh cervical vertebrae (C7) in the direction of movement. Stride length, and single-limb stance time in seconds were calculated using sensors placed on the calcaneus and distal phalanx of the hallux. A stride was defined as the distance from calcaneal minima to minima on the same side (i.e.: heel strike to heel strike). Local segment axes for the upper-torso, torso, pelvis, and hips were created from the calibration trials. Rotations for each segment measured as the rotations of each segment axis relative to the global axis. Segment rotations and coordination patterns were calculated using an XYZ Cardan angle sequence for each stride then interpolated to 100 data points for time-normalization [20,21]. Repeated measures ANOVA with task (Norm – without the iWalk, and iWalk), and walking velocity was used to analyze the results. Significant ANOVA results were followed by pairwise comparisons with a Tukey correction.

iWalk and Norm differences in Estimated Marginal Means (iWalk EMM – Norm EMM = ΔEMM) were reported to determine the magnitude and direction of significant comparisons.

Upper-torso, torso, pelvis, and hip axes were created using a multi-segment model similar to that of Needham's [22]. To create the torso axis, a vector was first drawn between the sacral and tenth thoracic vertebrae (SACR → T10 = $\vec{d}$). This would become the z-axis (transverse plane). Torso axial rotations were defined by movement about this axis. Another vector was drawn connecting the sternum and the sacrum (Stern → SACR = $\vec{e}$). The cross product of these two vectors created a third vector $\vec{f}$ which became the x-axis (sagittal plane). Rotations about this axis constituted torso flexion/extension. To ensure that the vectors were orthogonal, the vector $\vec{d}$ was crossed with the $\vec{f}$ ($\vec{d} \times \vec{f} = \overrightarrow{ee}$). This axis became the y-axis (frontal plane). Rotations about this axis comprised torso lateral bend.

4.3.4 Rotational amplitude calculations

Rotational amplitudes were calculated by taking the absolute value of the difference between the maximum and minimum rotations (Equation 3.1). Repeated measures ANOVA was also used to determine the effect of walking velocity and the use of the handless crutch on upper-torso, torso, pelvis, and intact and amputated (iWalk) hip rotations. Pairwise comparisons with Tukey corrections were used to further detect which rotations significantly impacted.

$$Rotational\ Amplitude = |Max_{rot} - Min_{rot}|$$

Equation 3.5

4.3.5 Continuous Relative Phase (CRP)

Coordination patterns between segments were calculated according to a method described by Hamill [23]. Methods used for this study are described in detail in previous papers. In brief: angular velocity was calculated from the angular position using the central difference method.

Angular position and velocity were then normalized using Equation 3.2 and Equation 3.3. Phase angle (φ) was calculated according to the unit circle normalization Figure 3.1. Lastly, coordination patterns were calculated using Equation 3.8. Mean and standard deviation were calculated using linear methods. Proportion of the gait cycle spent out-of-phase was calculated as the number datapoints in the CRP vector greater than 110º was divided by the length of the vector (100 data points) [16]. Repeated measures ANOVA followed by pairwise comparisons were used to compare walking velocities, and Norm and iWalk trials.

$$\theta_i{}' = \frac{2 * [\theta_i - min\ (\theta_i)]}{max(\theta_i) - min\ (\theta_i)}$$

Equation 3.6

$$\omega_i{}' = \frac{\omega_i}{max\ \{max(\omega_i), max(-\omega_i)\}}$$

Equation 3.7

$$CRP_{torso-pelvis} = |\varphi_{pelvis} - \varphi_{torso}|$$

Equation 3.8

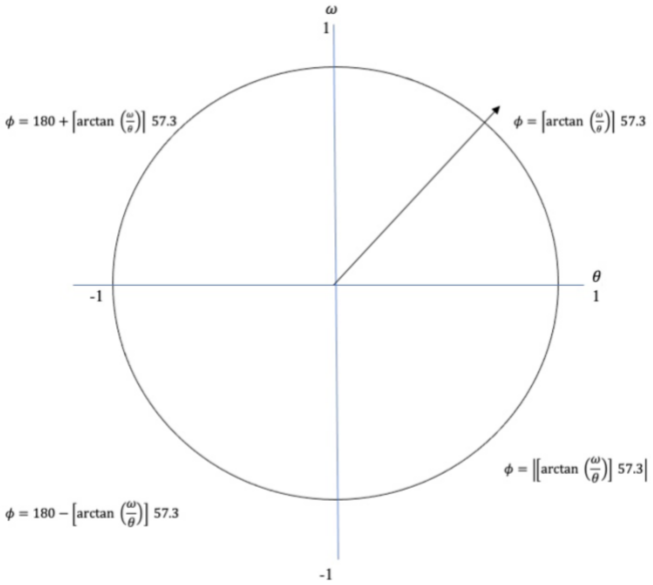

Figure 3.4: normalization of position-velocity phase angles (ϕ)

4.4 Results

4.4.1 Gait parameters

Mean walking velocities for Norm and iWalk tasks were compared. As expected, iWalk walking velocities were significantly slower ($p < 0.05$) than Norm tasks Table 3.7. Stride length and stance times for right and left sides for Norm tasks, and intact and amputated sides were compared (Figure 4.4,

Table 3.8). There were no statistically significant differences between right and left, or intact and amputated stride lengths. Statistically significant differences between intact and amputated side stance times were detected at all walking velocities except the SSS with the iWalk. In all cases, intact side stance time was greater than amputated side stance times.

Table 3.7: Walking velocity for each condition (Norm and iWalk). T-tests indicate that iWalk walking velocities were all significantly lower than Norm walking velocities.

Norm and iWalk walking velocities (m/s)		
	Norm	**iWalk**
Fast	1.02 ± 0.25	0.67 ± 0.22
SSS	1.02 ± 0.26	0.66 ± 0.23
Slow10	0.98 ± 0.25	0.64 ± 0.22
Slow20	0.98 ± 0.26	0.62 ± 0.26

Table 3.8: Table of gait parameters (stride length and stance time) in each task (Norm/iWalk). There were no statistically significant differences between right and left, or intact and amputated stride lengths. Statistically significant differences between intact and amputated side stance times were detected at all walking velocities except the SSS with the iWalk. In all cases, intact side stance time was greater than amputated side stance times.

Norm and iWalk Gait Parameters					
		Norm		**iWalk**	
		Left	**Right**	**Intact**	**iWalk**
Stride length (m)	**Fast**	1.39 ± 0.18	1.40 ± 0.17	0.94 ± 0.25	0.94 ± 0.24
	SSS	1.38 ± 0.18	1.38 ± 0.18	0.94 ± 0.26	0.93 ± 0.26
	Slow10	1.27 ± 0.17	1.26 ± 0.17	0.94 ± 0.26	0.93 ± 0.26
	Slow20	1.22 ± 0.17	1.22 ± 0.18	0.89 ± 0.23	0.88 ± 0.22
Stance time (s)	**Fast**	0.47 ± 0.11	0.48 ± 0.11	0.46 ± 0.19	0.49 ± 0.05
	SSS	0.49 ± 0.20	0.46 ± 0.10	0.48 ± 0.21	0.51 ± 0.14
	Slow10	0.47 ± 0.13	0.45 ± 0.16	0.44 ± 0.19	0.50 ± 0.07
	Slow20	0.47 ± 0.12	0.45 ± 0.13	0.47 ± 0.24	0.51 ± 0.07

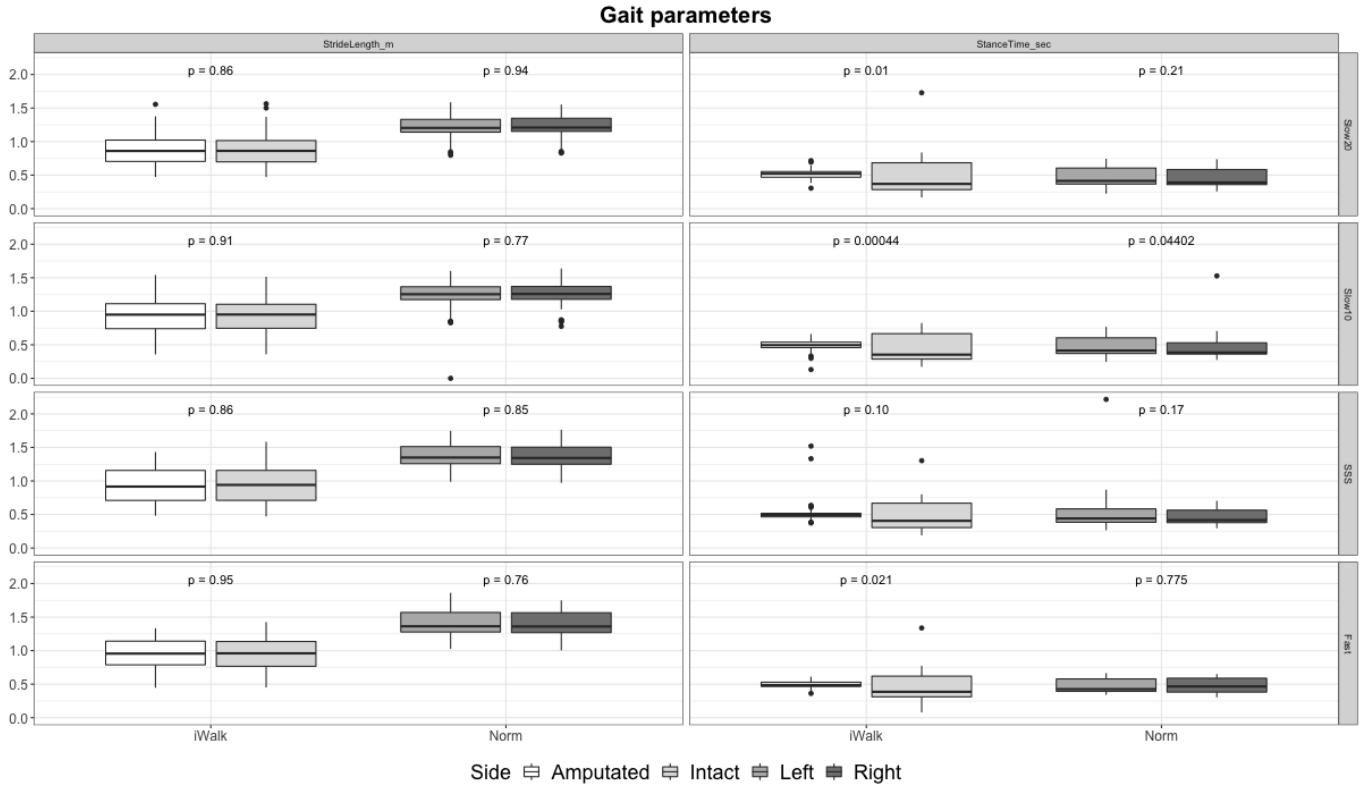

Figure 3.5:Box plots of iWalk intact and amputated and Norm right and left stride length (m) and stance time (sec) along with pairwise comparisons. No statistically significant differences were found in stride length between sides for either task at any walking velocity. However, there were statistically significant side differences in stance time for iWalk task at all walking velocities except SSS. To accommodate walking with the iWalk, subjects significantly increased intact side stance times.

4.4.2 Rotational amplitudes

Repeated measures ANOVA reported statistically significant two-way interactions between task (iWalk vs. Norm) and rotational amplitudes, task and walking velocity, and rotational amplitudes and speed ($p < 0.5$). There were also significant main effects of task, walking velocity, and rotational amplitudes. Pairwise comparisons for task and rotational amplitudes revealed statistically significant differences between iWalk and Norm tasks in all rotations (Table **3.9**, $p < 0.05$). However, all ΔEMM were less than 5º.

Table 3.9: Descriptive statistics (avg ± std) for each segment and its rotations for both iWalk and Norm tasks. Results of pairwise comparisons used to determine the effect of wearing the iWalk on segment rotation amplitudes are reported as the differences in estimated marginal means. Statistically significant differences were found between iWalk and Norm rotational amplitudes for all segments analyzed ($p < 0.05$). ΔEMM revealed that these differences were all below 5º.

iWalk – Norm rotational amplitudes pairwise comparisons					
	Rotation	**iWalk avg ± std (º)**	**Norm avg ± std (º)**	**ΔEMM(º)**	**P-value**
Upper-Torso	**Lat Bend**	7.69 ± 2.13	7.00 ± 1.90	0.7	**< 0.05**
	Flex/Ext	8.72 ± 2.61	6.57 ± 2.01	2.1	**< 0.05**
	Ax. Rot	19.92 ± 2.98	15.64 ± 2.63	4.3	**< 0.05**
Torso	**Lat Bend**	10.25 ± 2.17	8.33 ± 1.98	1.9	**< 0.05**
	Flex/Ext	7.89 ± 2.53	5.68 ± 2.03	2.2	**< 0.05**
	Ax. Rot	16.70 ± 2.54	13.42 ± 2.39	3.3	**< 0.05**
Pelvis	**Obliquity**	10.86 ± 2.10	9.70 ± 1.72	1.2	**< 0.05**
	A/P Tilt	6.73 ± 1.72	5.05 ± 1.28	1.7	**< 0.05**
	Ax. Rot	21.97 ± 3.18	17.80 ± 3.07	4.2	**< 0.05**
L/Intact Hip	**Add/Abd**	7.80 ± 2.26	7.45 ± 1.52	0.5	**< 0.05**
	Flex/Ext	6.50 ± 1.71	5.22 ± 1.33	1.3	**< 0.05**
	Ax. Rot	12.26 ± 2.08	9.90 ± 1.81	2.4	**< 0.05**
R/iWalk Hip	**Add/Abd**	8.26 ± 3.07	6.61 ± 1.46	1.7	**< 0.05**
	Flex/Ext	5.50 ± 1.64	4.36 ± 1.06	1.1	**< 0.05**
	Ax. Rot	11.02 ± 2.17	9.47 ± 1.92	1.6	**< 0.05**

4.4.3 CRP mean

Repeated measures ANOVA revealed significant three-way interactions between CRP mean, and walking velocity, segment coordination, and task. There were also significant two-way segment coordination and task interactions, and main effects for task, segment coordination and walking velocity.

Table 3.10 shows pairwise comparisons for CRP mean for each segment rotation at each walking velocity for iWalk – Norm, and their respective ΔEMM. Statistically significant differences were found between iWalk and Norm CRP mean at all walking velocities in all torso/upper-torso and pelvis/upper-torso segment coordination in lateral bend. Statistically significant CRP mean was

CRP mean iWalk-Norm pairwise comparisons across walking velocity										
		Lateral Bend			Flexion/Extension			Axial Rotation		
	Speed	iWalk avg ± std (•) Norm avg ± std (•)	ΔEMM (°)	P-value	iWalk avg ± std (•) Norm avg ± std (•)	ΔEMM(°)	P-value	iWalk avg ± std (•) Norm avg ± std (°)	ΔEMM(°)	P-value
Torso/Upper-torso	Slow20	90.04 ± 31.35 127.71 ± 23.60	-37.66	**< 0.05**	30.66 ± 14.29 47.71 ± 18.53	-17.05	**< 0.05**	22.97 ± 12.21 21.22 ± 19.91	1.75	**< 0.05**
	Slow10	100.18 ± 32.63 136.81 ± 22.07	-36.63	**< 0.05**	33.61 ± 14.61 45.61 ± 19.29	-12.00	**< 0.05**	20.45 ± 11.89 26.42 ± 24.73	-5.98	**< 0.05**
	SSS	109.35 ± 28.06 139.31 ± 22.82	-29.96	**< 0.05**	31.76 ± 12.48 43.80 ± 18.43	-12.04	**< 0.05**	21.68 ± 12.13 30.33 ± 25.70	-8.65	**< 0.05**
	Fast	114.97 ± 26.99 140.23 ± 23.90	-25.26	**< 0.05**	31.82 ± 12.95 41.75 ± 19.51	-9.93	**< 0.05**	19.71 ± 12.04 30.57 ± 26.75	-10.86	**< 0.05**
Pelvis/Upper-torso	Slow20	83.63 ± 28.62 116.07 ± 22.91	-32.44	**< 0.05**	37.99 ± 17.83 70.87 ± 20.61	-32.88	**< 0.05**	28.50 ± 15.82 49.33 ± 34.07	-20.84	**< 0.05**
	Slow10	95.07 ± 31.55 125.06 ± 21.62	-29.984	**< 0.05**	41.36 ± 18.76 68.15 ± 21.71	-26.79	**< 0.05**	30.39 ± 17.41 59.00 ± 35.94	-28.61	**< 0.05**
	SSS	101.95 ± 29.68 129.66 ± 20.43	-27.70	**< 0.05**	41.20 ± 19.66 60.68 ± 19.95	-19.48	**< 0.05**	34.16 ± 16.97 67.05 ± 31.30	-32.89	**< 0.05**
	Fast	107.76 ± 27.32 131.02 ± 21.93	-23.27	**< 0.05**	40.13 ± 18.51 61.77 ± 22.44	-21.63	**< 0.05**	36.98 ± 17.00 71.43 ± 33.11	-34.45	**< 0.05**
Pelvis/Torso	Slow20	28.79 ± 17.98 33.86 ± 12.13	-5.07	0.06	20.87 ± 11.83 55.40 ± 17.99	-34.54	**< 0.05**	19.13 ± 9.78 34.47 ± 28.02	-15.34	**< 0.05**
	Slow10	32.19 ± 18.09 34.20 ± 14.49	-2.00	0.45	23.04 ± 12.64 57.85 ± 19.62	-34.82	**< 0.05**	20.28 ± 9.65 38.56 ± 26.31	-18.29	**< 0.05**
	SSS	35.95 ± 18.25 32.33 ± 14.01	3.62	0.18	23.37 ± 12.35 57.35 ± 19.85	-33.98	**< 0.05**	19.34 ± 7.80 43.44 ± 24.26	-24.11	**< 0.05**
	Fast	34.94 ± 18.21 35.14 ± 18.84	-0.20	0.94	24.11 ± 11.97 53.36 ± 20.44	-29.25	**< 0.05**	23.64 ± 9.60 49.42 ± 28.05	-25.78	**< 0.05**

found for all flexion/extension coordination patterns at all walking velocities. In axial rotation, CRP mean was found to be statistically significant for all axial coordination patterns except for upper-torso/torso at Slow20. iWalk-Norm ΔEMM were greater than 10º. Negative ΔEMM indicate that the CRP mean for iWalk tasks were lower Norm tasks at all walking velocities.

In addition, pairwise comparisons also revealed that as walking velocity increased, there was a corresponding increase in CRP mean particularly in torso/upper-torso and pelvis/upper-torso lateral bend. Axial coordination CRP mean for pelvis/upper-torso and pelvis/torso coordination patterns showed an opposing pattern. That is, as walking velocity increased, there was a decrease in CRPmean. Overall change in CRP mean with increased walking velocity was more than 10º.

Table 3.10: CRP mean descriptive statistics and pairwise comparisons of iWalk and Norm tasks at all walking velocities for all segment coordination patterns of interest. Statistically significant differences were found between iWalk and Norm CRP mean at all walking velocities in torso/upper-torso and pelvis/upper-torso segment coordination in lateral bend. Statistically significant CRP mean was found for all flexion/extension coordination patterns at all walking velocities. In axial rotation, CRP mean was found to be statistically significant for all axial coordination patterns except for upper-torso/torso at Slow20. Except for statistically significant CRP mean for torso/upper-torso axial rotation in all walking velocities except Slow20, differences in iWalk-Norm ΔEMM were greater than 10º. Negative ΔEMM indicate that CRP mean for iWalk tasks were lower Norm tasks at all walking velocities. In addition, pairwise comparisons also revealed that as walking velocity increased, there was a corresponding increase in CRP mean particularly in torso/upper-torso and pelvis/upper-torso lateral bend. Axial coordination CRP mean for pelvis/upper-torso and pelvis/torso coordination patterns showed an opposing pattern. That is, as walking velocity increased, there was a decrease in CRP mean. Overall change in CRP mean with increased walking velocity was more than 10º.

CRP mean iWalk-Norm pairwise comparisons across walking velocity										
		Lateral Bend			**Flexion/Extension**			**Axial Rotation**		
	Speed	**iWalk avg ± std (•)** **Norm avg ± std (•)**	**ΔEMM (º)**	**P-value**	**iWalk avg ± std (•)** **Norm avg ± std (•)**	**ΔEMM(º)**	**P-value**	**iWalk avg ± std (•)** **Norm avg ± std (º)**	**ΔEMM(º)**	**P-value**
Torso/Upper-torso	**Slow20**	90.04 ± 31.35 127.71 ± 23.60	-37.66	**< 0.05**	30.66 ± 14.29 47.71 ± 18.53	-17.05	**< 0.05**	22.97 ± 12.21 21.22 ± 19.91	1.75	**< 0.05**
	Slow10	100.18 ± 32.63 136.81 ± 22.07	-36.63	**< 0.05**	33.61 ± 14.61 45.61 ± 19.29	-12.00	**< 0.05**	20.45 ± 11.89 26.42 ± 24.73	-5.98	**< 0.05**
	SSS	109.35 ± 28.06 139.31 ± 22.82	-29.96	**< 0.05**	31.76 ± 12.48 43.80 ± 18.43	-12.04	**< 0.05**	21.68 ± 12.13 30.33 ± 25.70	-8.65	**< 0.05**
	Fast	114.97 ± 26.99 140.23 ± 23.90	-25.26	**< 0.05**	31.82 ± 12.95 41.75 ± 19.51	-9.93	**< 0.05**	19.71 ± 12.04 30.57 ± 26.75	-10.86	**< 0.05**
Pelvis/Upper-torso	**Slow20**	83.63 ± 28.62 116.07 ± 22.91	-32.44	**< 0.05**	37.99 ± 17.83 70.87 ± 20.61	-32.88	**< 0.05**	28.50 ± 15.82 49.33 ± 34.07	-20.84	**< 0.05**
	Slow10	95.07 ± 31.55 125.06 ± 21.62	-29.984	**< 0.05**	41.36 ± 18.76 68.15 ± 21.71	-26.79	**< 0.05**	30.39 ± 17.41 59.00 ± 35.94	-28.61	**< 0.05**
	SSS	101.95 ± 29.68 129.66 ± 20.43	-27.70	**< 0.05**	41.20 ± 19.66 60.68 ± 19.95	-19.48	**< 0.05**	34.16 ± 16.97 67.05 ± 31.30	-32.89	**< 0.05**
	Fast	107.76 ± 27.32 131.02 ± 21.93	-23.27	**< 0.05**	40.13 ± 18.51 61.77 ± 22.44	-21.63	**< 0.05**	36.98 ± 17.00 71.43 ± 33.11	-34.45	**< 0.05**
Pelvis/Torso	**Slow20**	28.79 ± 17.98 33.86 ± 12.13	-5.07	0.06	20.87 ± 11.83 55.40 ± 17.99	-34.54	**< 0.05**	19.13 ± 9.78 34.47 ± 28.02	-15.34	**< 0.05**
	Slow10	32.19 ± 18.09 34.20 ± 14.49	-2.00	0.45	23.04 ± 12.64 57.85 ± 19.62	-34.82	**< 0.05**	20.28 ± 9.65 38.56 ± 26.31	-18.29	**< 0.05**
	SSS	35.95 ± 18.25 32.33 ± 14.01	3.62	0.18	23.37 ± 12.35 57.35 ± 19.85	-33.98	**< 0.05**	19.34 ± 7.80 43.44 ± 24.26	-24.11	**< 0.05**
	Fast	34.94 ± 18.21 35.14 ± 18.84	-0.20	0.94	24.11 ± 11.97 53.36 ± 20.44	-29.25	**< 0.05**	23.64 ± 9.60 49.42 ± 28.05	-25.78	**< 0.05**

4.4.4 CRP variability

CRP variability repeated measures ANOVA revealed a significant three-way interaction between task, walking velocity, and segment coordination variability. Indicating that both wearing the iWalk and walking velocity significantly impacted CRP variability. Pairwise comparisons showed statistically significant differences in CRP variability for all segments in lateral bend, flexion/extension and almost all axial rotations (

CRP variability iWalk-Norm pairwise comparisons across walking velocity										
		Lateral Bend			Flexion/Extension			Axial Rotation		
	Speed	iWalk avg ± std (•) Norm avg ± std (•)	ΔEMM(°)	P-value	iWalk avg ± std (•) Norm avg ± std (•)	ΔEMM(°)	P-value	iWalk avg ± std (•) Norm avg ± std (•)	ΔEMM(°)	P-value
Torso/Upper-torso	Slow20	42.19 ± 7.96 31.23 ± 10.93	10.96	**< 0.05**	24.70 ± 10.20 36.16 ± 10.39	-11.47	**< 0.05**	19.94 ± 9.85 15.74 ± 9.85	4.19	**< 0.05**
	Slow10	40.76 ± 9.15 26.82 ± 10.74	13.94	**< 0.05**	26.09 ± 11.35 34.64 ± 12.33	-8.55	**< 0.05**	17.61 ± 9.75 18.63 ± 11.43	-1.01	0.45
	SSS	40.90 ± 9.29 23.87 ± 10.46	17.03	**< 0.05**	25.21 ± 9.80 34.49 ± 12.23	-9.27	**< 0.05**	17.07 ± 7.70 21.36 ± 12.53	-4.29	**< 0.05**
	Fast	38.76 ± 8.60 24.19 ± 11.27	14.57	**< 0.05**	24.40 ± 11.11 30.79 ± 11.22	-6.39	**< 0.05**	15.20 ± 9.08 20.23 ± 12.18	-5.03	**< 0.05**
Pelvis/Upper-torso	Slow20	42.78 ± 7.89 34.78 ± 9.08	8.00	**< 0.05**	28.20 ± 11.68 41.59 ± 7.99	-13.40	**< 0.05**	20.74 ± 8.58 24.43 ± 11.17	-3.69	**< 0.05**
	Slow10	40.71 ± 8.89 30.11 ± 8.84	10.59	**< 0.05**	28.80 ± 12.35 39.32 ± 8.03	-10.53	**< 0.05**	20.67 ± 7.94 25.75 ± 9.67	-5.08	**< 0.05**
	SSS	41.78 ± 7.89 28.49 ± 10.16	13.30	**< 0.05**	29.56 ± 11.45 39.24 ± 8.10	-9.68	**< 0.05**	21.11 ± 6.89 28.74 ± 10.92	-7.63	**< 0.05**
	Fast	39.64 ± 8.52 29.28 ± 11.41	10.36	**< 0.05**	27.57 ± 11.71 37.62 ± 9.92	-10.05	**< 0.05**	21.06 ± 7.3 28.97 ± 11.24	-7.91	**< 0.05**
Pelvis/ Torso	Slow20	25.51 ± 9.70 27.18 ± 9.60	-1.66	0.22	18.19 ± 11.46 37.62 ± 9.12	-19.42	**< 0.05**	17.22 ± 10.27 21.63 ± 12.70	-4.41	**< 0.05**

	Slow10	27.83 ± 10.95 26.85 ± 11.63	0.98	0.47	18.67 ± 10.64 39.45 ± 9.60	-20.78	**< 0.05**	17.41 ± 8.49 23.53 ± 11.90	-6.12	**< 0.05**
	SSS	28.86 ± 8.67 25.27 ± 11.32	3.59	**< 0.05**	18.74 ± 9.87 38.86 ± 9.74	-20.12	**< 0.05**	15.47 ± 6.66 26.28 ± 13.28	-10.81	**< 0.05**
	Fast	28.53 ± 10.98 27.51 ± 12.62	1.02	0.45	18.78 ± 9.95 35.97 ± 9.42	-17.19	**< 0.05**	17.25 ± 7.04 28.41 ± 13.35	-11.17	**< 0.05**

Table 3.11). The only statistically insignificant differences between iWalk and Norm CRP variability was reported for torso/upper-torso axial rotation at Slow10 (Norm EMM = 18.6º, iWalk EMM = 17.6º, ΔEMM = -1.01º). Positive estimated marginal means in lateral signify Norm tasks generally had greater CRP variability than iWalk tasks. Negative values in flexion/extension and axial rotation show that in these rotations, iWalk tasks had greater CRP variability.

CRP variability showed some walking velocity effects. In lateral bend, as walking velocity deviated from SSS, the difference in CRP variability ΔEMM between tasks decreased by approximately 3º. Overall positive ΔEMM values indicate that lateral bend CRP variability (Table **3.11**). In flexion/extension CRP variability for all segment coordination patterns decreased with increased walking velocity. A similar pattern was seen in pelvis/upper-torso and pelvis/torso axial coordination patterns. Overall negative CRP variability values for flexion/extension and axial rotation reveal that coordination pattern variability was greater during Norm tasks.

Table 3.11: CRP variability descriptive statistics and pairwise comparisons of iWalk and Norm tasks at all walking velocities for all segment coordination patterns of interest. Results showed statistically significant differences in CRP variability for all segments in lateral bend, flexion/extension and almost all axial rotations. The only statistically insignificant differences between iWalk and Norm CRP variability was reported for torso/upper-torso axial rotation at Slow10. Positive estimated marginal means in lateral signify Norm tasks generally had greater CRP variability than iWalk tasks. Negative values in flexion/extension and axial rotation show that in these rotations, iWalk tasks had greater CRP variability.

CRP variability iWalk-Norm pairwise comparisons across walking velocity										
		Lateral Bend			**Flexion/Extension**			**Axial Rotation**		
	Speed	**iWalk avg ± std (•)** **Norm avg ± std (•)**	**ΔEMM(°)**	**P-value**	**iWalk avg ± std (•)** **Norm avg ± std (•)**	**ΔEMM(°)**	**P-value**	**iWalk avg ± std (•)** **Norm avg ± std (•)**	**ΔEMM(°)**	**P-value**
Torso/Upper-torso	**Slow20**	42.19 ± 7.96 31.23 ± 10.93	10.96	**< 0.05**	24.70 ± 10.20 36.16 ± 10.39	-11.47	**< 0.05**	19.94 ± 9.85 15.74 ± 9.85	4.19	**< 0.05**
	Slow10	40.76 ± 9.15 26.82 ± 10.74	13.94	**< 0.05**	26.09 ± 11.35 34.64 ± 12.33	-8.55	**< 0.05**	17.61 ± 9.75 18.63 ± 11.43	-1.01	0.45
	SSS	40.90 ± 9.29 23.87 ± 10.46	17.03	**< 0.05**	25.21 ± 9.80 34.49 ± 12.23	-9.27	**< 0.05**	17.07 ± 7.70 21.36 ± 12.53	-4.29	**< 0.05**
	Fast	38.76 ± 8.60 24.19 ± 11.27	14.57	**< 0.05**	24.40 ± 11.11 30.79 ± 11.22	-6.39	**< 0.05**	15.20 ± 9.08 20.23 ± 12.18	-5.03	**< 0.05**
Pelvis/Upper-torso	**Slow20**	42.78 ± 7.89 34.78 ± 9.08	8.00	**< 0.05**	28.20 ± 11.68 41.59 ± 7.99	-13.40	**< 0.05**	20.74 ± 8.58 24.43 ± 11.17	-3.69	**< 0.05**
	Slow10	40.71 ± 8.89 30.11 ± 8.84	10.59	**< 0.05**	28.80 ± 12.35 39.32 ± 8.03	-10.53	**< 0.05**	20.67 ± 7.94 25.75 ± 9.67	-5.08	**< 0.05**
	SSS	41.78 ± 7.89 28.49 ± 10.16	13.30	**< 0.05**	29.56 ± 11.45 39.24 ± 8.10	-9.68	**< 0.05**	21.11 ± 6.89 28.74 ± 10.92	-7.63	**< 0.05**
	Fast	39.64 ± 8.52 29.28 ± 11.41	10.36	**< 0.05**	27.57 ± 11.71 37.62 ± 9.92	-10.05	**< 0.05**	21.06 ± 7.3 28.97 ± 11.24	-7.91	**< 0.05**
Pelvis/Torso	**Slow20**	25.51 ± 9.70 27.18 ± 9.60	-1.66	0.22	18.19 ± 11.46 37.62 ± 9.12	-19.42	**< 0.05**	17.22 ± 10.27 21.63 ± 12.70	-4.41	**< 0.05**
	Slow10	27.83 ± 10.95 26.85 ± 11.63	0.98	0.47	18.67 ± 10.64 39.45 ± 9.60	-20.78	**< 0.05**	17.41 ± 8.49 23.53 ± 11.90	-6.12	**< 0.05**
	SSS	28.86 ± 8.67 25.27 ± 11.32	3.59	**< 0.05**	18.74 ± 9.87 38.86 ± 9.74	-20.12	**< 0.05**	15.47 ± 6.66 26.28 ± 13.28	-10.81	**< 0.05**
	Fast	28.53 ± 10.98 27.51 ± 12.62	1.02	0.45	18.78 ± 9.95 35.97 ± 9.42	-17.19	**< 0.05**	17.25 ± 7.04 28.41 ± 13.35	-11.17	**< 0.05**

Table 3.12: iWalk – Norm pairwise comparisons and their resulting ΔEMM. Results for this analysis are collapsed over running velocities. A statistically significant effect of wearing the iWalk on CRP variability was found for nearly all rotations except pelvis/torso lateral bend. Overall positive ΔEMM in lateral bend CRP variability indicates that in this rotation, the iWalk tasks generally had greater coordination pattern variability. Negative ΔEMM for flexion/extension and axial rotation CRP variability indicate that the Norm tasks had greater coordination pattern variability.

CRP variability iWalk – Norm pairwise comparisons						
	Torso/Upper-torso		**Pelvis/Upper-torso**		**Pelvis/Torso**	
	ΔEMM(°)	**P-value**	**ΔEMM(°)**	**P-value**	**ΔEMM(°)**	**P-value**
Lateral Bend	14.24	**< 0.05**	10.56	**< 0.05**	0.98	0.15
Flexion/Extension	-8.92	**< 0.05**	-10.91	**< 0.05**	-19.38	**< 0.05**
Axial Rotation	1.54	**< 0.05**	-6.08	**< 0.05**	-8.13	**< 0.05**

4.4.5 Proportion of gait cycle spent out-of-phase

Repeated measures ANOVA was used to determine how walking velocity and the use of the iWalk impacted the proportion of the gait cycle spent in an out-of-phase pattern. Out-of-phase was defined as an CRP value greater than 110º. Repeated measures ANOVA analysis determined that there was a significant three-way interaction between task, walking velocity, and proportion of the gait cycle spent out-of-phase. Pairwise comparisons revealed statistically significant differences in the proportion of the gait cycle spent out-of-phase patterns at all walking velocities in lateral bend for torso/upper-torso and pelvis/upper-torso segment coordination, all segment coordination patterns for flexion/extension, and pelvis/upper-torso and pelvis/torso in axial rotation (Table 3.13). Negative iWalk-Norm ΔEMM imply that subjects spent a greater portion of the gait cycle in an out-of-phase pattern during the iWalk task than during the Norm task. In lateral bend especially, subjects saw a 20% - 30% increase in the proportion of the gait cycle spent out-of-phase when walking with the iWalk then under normal walking conditions.

A slight effect of walking velocity was also seen in the proportion of the gait cycle spent out-of-phase. In torso/upper-torso lateral bend as walking velocity increased there was a 10% increase in the proportion of the gait cycle spent out of phase. In pelvis/upper-torso flexion/extension there was a 6% increase. In pelvis/upper-torso axial rotation, there was a 6% decrease in the proportion of the gait cycle spent out-of-phase.

Table 3.13: Descriptive statistics and pairwise comparisons for iWalk and Norm tasks for proportion of the gait cycle spent out-of-phase for each coordination pattern of interest at all walking velocities. Out-of-phase was defined as CRP greater than 110º. Pairwise comparisons revealed statistically significant differences out-of-phase patterns at all walking velocities in lateral bend for torso/upper-torso and pelvis/upper-torso segment coordination, all segment coordination patterns for flexion/extension, and pelvis/upper-torso and pelvis/torso in axial rotation. Negative iWalk-Norm difference in estimated marginal means imply that subjects spent a greater portion of the gait cycle in an out-of-phase pattern during the iWalk task than during the Norm task. In lateral bend especially, subjects saw a 20% - 30% increase in the proportion of the gait cycle spent out-of-phase when walking with the iWalk then under normal walking conditions. A slight effect of walking velocity was also seen in the proportion of the gait cycle spent out-of-phase. In torso/upper-torso lateral bend as walking velocity increased there was a 10% increase in the proportion of the gait cycle spent out of phase. In pelvis/upper-torso flexion/extension there was a 6% increase. In pelvis/upper-torso axial rotation, there was a 6% decrease in the proportion of the gait cycle spent out-of-phase.

Proportion of the gait cycle spent-out-of-phase										
		Lateral Bend			**Flexion/Extension**			**Axial Rotation**		
	Speed	**iWalk avg ± std** **Norm avg ± std**	**ΔEMM**	**P-value**	**iWalk avg ± std** **Norm avg ± std**	**ΔEMM**	**P-value**	**iWalk avg ± std** **Norm avg ± std**	**ΔEMM**	**P-value**
Torso/Upper-torso	**Slow 20**	0.42 ± 0.24 0.74 ± 0.23	-0.32	**< 0.05**	0.05 ± 0.07 0.12 ± 0.10	-0.07	**< 0.05**	0.03 ± 0.04 0.03 ± 0.09	0.00	0.83
	Slow10	0.49 ± 0.25 0.80 ± 0.21	-0.31	**< 0.05**	0.06 ± 0.07 0.12 ± 0.10	-0.06	**< 0.05**	0.02 ± 0.04 0.05 ± 0.12	-0.03	0.15
	SSS	0.56 ± 0.22 0.80 ± 0.21	-0.24	**< 0.05**	0.05 ± 0.05 0.11 ± 0.09	-0.05	**< 0.05**	0.01 ± 0.03 0.05 ± 0.13	-0.04	**< 0.05**
	Fast	0.59 ± 0.21 0.80 ± 0.24	-0.20	**< 0.05**	0.06 ± 0.06 0.11 ± 0.12	-0.06	**< 0.05**	0.01 ± 0.03 0.06 ± 0.14	-0.04	**< 0.05**
Pelvis/Upper-torso	**Slow20**	0.37 ± 0.23 0.61 ± 0.24	-0.24	**< 0.05**	0.07 ± 0.09 0.23 ± 0.14	-0.16	**< 0.05**	0.03 ± 0.06 0.13 ± 0.22	-0.10	**< 0.05**
	Slow10	0.44 ± 0.25 0.70 ± 0.21	-0.25	**< 0.05**	0.09 ± 0.10 0.21 ± 0.14	-0.12	**< 0.05**	0.03 ± 0.07 0.15 ± 0.23	-0.12	**< 0.05**
	SSS	0.50 ± 0.24 0.76 ± 0.20	-0.26	**< 0.05**	0.09 ± 0.09 0.17 ± 0.11	-0.09	**< 0.05**	0.03 ± 0.05 0.17 ± 0.21	-0.14	**< 0.05**
	Fast	0.54 ± 0.23 0.76 ± 0.21	-0.22	**< 0.05**	0.08 ± 0.08 0.18 ± 0.12	-0.10	**< 0.05**	0.03 ± 0.07 0.19 ± 0.22	-0.16	**< 0.05**
Pelvis/Torso	**Slow20**	0.05 ± 0.09 0.05 ± 0.06	0.00	0.93	0.03 ± 0.04 0.14 ± 0.11	-0.11	**< 0.05**	0.02 ± 0.04 0.08 ± 0.15	-0.05	**< 0.05**
	Slow10	0.06 ± 0.10 0.06 ± 0.09	0.00	1.00	0.03 ± 0.05 0.15 ± 0.11	-0.12	**< 0.05**	0.02 ± 0.03 0.07 ± 0.12	-0.05	**< 0.05**
	SSS	0.07 ± 0.10 0.07 ± 0.08	0.00	0.90	0.03 ± 0.04 0.14 ± 0.11	-0.11	**< 0.05**	0.01 ± 0.01 0.08 ± 0.11	-0.07	**< 0.05**
	Fast	0.07 ± 0.09 0.08 ± 0.10	-0.01	0.57	0.03 ± 0.04 0.13 ± 0.11	-0.09	**< 0.05**	0.01 ± 0.02 0.11 ± 0.13	-0.09	**< 0.05**

4.5 Discussion

In this study, the iWalk 2.0 was used to mimic unilateral knee disarticulation. This allowed for a standardized comparison of gait, segment rotation and coordination with and without the iWalk which may translate into understanding adaptations LLAs make early in their prosthetic use. In addition, it minimized variability due to changes in lower-limb structure and musculature, varying prostheses, and underlying disease/injury, and other comorbidities. While in this study there was no comparison amputee population, there is other literature that these results can be compared to.

Other studies that have evaluated the effects of LLA on gait parameters have found that LLAs generally have slower walking velocities than controls [6–8,24–27]. Transfemoral amputees (TFAs) are more likely to show gait asymmetries such as increased stride lengths and stance times on the intact side [6,8,25]. In this study, during iWalk tasks, subjects showed significant decreases in stance time on the intact side (the side on which the iWalk was not worn). While TFA also present with shorter stride lengths for prosthetic side strides than on intact side strides, there were no intact/amputated side stride length asymmetries in this study as seen in studies by Burkett, Hof and others [7,8,25–27]. Subjects in this study may not have exhibited stride length asymmetry due to having intact hip abductor musculature. A study by Nadolleck and colleagues found that stronger hip abductor musculature was correlated with faster walking velocities, longer step lengths and stride lengths and smaller swing and stance time ratios [7]. Hip abductor weakness is common in transtibial amputees and atrophy is common TFAs [7]. However, there were significant differences between amputated and intact sides in stance times.

Analysis of rotational amplitudes showed a statistically significant effect of wearing the iWalk on upper-torso, torso, pelvis, and hip rotations. Positive ΔEMM indicate subjects generally had greater rotational amplitudes under Norm tasks than during iWalk tasks. Other authors have also found statistically higher range of motion in LLAs particularly in pelvic anterior/posterior tilt and obliquity [6]. While rotational amplitude differences between tasks were statistically significant, the difference in ΔEMM between iWalk and Norm tasks below 5º. While these results are statistically significant, the clinical significance of these results is questionable.

Results from mean CRP analysis exposed significant effects of both walking velocity and task. Negative differences in ΔEMM indicate that for the iWalk task CRP mean was significantly less than for the Norm task. This was particularly apparent in torso/upper-torso and pelvis/upper-torso lateral bend, pelvis/upper-torso flexion/extension, and pelvis/upper-torso and pelvis/torso CRP mean ΔEMM which were almost all greater than 20º. Lower CRP mean indicates a less out-of-phase coordination pattern between the segments analyzed. Seay and colleagues have reported such differences between controls, and those with LBP or a history of LBP [12]. More specifically, Seay reported decreased CRP mean in the frontal plane (lateral bend rotations) than in other rotations. A similar pattern was identified in this study particularly at slower walking velocities. For instance, for torso/upper-torso lateral coordination patterns, CRP mean ΔEMM ranged from approximately -25º to -30º ($p < 0.05$) from fastest walking velocity to slowest. This indicates that during iWalk tasks, subjects adopted a more in-phase torso/upper-torso lateral coordination pattern. For the same segments CRP mean ΔEMM in axial rotation ranged from -10º ($p < 0.05$) to 1.75º ($p = 0.51$) across walking velocities. Pelvis/upper-torso lateral bend and axial coordination patterns seemed to be equally impacted by task. However, pelvis/torso

coordination patterns showed an opposing pattern where lateral bend coordination were less impacted than axial coordination. However, results from pelvis/torso lateral bend coordination did not reach statistical significance.

CRP mean also shows an impact of walking velocity. In torso/upper-torso lateral coordination, as walking velocity increases, there is an accompanying increase CRP mean ΔEMM from approximately -38º to -25º. A similar pattern was identified in torso/upper-torso lateral bend, pelvis/upper-torso lateral bend and flexion/extension, and pelvis/torso flexion/extension. This aligns with other studies which have reported walking velocity effects on trunk and pelvis coordination patterns [12,13,16]. Interestingly, there were increases in axial coordination CRP mean for pelvis/torso and pelvis/upper-torso segments. To the author's knowledge such results have not been reported in other studies.

To the author's knowledge there has only been one study which evaluated relative phasing between spinal segments in LLAs [6]. Goujon-Pillet et al. reported significant changes in pelvis-thorax coordination particularly in the transverse plane in TFAs. On average, they saw a 30º decrease in pelvis-thorax CRP mean in TFAs when compared to controls. This is in-line with results from this study where iWalk-Norm CRP mean ΔEMM of transverse plane coordination patterns ranged from -15º to -35º for coordination patterns that involved the pelvis. Significant differences in coordination patterns between controls and TFAs were not reported for frontal (lateral bend) and sagittal (flexion/extension) and therefore results could not be compared.

Statistically significant differences between tasks at all walking velocities were seen in CRP variability in almost all segments. All segments in lateral bend show positive CRP variability ΔEMM indicate that Norm tasks generally have higher CRP variability in lateral bend

than iWalk tasks. This trend is reversed for flexion/extension and axial rotation where subjects had greater CRP variability during the iWalk task than during the Norm task. In LBP populations, there is generally a decrease in CRP variability. It is hypothesized that those with LBP or a history of LBP decrease CRP variability and adopt a more guarded gait pattern to avoid counterrotations between segments and therefore decrease the likelihood of developing future pain [12,13,15,17]. Increases in flexion/extension and axial rotation coordination variability are not unexpected for this population. Subjects may have increased variability to adjust for the inability to use the knee to clear the iWalk during amputated side swing. Results indicate that to clear the iWalk swing limb, subjects tilted forward and had more transverse (axial) rotations. However, increases in CRP variability were accompanied by decreases in CRP mean, indicating that there was no increase in counterrotation between these segments.

Van Emmerik and colleagues as well as others have reported some velocity effects on CRP variability [12,13,16]. Mainly, that at walking velocities closer to preferred, CRP variability is high and decreases at walking velocities further from preferred. This pattern was observed in lateral bend CRP variability where CRP variability at SSS was higher than at both Slow20 and Fast walking velocities. In axial coordination patterns for all segments as walking velocity increased there was an accompanying decrease in CRP variability. This phenomenon may have been driven primarily by the added challenge of walking at higher velocities with the iWalk.

Whether wearing the iWalk impacts the proportion of the gait cycle was also calculated because such a measure is more descriptive than CRP mean. Some authors assume that increases in CRP mean indicate a transition from an in-phase coordination pattern to an out-of-phase coordination pattern [12,13,15–17]. However, that may not always be the case. In addition, clinical implications for CRP mean are difficult to determine. Proportion of the gait cycle spent

out-of-phase may have more diagnostic weight and give clearer targets for therapeutic interventions. Overall, there were statistically significant differences in proportion of the gait cycle spent out-of-phase between iWalk and Norm tasks for nearly all segments at most walking velocities. Negative differences in ΔEMM indicate that during iWalk tasks subjects spent a smaller proportion of the gait cycle out-of-phase than during Norm tasks. Combined with results from CRP mean, this indicates that during the iWalk tasks subjects maintained a more in-phase coordination pattern.

4.6 Conclusions

Overall, results from this study are well aligned with others that evaluate the effects of LLA or LBP on gait. While stride length results from this study do not align with other studies that evaluate the effects TFA on these measures, results here can easily be explained by the presence of intact hip abductor musculature. Other authors have reported that strong hip abductor musculature in LLAs can greatly impact gait parameters and significantly reduce gait asymmetries [7].

While the population studied here was not a true amputee population, using the iWalk to mimic amputation in a healthy control population can provide insight into early adaptations to prosthetic use. To the author's knowledge a study conducted by Goujon-Pillet is the only one to evaluate pelvis-trunk coordination in LLAs [6]. While their study only evaluated transverse plane (axial rotation) coordination patterns, the results from this study are well aligned with theirs. Overall, amputees/iWalk adopt a more-in-phase coordination pattern than their healthy controls or during Norm tasks.

This study also introduced a new measure: proportion of the gait cycle spent out-of-phase. This measure was chosen because it is more descriptive than CRP mean and CRP

variability and can give insight into motor control changes. In addition, it is a potential diagnostic tool and physical therapy target. Patients who show significant decreases in proportion of the gait cycle spent out-of-phase may be adopting a guarded gait pattern which could increase their likelihood of musculoskeletal or low-back injury. Teaching patients how to decouple these movements and maintain a healthy out-of-phase pattern may decrease the likelihood of injury. Further studies using amputee populations will need to be conducted to verify these findings and determine whether using the iWalk 2.0 to mimic knee disarticulation is valid.

4.7 References

[1] C.S. Molina, J. Faulk, Lower Extremity Amputation, in: StatPearls, StatPearls Publishing, Treasure Island (FL), 2021. http://www.ncbi.nlm.nih.gov/books/NBK546594/ (accessed November 13, 2021).

[2] P.L. Ephraim, S.T. Wegener, E.J. MacKenzie, T.R. Dillingham, L.E. Pezzin, Phantom Pain, Residual Limb Pain, and Back Pain in Amputees: Results of a National Survey, Archives of Physical Medicine and Rehabilitation. 86 (2005) 1910–1919. https://doi.org/10.1016/j.apmr.2005.03.031.

[3] D.M. Ehde, D.G. Smith, J.M. Czerniecki, K.M. Campbell, D.M. Malchow, L.R. Robinson, Back pain as a secondary disability in persons with lower limb amputations, Archives of Physical Medicine and Rehabilitation. 82 (2001) 731–734. https://doi.org/10.1053/apmr.2001.21962.

[4] L. Vogt, K. Pfeifer, M. Portscher, W. Banzer, Influences of Nonspecific Low Back Pain on Three- Dimensional Lumbar Spine Kinematics in Locomotion, Spine. 26 (2001) 1910–1919.

[5] Y. Barzilay, B.S. Lonner, B. Amit Mor, B. Avi Elbaz, Patients with chronic non-specific low back pain who reported reduction in pain and improvement in function also demonstrated an improvement in gait pattern, European Spine Journal. 25 (2015) 2761–2766. https://doi.org/10.1007/s00586-015-4004-0.

[6] H. Goujon-Pillet, E. Sapin, P. Fodé, F. Lavaste, Three-Dimensional Motions of Trunk and Pelvis During Transfemoral Amputee Gait, Archives of Physical Medicine and Rehabilitation. 89 (2008) 87–94. https://doi.org/10.1016/j.apmr.2007.08.136.

[7] H. Nadollek, S. Brauer, R. Isles, Outcomes after trans-tibial amputation: the relationship between quiet stance ability, strength of hip abductor muscles and gait, Physiotherapy Research International. 7 (2002) 203. https://doi.org/10.1002/pri.260.

[8] S.M.H.J. Jaegers, Prosthetic gait of unilateral transfemoral amputees: A kinematic study, Archives of Physical Medicine and Rehabilitation. 76 (1995) 736–743. https://doi.org/10.1016/S0003-9993(95)80528-1.

[9] Y. Sagawa Jr, K. Turcot, S. Armand, A. Thevenon, N. Vuillerme, E. Watelain, Biomechanics and physiological parameters during gait in lower-limb amputees: A systematic review, Gait & Posture. 33 (2011) 511–526. https://doi.org/10.1016/j.gaitpost.2011.02.003.

[10] C. Sjödahl, G.-B. Jarnlo, B. Söderberg, B.M. Persson, Pelvic motion in trans-femoral amputees in the frontal and transverse plane before and after special gait re-education, Prosthetics and Orthotics International. 27 (2003) 227–237. https://doi.org/10.1080/03093640308726686.

[11] N.F. Taylor, O.M. Evans, P.A. Goldie, The effect of walking faster on people with acute low back pain, European Spine Journal. 12 (2003) 166–172. https://doi.org/10.1007/s00586-002-0498-3.

[12] J.F. Seay, R.E.A. Van Emmerik, J. Hamill, Low back pain status affects pelvis-trunk coordination and variability during walking and running, Clinical Biomechanics. 26 (2011) 572–578. https://doi.org/10.1016/j.clinbiomech.2010.11.012.

[13] J.F. Seay, Influence of Low Back Pain Status on Pelvis-Trunk Coordination During Walking and Running, Spine (Philadelphia, Pa. 1976). 36 (2011) E1070–E1079. https://doi.org/10.1097/BRS.0b013e3182015f7c.

[14] J.F. Seay, R.E.A. Van Emmerik, J. Hamill, Trunk bend and twist coordination is affected by low back pain status during running, European Journal of Sport Science. 14 (2014) 563–568. https://doi.org/10.1080/17461391.2013.866167.
[15] C.J.C. Lamoth, Pelvis-Thorax Coordination in the Transverse Plane During Walking in Persons With Nonspecific Low Back Pain, Spine (Philadelphia, Pa. 1976). 27 (2002) E92–E99. https://doi.org/10.1097/00007632-200202150-00016.
[16] R.E.A. van Emmerik, R.C. Wagenaar, Effects of walking velocity on relative phase dynamics in the trunk in human walking, Journal of Biomechanics. 29 (1996) 1175–1184. https://doi.org/10.1016/0021-9290(95)00128-X.
[17] C.J.C. Lamoth, P.J. Beek, O.G. Meijer, Pelvis–thorax coordination in the transverse plane during gait, Gait & Posture. 16 (2002) 101–114. https://doi.org/10.1016/S0966-6362(01)00146-1.
[18] M.P. Kadaba, H.K. Ramakrishnan, M.E. Wootten, Measurement of lower extremity kinematics during level walking, Journal of Orthopaedic Research. 8 (1990) 383–392. https://doi.org/10.1002/jor.1100080310.
[19] D. Winter, Biomechanics and motor control of human movement, Fourth, John Wiley & Sons Inc, Hoboken, 2009.
[20] R. Needham, R. Naemi, N. Chockalingam, Quantifying lumbar-pelvis coordination during gait using a modified vector coding technique, Journal of Biomechanics. 47 (2014) 1020–1026. https://doi.org/10.1016/j.jbiomech.2013.12.032.
[21] J.A. Smith, K. Kulig, Trunk-pelvis coordination during turning: A cross sectional study of young adults with and without a history of low back pain, Clinical Biomechanics. 36 (2016) 58–64. https://doi.org/10.1016/j.clinbiomech.2016.05.011.
[22] R. Needham, N. Chockalingam, R. Naemi, T. Shannon, A. Healy, Validation of a multi-segment spinal model for kinematic analysis and a comparison of different data processing techniques, Stud Health Technol Inform. 176 (2012) 151–154.
[23] J. Hamill, R.E.A. van Emmerik, B.C. Heiderscheit, L. Li, A dynamical systems approach to lower extremity running injuries, Clinical Biomechanics. 14 (1999) 297–308. https://doi.org/10.1016/S0268-0033(98)90092-4.
[24] B.S. Baum, B.L. Schnall, J.E. Tis, J.S. Lipton, Correlation of residual limb length and gait parameters in amputees, Injury. 39 (2008) 728–733. https://doi.org/10.1016/j.injury.2007.11.021.
[25] A.L. Hof, EMG and muscle force: An introduction, Human Movement Science. 3 (1984) 119–153. https://doi.org/10.1016/0167-9457(84)90008-3.
[26] L. Nolan, A. Lees, The functional demands on the intact limb during walking for active transfemoral and transtibial amputees, Prosthet Orthot Int. 24 (2000) 117–125. https://doi.org/10.1080/03093640008726534.
[27] L. Nolan, A. Wit, K. Dudziñski, A. Lees, M. Lake, M. Wychowañski, Adjustments in gait symmetry with walking speed in trans-femoral and trans-tibial amputees, Gait & Posture. 17 (2003) 142–151. https://doi.org/10.1016/S0966-6362(02)00066-8.

Chapter 5 A comparison of continuous methods for relative phase analysis

5.1 Abstract

The three most common continuous methods for calculating coordination patterns between segments: Continuous Relative Phase (CRP), Continuous Relative Phase using the Hilbert Transform (CRP_{HT}) and Relative Fourier Phase (RFP). How each method's underlying assumptions impact relative phase interpretation remains unknown. The aims of this study were to 1) provide a complete comparison of these methods using computer generated and human movement data. 2) Outline calculation methods. 3) Specify best practices for each method. To address these aims three sets of sinusoidal signals were created. *Scenario 1:* three sinusoidal signals of the same frequency with phase shifts of 0º, 18º, and 126º. *Scenario 2:* two sinusoidal signals of different frequencies. *Scenario 3:* three non-sinusoidal signals with phase shifts of 0º, 18º, and 126º. In addition, rectangular, Hanning, and Hamming windows were compared when analyzing signals using RFP. All method estimated the phase shifts of signals from *Scenario 1* and *Scenario 2* accurately. CRP_{HT} had the greatest standard deviation, while CRP had the lowest. For *Scenario 3* the average signal for each method was approximately equal to the phase shift of the signal. When analyzing upper-torso, torso, and pelvic coordination patterns RFP returned a higher-than-average relative phase and standard deviation than both CRP and CRP_{HT}. CRP and CRP_{HT} are recommended when analyzing overground gait trials or tasks where a single cycle of a movement will be analyzed. RFP is recommended for treadmill gait tasks, or tasks where multiple cycles are collected. Lastly, the Hamming window is recommended when using RFP for analysis.

5.2 Background

Relative phase in biomechanics is often used to describe inter-joint, intra-joint, or segment coordination during tasks that have a repetitive motion such as walking, running, lifting, or balance [1–18]. Coordination patterns between segments are of interest because changes to coordination patterns and their variability may lend insight into the development of various musculoskeletal pathologies. Authors that have evaluated variability during postural sway and coordination patterns during gait tasks often do so as a proxy for stability and interpret the results as a subject's ability or inability to adjust to perturbations that require increasing or decreasing walking velocity [19,20]. Studies conducted by van Emmerik and colleagues have found at walking velocities that deviate from comfortable there is an increase the thorax-pelvis relative phase variability of healthy controls. That is, as walking velocity changes there is a decrease in stability. In addition pelvis-thorax coordination transitions from an in-phase pattern where the pelvis and thorax are rotating together at similar frequencies to an out-of-phase pattern where there is counterrotation between the segments [17]. Studies that evaluate relative phase in those with low-back pain (LBP) have found that this transition from an in-phase pattern to an out-of-phase pattern is often delayed or non-existent [6,13,14,20,21]. This is also often accompanied by decreases in variability indicating those with LBP adopt a more stable pattern which may be overly rigid because it does not allow for this transition.

To the author's knowledge there are four common methods that appear in the literature for calculating relative phasing between segments. These are, discrete relative phase (DRP), continuous relative Fourier phase analysis (RFP), continuous relative phase analysis also known as portrait analysis (CRP), and continuous relative phase using the Hilbert Transform (CRP_{HT}). Of these, DRP is discrete while the rest are continuous. Relative phase analysis involves taking

the difference of the phase angles of the signals of interest. CRP, CRP_{HT}, and RFP begin with angular position but go about obtaining phase angles (ϕ) in different ways. CRP as described by Hamill obtains phase angles from the arctangent of the position and velocity signals. ϕ_{CRP_HT} is calculated from the imaginary and analytical signals of the Hilbert transformed signal. Lastly, ϕ_{RFP} is calculated from the windowed short-time Fourier transform of the angular position at the fundamental frequency of the signal.

A comprehensive comparison of DRP and CRP has been carried out by Peters and Haddad, while Kurz and Stergiou compare phase-plane normalization methods [22,23]. Lamb and Stöckl provided an equally robust comparison of CRP and CRP_{HT} [5]. Using methods outlined by Peters and Haddad, they were able to show how that CRP_{HT} performs better than CRP regardless of normalization technique particularly when evaluating non-sinusoidal signals. RFP is an analysis method that was preferred by Lamoth and colleagues as well as Li and Kakar [6–8,24]. Li and Kakar, and Lamb and Stöckl provide the most complete outline for coordination pattern calculations using RFP and CRP_{HT} respectively. Analysis of computer generated sinusoidal and non-sinusoidal signals using RFP has yet to be carried out. In addition, while Lamb and Stöckl, and Li and Kakar provide the most thorough outline of these analysis methods, they omit details critical for replication. Therefore, the aim of this study is three-fold. Firstly, to provide a complete comparison of CRP, CRP_{HT}, and RFP using sinusoidal and non-sinusoidal signals with known phase shifts using a protocol similar to that used by Lamb and Stöckl and Peters and Haddad [5,22]. In addition, relative phasing of the upper-torso, torso, and pelvis a subject will be assessed using each of these methods to showcase the real-world implications of these analyses. Secondly, this paper will provide a detailed outline for calculating coordination patterns using each of these methods. Lastly, this paper will also specify best practices for each

method based on analysis of computer generated signals, human movement data, and from the literature.

In recent years, coordination patterns have come to the fore as a potentially sensitive measure for identifying changes to pelvic and torso rotations in those with and without LBP and a history of LBP [6,13,14,25]. Persistent coordination pattern adaptations found in those with LBP could explain the recurrent nature of LBP. CRP and RFP have been used successfully to identify changes in coordination in those with and without LBP at varying walking velocities [6,13,14,20,25]. While CRP has proven to be sensitive to a history of LBP, the use of this method and interpretation of results is often challenged by the need for normalization [3,13,14,22,23]. Conducting a systematic evaluation of these methods within the same context will give researchers much-needed guidance for choosing the proper method for analysis given the type of data they wish to analyze, present their strengths, weaknesses, and limitations clearly, and inform the interpretation of results using each method.

5.3 Methods

5.3.1 Computer generated signals

All analysis was carried out in MATLAB (MathWorks, Natick, MA). To conduct a thorough analysis of continuous methods for calculating relative phase, sinusoidal and non-sinusoidal signals of known phase shift which were mathematically described as:

$$x(t) = \sin(\omega\pi t + \psi)$$

Equation 3.9

Where $\omega\pi$ is the frequency, and ψ denotes the phase shift along the x-axis at a resolution of 4,000 data points.

Sinusoidal Signals: In the first scenario, the effects of a phase shift were tested using three sinusoidal signals of the same frequency:

$$x_1(t) = sin(3\pi t) \qquad \text{for } t \in [0,2\pi]$$

Equation 3.10

$$x_2(t) = sin(3\pi t - 18°) \qquad \text{for } t \in [0,2\pi]$$

Equation 3.11

$$x_3(t) = sin(3\pi t - 126°) \qquad \text{for } t \in [0,2\pi]$$

Equation 3.12

X_1 was then compared to x_2 and x_3. These signals have the same fundamental frequency but have a phase shift of 18º or 126º respectively (Figure 5.1a-b). In the second scenario, the effects of two signals of different frequencies were tested. These signals were created using Equation 3.13 andEquation 3.14

$$x_4(t) = sin(3\pi t) \text{ for } t \in [0,2\pi]$$

Equation 3.13

$$x_5(t) = sin(4\pi t) \text{ for } t \in [0,2\pi]$$

Equation 3.14

Non-sinusoidal signals: For the third scenario, the effects of non-sinusoidal signals were tested. The signals had the following equations (Figure 5.1d-e):

$$x_6(t) = \frac{cos(3\pi t - 0.25\pi)}{\sqrt{1 + 0.4148^2 - 2 \times 0.4148\, sin(3\pi t - 0.25\pi)}}$$

Equation 3.15

$$x_7(t) = \frac{cos(3\pi t - 0.25\pi)}{\sqrt{1 + 0.4148^2 \; - \; 2 \; \times \; 0.4148 \, sin(3\pi t - 0.25\pi - 126°)}}$$

Equation 3.16

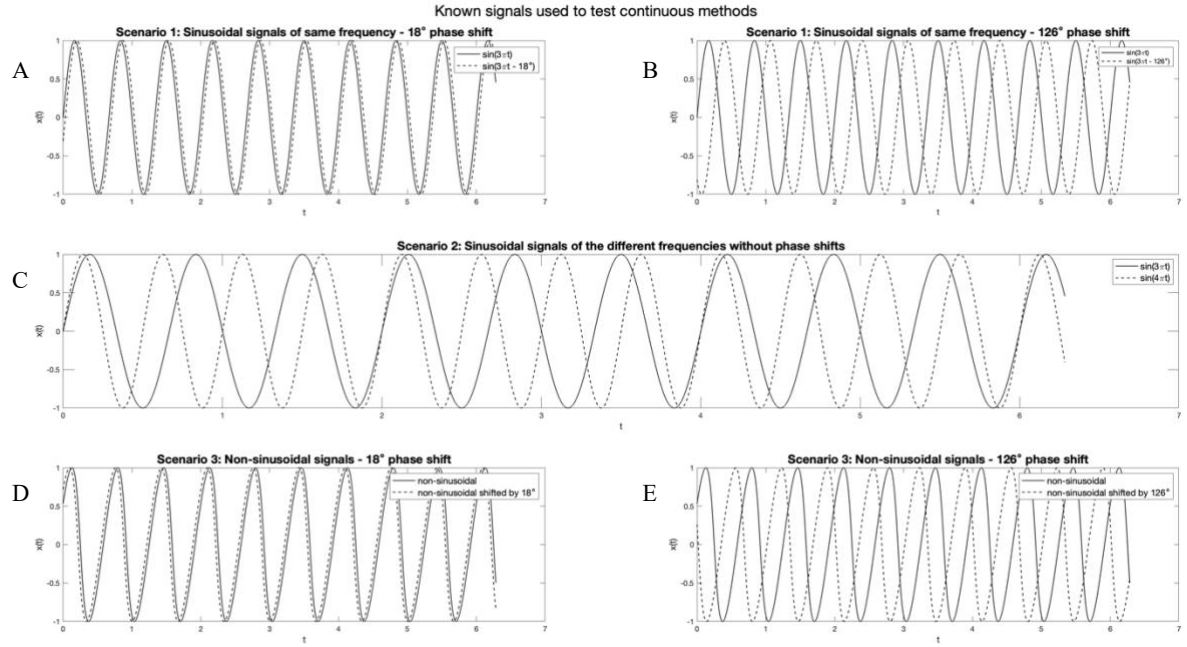

Figure 3.6: A-B) Computer generated signals for *scenario 1:* sinusoidal signals of the same frequency with phase shifts of A) sinusoidal signal of $x_1(t) = \sin(3\pi t)$ (solid) and $x_2(t) = \sin(3\pi t - 18°)$ (dashed). B) A sinusoidal signal of $x_1(t) = \sin(3\pi t)$ (solid) and $\sin(3\pi t - 126°)$ (dashed). C) Sinusoidal signals for *scenario 2*: sinusoidal signals of different frequencies. $x_4(t) = \sin(2\pi t)$ (solid) and $x_5(t) = \sin(3\pi t)$ (dashed). D-E); Non-sinusoidal signals for *scenario 3*: D) $x_6(t) = \frac{\cos(3\pi t - 0.25\pi)}{\sqrt{1+0.4148^2 - 2 \times 0.4148 \sin(\pi 3t - 0.25\pi)}}$ (solid) with a phase shift of 18º (dashed) and E) with a phase shift of 126º (dashed)

5.3.2 Continuous Relative Phase (CRP)

The datapoints for each original vector were taken to reflect angular position ($x(t_i) = \theta$). Angular velocity was obtained by taking the first derivative of the angular position using the central difference method ($\dot{x}(t_i) = \omega$). Angular position and angular velocity were then normalized according to a protocol established by Hamill using Equation 3.17 and Equation 3.18 [4]. The goal of the normalization was to obtain a circular position-velocity phase plane graph for the vectors of sinusoidal signals. Vectors of non-sinusoidal signals present with distortion in the position-velocity phase plane graphs. Phase angles for each signal were calculated as the

arctangent of the angular velocity and angular position according to Equation 3.19. CRP was then calculated as the difference between original and shifted vector phase angles using

$$\theta_i = \frac{2*[\theta_i - \min(\theta_i))}{\max(\theta_i) - \min\theta_i}$$

Equation 3.17

$$\omega_i = \frac{\omega_i}{\max|\omega_i|}$$

Equation 3.18

$$\phi_i = arctan\left(\frac{\omega_i}{\theta_i}\right)$$

Equation 3.19

$$CRP_{ref-shift} = |\varphi_{shift} - \varphi_{ref}|$$

Equation 3.20

5.3.3 Continuous Relative Phase using the Hilbert Transform (CRP_{HT})

All methods used to calculate coordination patterns require the calculation of phase angles. In the CRP method described previously, phase angles are calculated from the original vector and it's first derivative. To obtain phase angles using CRP_{HT} first the measured vector $x(t_i)$ must undergo convolution using the Hilbert Transform. This transform acts as a filter maintaining the amplitudes and spectral components of the original vector but shifting the phase by $-\pi/2$ [26].

Recall that the Hilbert Transform can be used in two ways. First, to analyze complex signals in the time domain by providing frequency, phase, and amplitude. Second, for signal analysis in the frequency domain. This latter method is the way in which the Hilbert Transform

is being used here. Once $x(t_i)$ undergoes convolution by the Hilbert Transform, the analytic signal is obtained ($X(t_i)$) which consists of the original signal (real portion $x(t_i)$) and its Hilbert Transform conjugation (imaginary part $\tilde{x}(t_i)$). The phase angle is therefore obtained by taking the arctangent of the real and imaginary portions according to Equation 3.21.

$$\phi(t_i) = tan^{-1}\frac{\tilde{x}(t_i)}{x(t_i)}$$

Equation 3.21

5.3.4 Relative Fourier Phase Analysis (RFP)

The RFP methodology described below follows the outline by Li and Lamoth, with adjustments for analyzing overground walking trials [6,24,27]. First, the power spectrum densities (PSD) for each vector were obtained using a discrete Fourier transform using a Hanning window. This window type was chosen because studies by Lamoth and Li both show that human data has frequency signals that are well separated, and the Hanning window is the most ubiquitous window type [6,24,27]. One drawback of this window type is that it tends to overestimate amplitudes. However, this is not of concern because amplitude in this case is only used to identify the fundamental frequency of the signal. From the PSD, the fundamental frequency (f_1) was identified as the frequency with the highest amplitude. The first five harmonics were also calculated as multiples of the fundamental frequency (i.e.: $f_4 = 4f_1$).

For each signal, the Fourier phase angle (ϕ_{RFP}) was calculated using a windowed short-time discrete Fourier transform with rectangular, Hanning, and Hamming windows to compare them. A window length equivalent to stride length was used. A stride was measured form heel strike to heel strike of the right side. According to Li, the short-time discrete Fourier transform is used because it detects time-dependent changes at the frequencies of interest and filters out the effects of higher harmonics [24]. The windowed phase angles for each signal were then

converted into a continuous time series, by extracting the short-time Fourier transform at the fundamental frequency. This vector was then converted into angles using the built-in angle function in MATLAB.

Relative Phase calculations: After phase angles (ϕ) was calculated using each method, relative phase for each signal was calculated using Equation 3.22.

$$\text{RP} = |\phi_{original}(t) - \phi_{shifted}(t)|$$

Equation 3.22

RP was then calculated as (**Error! Reference source not found.**). This eliminated the need to use circular statistics to measure RP mean and variability. Therefore, linear methods were used to calculate RP descriptive statistics.

A

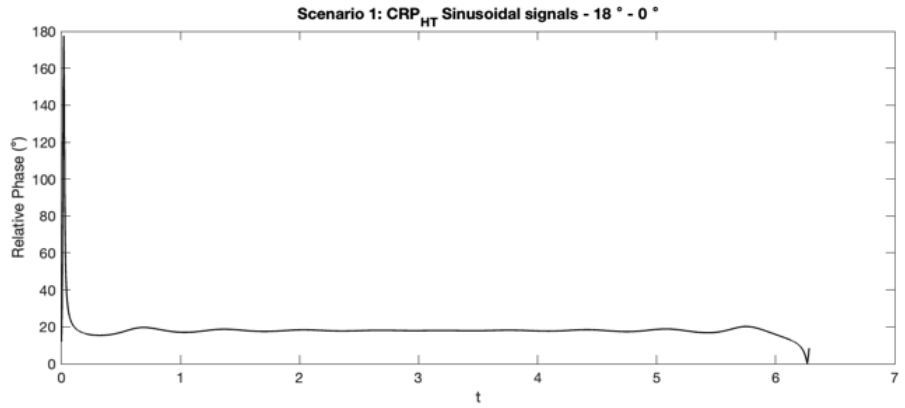

B

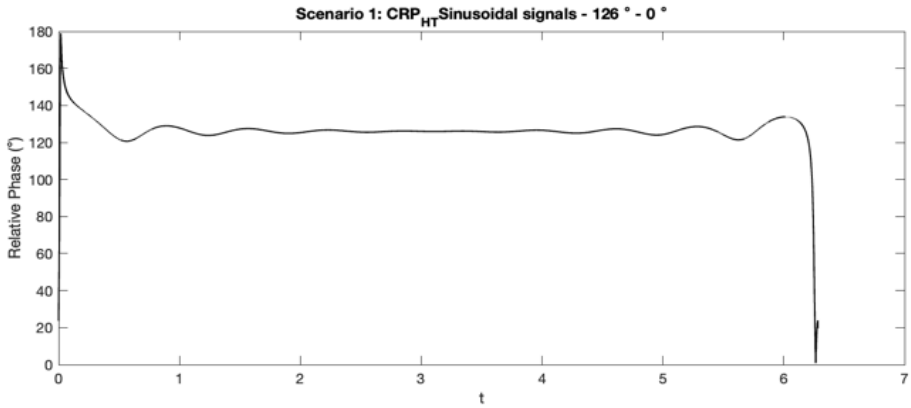

Figure 3.7: Sinusoidal signals with phase shifts of 18º (a) and 126º (b) degrees respectively calculated using CRP_{HT}. Overestimation of the relative phase shifts at the beginning and end of the signal likely contribute to the higher standard deviations.

5.4 Results

5.4.1 Analysis of computer-generated signals

As stated previously, sinusoidal signals of known frequency and phase shift were created to accurately compare the effect of each relative phase analysis methodology (

	S1: phase = 18º	**S1: phase = 126º**	**S2**	**S3: phase = 18dº**	**S3: phase = 126º**
CRP mean	18.000 ± 0.002	126.000 ± 0.004	87.077 ± 52.615	18.072 ± 9.138	126.944 ± 27.142
CRP_{HT} means	18.187 ± 7.325	126.091 ± 9.789	87.627 ± 52.769	18.133 ± 5.042	126.686 ± 17.819
RFP (rect) mean	18.000 ± 0.009	126.000 ± 0.024	93.763 ± 51.314	18.000 ± 0.013	125.999 ± 0.036

RFP (hann) mean	18.000 ± 0.023	126.001 ± 0.060	93.762 ± 51.316	17.956 ± 1.297	125.615 ± 7.384
RFP (hamm) mean	18.000 ± 0.018	126.000 ± 0.047	93.762 ± 51.316	17.963 ± 1.104	125.672 ± 6.290

Table 3.14). In scenario 1 (S1), three sinusoidal signals of the same frequency and phase shifts of 0º, 18º and 126º were created. Signals with phase shifts of 18º and 126º were compared to 0º phase shift signal. For the second scenario (S2), the relative phase of two signals with different frequencies were calculated. In scenario 3, non-sinusoidal signals with phase shifts of 18º and 126º were compared to a non- sinusoidal signal with a 0º phase shift (S3).

All methods estimate relative phasing between sinusoidal signals accurately. However, CRP_{HT} had the highest standard deviations for sinusoidal signals, and second highest for non-sinusoidal signals behind CRP. However, this is likely due to overestimation of the relative phase at the beginning and the end of the signals (Figure 5.2). RFP using different window types showed no differences in the average or standard deviation of the relative phase. For sinusoidal signals of different frequencies (S2), each method approximates a phase shift between 87º and 93º. CRP and CP_{HT} have similar relative phase and standard deviation estimates, while RFP with different window sizes also all have similar values. The standard deviation is high for these calculations because of the natural rise and fall in the relative phase signal (Figure 5.3). For the non-sinusoidal signals (S3), all methods on average estimated the phase shifts between the signals accurately. RFP using the rectangular window showed had the least amount of variation (SD: 0.036º), while CRP had the highest (SD: 27.14º). These higher standard deviations are likely due to the oscillations in the relative phase graphs (Figure 5.4).

Table 3.14: Means and standard deviations for relative phase calculated using CRP, CRP_{HT}, and RFP for computer generated signals. All methods accurately detect phase shifts in sinusoidal signals (S1) with very low standard deviations. Sinusoidal signals of different frequencies (S2) analyzed using CRP and CRP_{HT} showed similar averages and standard deviations. RFP analysis showed much higher average relative phase but similar standard deviations. For non-sinusoidal signals (S3) results for all methods were similar. Surprisingly, RFP using a rectangular window showed the least amount of variation, while the Hanning window showed the greatest variation among RFP window types.

	S1: phase = 18º	**S1: phase = 126º**	**S2**	**S3: phase = 18dº**	**S3: phase = 126º**
CRP mean	18.000 ± 0.002	126.000 ± 0.004	87.077 ± 52.615	18.072 ± 9.138	126.944 ± 27.142
CRP_{HT} means	18.187 ± 7.325	126.091 ± 9.789	87.627 ± 52.769	18.133 ± 5.042	126.686 ± 17.819
RFP (rect) mean	18.000 ± 0.009	126.000 ± 0.024	93.763 ± 51.314	18.000 ± 0.013	125.999 ± 0.036
RFP (hann) mean	18.000 ± 0.023	126.001 ± 0.060	93.762 ± 51.316	17.956 ± 1.297	125.615 ± 7.384
RFP (hamm) mean	18.000 ± 0.018	126.000 ± 0.047	93.762 ± 51.316	17.963 ± 1.104	125.672 ± 6.290

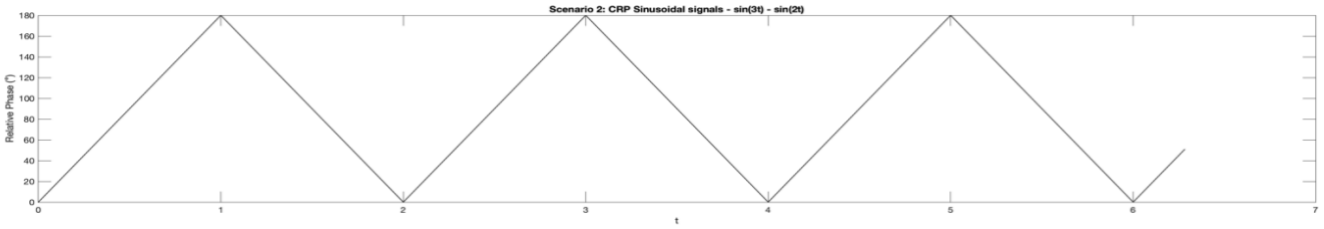

Figure 3.9: Relative phase plots for two sinusoidal signals of two different frequencies using CRP. The rise and fall of the relative phase plot show the progression of the phase of the signal from in-phase (closer to 0º) to out-of-phase (closer to 180º) as the signal progresses. This shift from in-phase to out-of-phase pattern accounts for the higher standard deviations recorded

A

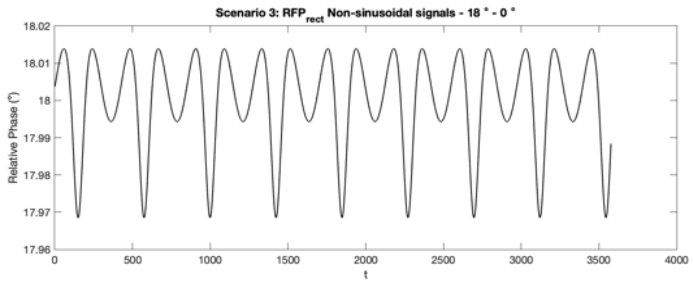

B

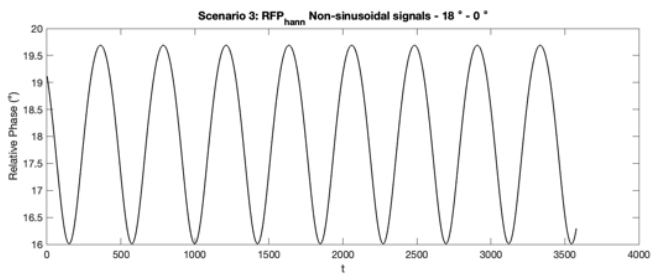

C

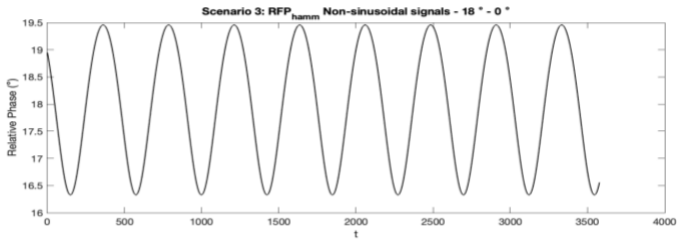

Figure 3.8: Relative phase plots for non-sinusoidal signals with phase shifts of 180º for RFP using the rectangular window (a), Hanning window (b), and Hamming window (c). While the rectangular window has the lowest standard deviation of the three window types, additional peaks appear in the signal likely due to transients. Figures b and c show that Hanning and Hamming windows perform better.

5.4.2 Kinematic Data

Kinematic data from a healthy control walking performing overground walking trials at four velocities, self-selected speed (SSS), SSS – 10 % (Slow10), SSS – 20% (Slow20) and SSS + 10 % (Fast), and under two conditions without the iWalk (Norm and with the iWalk 2.0 (iWalk) which was used to mimic unilateral knee disarticulation. Results Relative phasing between the upper-torso, torso and pelvis were calculated using the three methods outlined above. Given the relatively equal performance of RFP using Hamming and Hanning windows in the previous section, the Hanning window was used for the short-time Fourier transform because of its wide applicability. Results for subject 2 Norm trials at all speeds using all three methods for calculating relative phase are reported below in tables

Table 3.15 - Table **3.16.**

Table 3.18 reports relative phase average and standard deviations for subject 2 with the iWalk at all

Norm CRP	Torso/Upper-Torso			Pelvis/Upper-Torso			Pelvis/Torso		
	Flex/Ext	Lat Bend	Ax. Rot	Flex/Ext	Lat Bend	Ax. Rot	Flex/Ext	Lat Bend	Ax. Rot
Slow20 avg ± std (•)	45.6 ± 29.6	115.0 ± 13.3	13.1 ± 5.3	51.6 ± 33.7	105.7 ± 15.6	15.5 ± 6.5	18.7 ± 7.3	34.4 ± 11.6	10.5 ± 4.7
Slow10 avg ± std (•)	60.7 ± [illegible]	[illegible]	9.0 ± [illegible]	71.1 ± [illegible]	[illegible]	14.8 ± [illegible]	27.0 ± [illegible]	[illegible]	8.8 ± 4.5
SSS avg ± std (•)	[illegible]	[illegible]	[illegible]	[illegible]	[illegible]	[illegible]	[illegible]	[illegible]	[illegible]
Fast avg ± std (•)	[illegible]	[illegible]	[illegible]	[illegible]	[illegible]	[illegible]	[illegible]	[illegible]	[illegible]

iWalk CRP	Torso/Upper-Torso			Pelvis/Upper-Torso			Pelvis/Torso		
	Flex/Ext	Lat Bend	Ax. Rot	Flex/Ext	Lat Bend	Ax. Rot	Flex/Ext	Lat Bend	Ax. Rot
Slow20 avg ± std (•)	25.2 ± 19.9	47.7 ± 15.5	32.0 ± 12.4	25.7 ± 21.7	58.6 ± 14.6	20.2 ± 9.9	22.1 ± 18.7	26.2 ± 5.9	13.5 ± 11.9
Slow10 avg ± std (•)	19.5 ± 7.5	45.7 ± 16.5	31.7 ± 14.4	22.5 ± 8.6	53.7 ± 17.8	22.5 ± 7.1	22.2 ± 13.9	29.9 ± 6.5	15.1 ± 8.7
SSS avg ± std (•)	30.2 ± 9.0	61.5 ± 16.2	19.6 ± 5.4	27.8 ± 14.3	76.8 ± 15.3	12.2 ± 2.6	26.1 ± 12.8	33.6 ± 6.7	12.0 ± 5.2
Fast avg ± std (•)	30.9 ± 11.8	68.1 ± 21.7	35.1 ± 21.6	32.0 ± 11.6	86.9 ± 11.8	31.4 ± 17.9	18.6 ± 8.2	47. ± 31.2	29.5 ± 17.7

walking velocities.

Analysis using RFP showed higher average relative phase and relative phase standard deviation than CRP and CRP_{HT}. CRP and CRP_{HT} had very similar results. However, CRP_{HT} generally showed greater standard deviations for all axial relative phases. Previous studies have reported that as walking velocity increases, there is a transition from in-phase coordination patterns (< 110º) to out-of-phase patterns (≥ 110º) [8,13]. This transition was not clearly seen in

any of the methods below. These results show that as walking velocity increases relative phasing tends to become more out-of-phase starting between 105º and 115º and reaching a peak of between 146º and 160º depending on the method used.

Table 3.18 shows means and standard deviations for the same subject but for overground walking trials using the iWalk 2.0. Relative phase between segments was analyzed using CRP. When compared to results from

iWalk CRP	Torso/Upper-Torso			Pelvis/Upper-Torso			Pelvis/Torso		
	Flex/Ext	Lat Bend	Ax. Rot	Flex/Ext	Lat Bend	Ax. Rot	Flex/Ext	Lat Bend	Ax. Rot
Slow20 avg ± std (•)	25.2 ± 6.9	47.7 ± 12.4	32.0 ± 14.2	25.7 ± 8.2	58.6 ± 12.3	20.2 ± 6.9	22.1 ± 12.2	26.2 ± 5.9	13.5 ± 8.4
Slow10 avg ± std (•)	19.5 ± 7.5	45.7 ± 16.5	31.7 ± 14.4	22.5 ± 8.6	53.7 ± 17.8	22.5 ± 7.1	22.2 ± 13.9	29.3 ± 6.5	15.1 ± 8.7
SSS avg ± std (•)	30.9 ± 11.8	68.1 ± 21.7	33.1 ± 21.6	32.0 ± 11.6	86.9 ± 11.8	31.4 ± 17.9	18.6 ± 8.2	47 ± 11.6	29.5 ± 17.7
Fast avg ± std (•)	45.6 ± 29.6	115.0 ± 13.3	13.1 ± 5.3	51.6 ± 33.7	105.7 ± 15.6	15.5 ± 6.5	18.7 ± 7.3	34.4 ± 11.6	10.5 ± 4.7
Slow10 avg ± std (•)	60.7 ± 37.3	117.7 ± 12.4	9.0 ± 2.5	71.1 ± 39.6	98.6 ± 17.3	14.8 ± 4.0	27.0 ± 15.4	24.7 ± 8.3	8.8 ± 4.5
SSS avg ± std (•)	53.1 ± 19.9	145.7 ± 15.5	9.1 ± 3.1	44.4 ± 21.7	127.0 ± 14.6	16.7 ± 9.9	42.5 ± 18.7	39.2 ± 10.5	16.5 ± 11.9
Fast avg ± std (•)	42.2 ± 36.2	152.9 ± 17.7	15.4 ± 11.4	53.9 ± 43.6	143.3 ± 23.4	29.3 ± 19.8	27.7 ± 23.0	21.4 ± 13.3	23.6 ± 22.0

Table 3.15, we see that this subject no longer adopts an out-of-phase pattern between all segments. This is accompanied by a marked decrease in standard deviation

Table 3.15: Average and standard deviations of upper-torso and torso, pelvis and upper-torso, and pelvis and torso relative phase calculated using CRP. This data comes from a healthy control performing overground walking tasks at four speeds under normal conditions. These speeds were Slow20 (SSS – 20%), Slow10 (SSS – 10%), self-selected speed (SSS), Fast (SSS + 10%). This method shows the previously reported transition from an in-phase coordination pattern

Norm CRP	Torso/Upper-Torso			Pelvis/Upper-Torso			Pelvis/Torso		
	Flex/Ext	Lat Bend	Ax. Rot	Flex/Ext	Lat Bend	Ax. Rot	Flex/Ext	Lat Bend	Ax. Rot
Slow20 avg ± std (•)	45.6 ± 29.6	115.0 ± 13.3	13.1 ± 5.3	51.6 ± 33.7	105.7 ± 15.6	15.5 ± 6.5	18.7 ± 7.3	34.4 ± 11.6	10.5 ± 4.7
Slow10 avg ± std (•)	60.7 ± 37.3	117.7 ± 12.4	9.0 ± 2.5	71.1 ± 39.6	98.6 ± 17.3	14.8 ± 4.0	27.0 ± 15.4	24.7 ± 8.3	8.8 ± 4.5
SSS avg ± std (•)	53.1 ± 19.9	145.7 ± 15.5	9.1 ± 3.1	44.4 ± 21.7	127.0 ± 14.6	16.7 ± 9.9	42.5 ± 18.7	39.2 ± 10.5	16.5 ± 11.9
Fast avg ± std (•)	42.2 ± 36.2	152.9 ± 17.7	15.4 ± 11.4	53.9 ± 43.6	143.3 ± 23.4	29.3 ± 19.8	27.7 ± 23.0	21.4 ± 13.3	23.6 ± 22.0

Table 3.16: Averageand standard deviations of upper-torso and torso, pelvis and upper-torso, and pelvis and torso relative phase calculated using RFP. This data comes from a healthy control performing overground walking tasks at four speeds under normal conditions. These speeds were Slow20 (SSS – 20%), Slow10 (SSS – 10%), self-selected speed (SSS), Fast (SSS + 10%).

Norm RFP	Torso/Upper-Torso			Pelvis/Upper-Torso			Pelvis/Torso		
	Flex/Ext	Lat Bend	Ax. Rot	Flex/Ext	Lat Bend	Ax. Rot	Flex/Ext	Lat Bend	Ax. Rot
Slow20 avg ± std (•)	54.2 ± 48.7	127.5 ± 48.9	8.8 ± 7.4	59.8 ± 48.7	109.9 ± 44.1	15.5 ± 11.8	30.9 ± 36.3	34.3 ± 24.1	10.9 ± 9.5
Slow10 avg ± std (•)	67.5 ± 49.7	132.2 ± 40.7	8.4 ± 7.3	71.2 ± 52.0	111.8 ± 39.9	14.7 ± 11.6	47.3 ± 43.7	36.4 ± 27.1	9.7 ± 8.8
SSS avg ± std (•)	60.8 ± 48.3	137.7 ± 40.0	8.8 ± 7.9	65.9 ± 49.4	129.8 ± 38.7	27.0 ± 23.0	39 ± 40.1	35.1 ± 17.7	22.7 ± 19.7
Fast avg ± std (•)	53.1 ± 44.0	146.0 ± 30.4	8.7 ± 8.6	78.4 ± 48.0	135.4 ± 30.3	29.4 ± 21.3	48.4 ± 42.7	31.5 ± 22.3	24.6 ± 16.7

Table 3.17: Means and standard deviations of upper-torso and torso, pelvis and upper-torso, and pelvis and torso relative phase calculated using CRP with the Hilbert Transform. This data comes from a healthy control performing overground walking tasks at four speeds under normal conditions. These speeds were Slow20 (SSS – 20%), Slow10 (SSS – 10%), self-selected speed (SSS), Fast (SSS + 10%).

Norm CRPHT	Torso/Upper-Torso			Pelvis/Upper-Torso			Pelvis/Torso		
	Flex/Ext	Lat Bend	Ax. Rot	Flex/Ext	Lat Bend	Ax. Rot	Flex/Ext	Lat Bend	Ax. Rot
Slow20 avg ± std (•)	45.6 ± 29.5	115.0 ± 13.3	13.1 ± 5.3	51.6 ± 33.6	105.7 ± 15.6	15.5 ± 6.5	18.6 ± 7.3	34.4 ± 11.5	10.4 ± 4.6
Slow10 avg ± std (•)	60.7 ± 37.2	117.7 ± 12.3	9.0 ± 2.5	71.0 ± 39.6	98.6 ± 17.3	14.7 ± 3.9	26.9 ± 15.4	24.7 ± 8.2	8.8 ± 4.4
SSS avg ± std (•)	53.1 ± 19.8	145.6 ± 15.4	9.0 ± 3.1	44.4 ± 44.4	127.0 ± 14.5	16.6 ± 9.9	42.5 ± 186	39.2 ± 10.5	16.5 ± 11.9
Fast avg ± std (•)	63.4 ± 39.7	160.0 ± 12.7	8.1 ± 4.4	71.7 ± 46.5	144.8 ± 11.0	27.2 ± 8.9	23.7 ± 10.6	24.9 ± 13.8	23.5 ± 10.8

Table 3.18: Means and standard deviations of upper-torso and torso, pelvis and upper-torso, and pelvis and torso relative phase calculated using CRP. This data comes from a healthy control performing overground walking tasks using the iWalk 2.0 at four speeds under normal conditions. These speeds were Slow20 (SSS – 20%), Slow10 (SSS – 10%), self-selected speed (SSS), Fast (SSS + 10%). The iWalk 2.0 was used to mimic unilateral lower-limb amputation through the knee. When compared to Norm tasks this subject is unable to adopt the characteristic out-of-phase pattern seen in Norm tasks. This is also accompanied by a decrease in standard deviation indicating an overall more rigid coordination pattern between segment.

iWalk CRP	Torso/Upper-Torso			Pelvis/Upper-Torso			Pelvis/Torso		
	Flex/Ext	Lat Bend	Ax. Rot	Flex/Ext	Lat Bend	Ax. Rot	Flex/Ext	Lat Bend	Ax. Rot
Slow20 avg ± std (•)	25.2 ± 6.9	47.7 ± 12.4	32.0 ± 14.2	25.7 ± 8.2	58.6 ± 12.3	20.2 ± 6.9	22.1 ± 12.2	26.2 ± 5.9	13.5 ± 8.4
Slow10 avg ± std (•)	19.5 ± 7.5	45.7 ± 16.5	31.7 ± 14.4	22.5 ± 8.6	53.7 ± 17.8	22.5 ± 7.1	22.2 ± 13.9	29.9 ± 6.5	15.1 ± 8.7
SSS avg ± std (•)	30.2 ± 9.0	61.5 ± 16.2	19.6 ± 5.4	27.8 ± 14.3	76.8 ± 15.3	12.2 ± 2.6	26.1 ± 12.8	33.6 ± 6.7	12.0 ± 5.2
Fast avg ± std (•)	30.9 ± 11.8	68.1 ± 21.7	35.1 ± 21.6	32.0 ± 11.6	86.9 ± 11.8	31.4 ± 17.9	18.6 ± 8.2	47. ± 31.2	29.5 ± 17.7

5.5 Discussion

This paper analyzed three continuous methods that can be used for calculating relative phasing or coordination patterns of signals or segments of interest. These methods have been previously used by various authors to analyze coordination patterns between body segments in various populations [4–9,12–14,16,20,24,25,27,28]. However, how each method could impact the interpretation of coordination patterns remained unknown. There is some literature which compare continuous and discrete methods for calculating coordination patterns, and which compare CRP_{HT} and CRP and its various forms of normalization [5,22,28]. However, to the author's knowledge there is only one study that uses computer generated sinusoidal and non-sinusoidal signals with known phase shifts to compare CRP and CRP_{HT}, and there are no papers which include RFP. The aim of this paper was three-fold. Firstly, to run a comprehensive comparison of all known continuous methods for calculating relative phase between signals. Secondly, to provide a step-by-step guide for analyzing overground walking or running data using all three methods. Lastly, to specify best practices for each analysis method.

Analysis of computer-generated signals reported surprising similarities between CRP and CRP_{HT}. Good estimation of relative phasing between sinusoidal signals was expected. Average relative phase for non-sinusoidal signals was also equal to the phase shift between the signals. The similarity between these two methods was surprising given the methodological differences between CRP and CRP_{HT}. CRP takes rotation data calculated from sensor positions and calculates angular velocity. Normalization of angular position and angular velocity are carried out to ensure that the position-velocity phase plane is close to circular. This normalization is intended to normalize the frequencies between the signals and ensure that frequency does not overpower phase. Phase angles for each segment are then obtained from angular position and

velocity vectors and CRP is calculated as the difference between distal and proximal phase angles. CRP_{HT} in comparison does not require calculation of angular velocity, but rather relies on the angular position and it's Hilbert transform to calculate phase angles. Since human movement data is more complex, greater differences between CRP and CRP_{HT} in segment coordination analysis were expected. Additionally, variability of relative phase for CRP_{HT} were more in line CRP. Inspection of the CRP_{HT} plots for the example subject show that the characteristic overestimation at the beginning and end of the signal is dampened (Figure 5.5). This may be due in part to individual stride analysis of the data rather than analysis of whole signal. Interestingly, Lamb and Stöckl did not report overestimation at the beginning and end of their computer-generated signals. This may be because they analyzed a single cycle of their signals rather than multiple cycles. They also used the full range from 0º to 360º for their analysis. Overall, results from the computer-generated signals align with those found in this study.

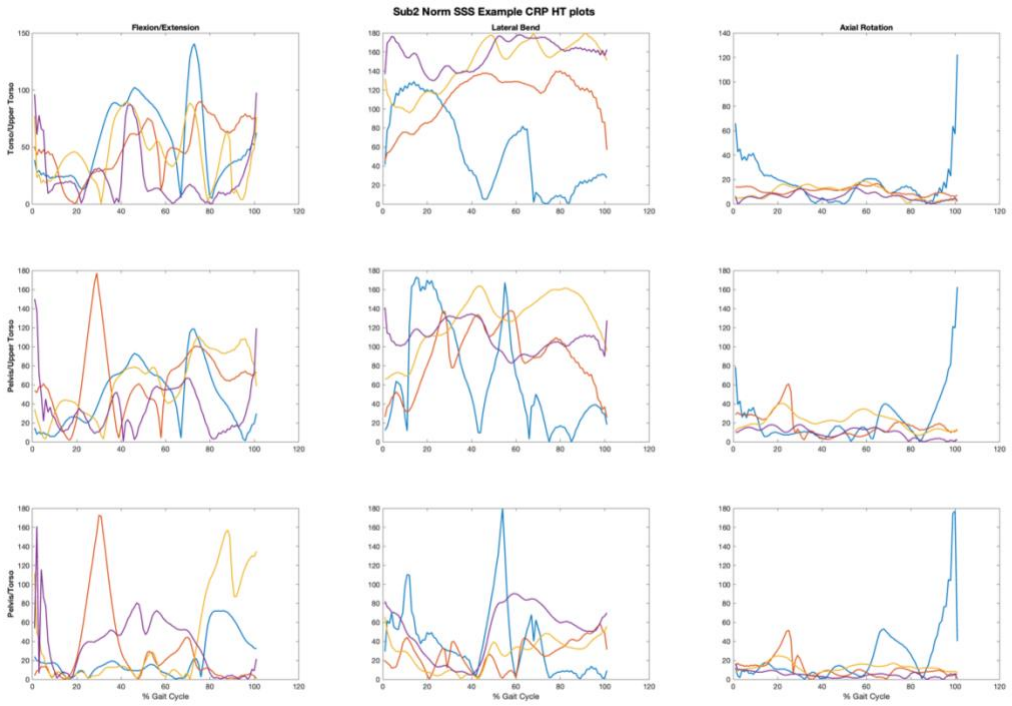

Figure 3.10: Example CRP_{HT} plots for subject 2 performing overground walking trials at a self-selected speed. Each line in the graph represents a stride. When compared to Figure **3.7** these graphs do not have the characteristic overestimation at the beginning and end of the signal. This is likely because the data was analyzed on a stride-to-stride basis whereas the entire computer-generated signals was analyzed.

Analysis of computer-generated signals using RFP shows that this method also accurately detects phase shifts between signals. Like CRP and CRP_{HT} it performs well with both sinusoidal signals with or without the same frequency, and non-sinusoidal signals with less variability. The different window types did not affect average relative phase calculations. There were differences between window types in relative phase standard deviation, however they were all less than 10º.

Segment coordination pattern analyzed using RFP show that this method estimates a higher relative phase than both CRP and CRP_{HT} for almost all rotations. This is because in essence, RFP is creating a sinusoidal signal that has a frequency equivalent to the fundamental frequency found in the human movement data. Doing so acts as a filter removing higher frequencies. However, this assumes that higher frequencies in a signal are primarily noise and fine to ignore when this may not be the case. Figure 5.6 shows an example power spectrum for the upper-torso in lateral bend for a subject performing a Fast overground walking trial using the iWalk 2.0. Power spectrum shows a primary peak occurring at approximately 0.6Hz, harmonics at 0.8Hz, 1.2Hz, and 1.8Hz. The presence of additional peaks was also reported by Lamoth in pelvis transverse plane rotations of healthy controls [8]. They concluded that this supports the hypothesis that velocity dependent changes to coordination patterns

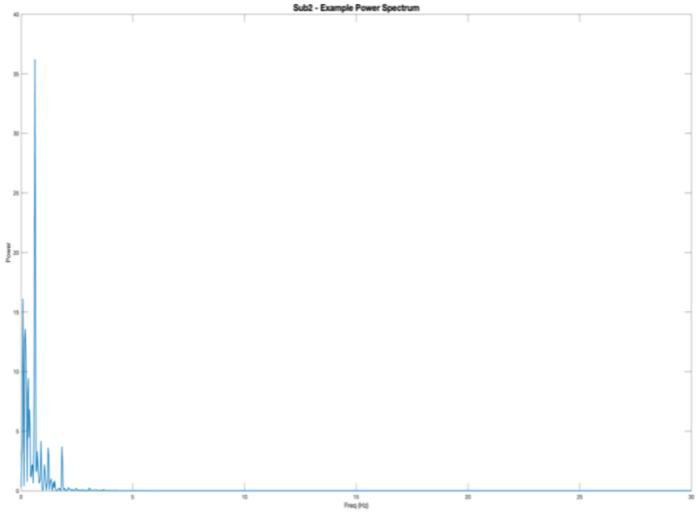

Figure 3.11: Example power spectrum plot of the upper-torso lateral bend for subject 2 performing an overground walking trial with the iWalk 2.0 Fast (SSS + 10%). While the most prominent peak occurs at a frequency of 0.6Hz, there are additional peaks above 0.6Hz some which occur at multiples of the fundamental frequency (i.e: 1.2Hz, and 1.8Hz. A similar phenomenon was seen by Lamoth but only in pelvis rotations. In healthy controls these higher harmonics reflect the changing pattern of the pelvis at higher walking velocities. In this case, this may represent an adaptation to prosthetic use

are driven primarily by changes to the frequency of pelvis rotations. The presence of higher harmonics in upper-torso lateral rotations during a task meant to mimic knee disarticulation suggests that impairments of the lower limb have consequences further upstream than previously reported, and that these changes may be used to adapt to the new conditions.

Previous studies that have used RFP to analyze segment coordination patterns have used gait data collected on a treadmill [6–8,27,28]. Li in their analysis used 12 cycles of data, while Lamoth suggests at least 10. This is primarily because of they suggest a window size of $4 \times \frac{1}{f_{1max}} \times$ sample rate. To ensure there were enough cycles for analysis, data from all trials of the same task were concatenated. To ensure there were no discontinuities data from one trial's last heel strike was concatenated with the data from the next trial's first heel strike. After concatenation, the window size was still too large for analysis. A large window size would not be able to adequately capture changes in phase. Therefore, for this analysis a window of the average length of a stride was used.

5.5.1 Relative Phase Analysis: Best Practices

CRP and CRP_{HT}: CRP as described by Hamill has been used by several researchers to characterize coordination patterns of both upper and lower extremities. In the known signal processing CRP and CRP_{HT} show little difference in average and standard deviations of relative phase. The main difference appears in the graphs of the relative phase plots particularly when analyzing non-sinusoidal signals. CRP plots show additional peaks that do not appear in the CRP_{HT} plots. Interestingly these additional peaks only appear in S1 where the average relative phase between the signals is 18º. CRP_{HT} does not present with these additional peaks, however,

there is distortion of the signal at the beginning and end of the signal which contributes to the increased standard deviation calculations using this method.

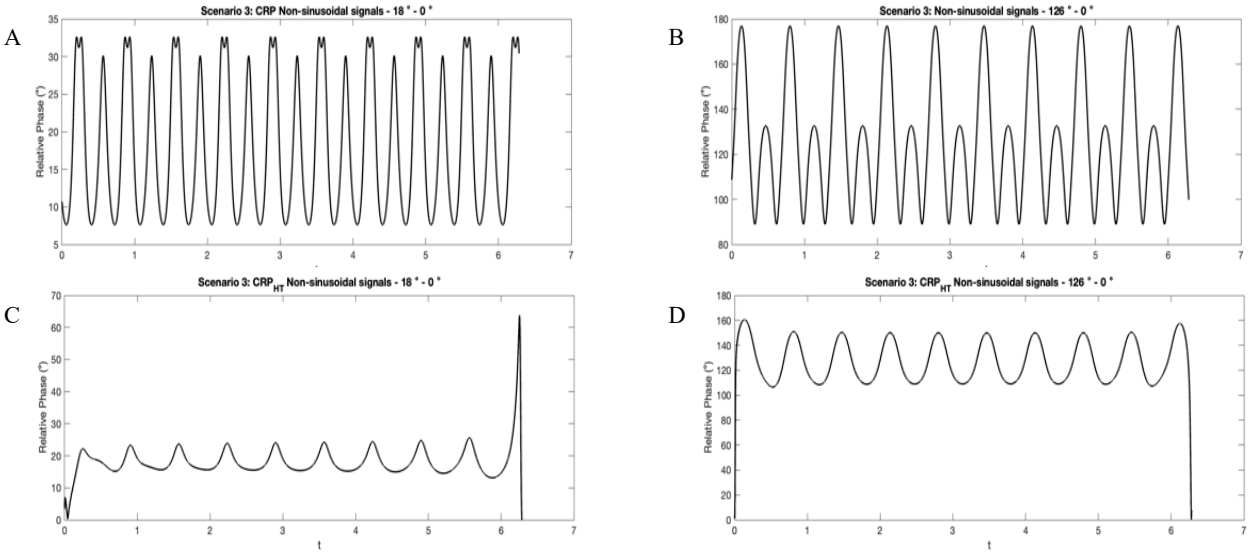

Figure 3.12: Computer generated non-sinusoidal signals with phase shifts of 18º (a,c), and 126º analyzed using CRP (a,b), and CRP_{HT} (c,d). Additional peaks appear when analyzing non-sinusoidal signals with phase shifts of 18º using CRP (a), that are not present when analyzing using CRP_{HT} (c). However, CRP_{HT} plots have distortions at the beginning and the ends of the signals which impact standard deviation calculations.

When analyzing human movement data using CRP or CRP_{HT} it is best to analyze a single cycle at a time. When using CRP this is important because of the angular position and velocity normalizations which are based on the minimum and maximum values of the vectors. A within stride minima or maxima may not be equivalent to the minima/maxima over multiple strides. This also prevents within stride distortions. Analysis of shorter datasets seems to reduce the distortion at the beginning and end of the CRP_{HT} data as well.

Lamb and Stöckl used CRP and CRP_{HT} to compare hip and knee coordination during treadmill running tasks. While they did not report averages and standard deviations from their data, from their figures the Hilbert centered and CRP when normalized as described in this paper are very similar. Therefore, it seems that CRP and CRP_{HT} can be used to calculate coordination patterns between many different types of segments of both upper and lower extremity.

RFP: To the author's knowledge, RFP has only been used to characterize coordination patterns between upper-trunk/trunk and pelvis segments [6–8,24,27]. This method seems to be better suited for treadmill tasks because of the need for multiple cycles to use the window size described by Li and Lamoth [6,24,27]. To ensure a sufficient vector length for RFP analysis, trials from the same task were concatenated using heel strike data and a new window size was proposed. Window sizes are important because they can negatively affect calculations of relative phase. A window that is too long will miss potentially important phase changes. Windows that are too short may cause aliasing. This could account for the additional frequencies, especially non-harmonic frequencies, seen in the example iWalk figures (Figure 5.6). However, additional frequencies were also seen in pelvis transverse plane power spectra by Lamoth in healthy controls as walking velocity increased [8]. In addition, the window type can also distort the data. Computer generated signals showed little difference in window types. The only major difference was seen in when using the Hanning window where the RFP standard deviation was higher than for all the other window types. Using a uniform or rectangular window was not an option for human movement data because of potential transients created when shifting the window. Both Hanning and Hamming windows seemed to perform well. However, the Hanning window was chosen because of its wide applicability. One drawback of RFP is that identification of coordination patterns at specific gait events is not possible because multiple cycles are needed to adequately calculate fundamental frequency and to perform the short-time Fourier transform.

Beyond mean and standard deviations, another measure that may be of interest is the percentage of the gait cycle subjects spend in an out-of-phase pattern. Example results of this analysis are shown in Table **3.19** and

Table 3.20. Table **3.19** displays torso/upper-torso, pelvis/upper-torso, and pelvis/torso coordination patterns in all planes at four different walking velocities. As walking velocity increases the proportion of the gait cycle spent out-of-phase increases in torso/upper-torso lateral bend from 0.7 to 1.0, and in pelvis/upper-torso lateral bend from 0.4 to 0.9. This is in line with previous studies that show a transition to an out-of-phase coordination pattern as walking velocity increases.

Table **3.20** shows similar results, but from overground walking tasks with the iWalk 2.0. This table clearly shows that this subject maintains an in-phase coordination pattern even as walking velocity increases. There is a slight increase in the proportion of the gait cycle spent out-of-phase in pelvis/upper-torso lateral bend, however this increase is only 10%.

Table 3.19: Proportion of torso/upper-torso, pelvis/upper-torso, and pelvis/torso coordination patterns spent out-of-phase during overground walking trials without iWalk 2.0 at four speeds. This data was calculated using CRP. This table gives a clearer picture of changes to coordination patterns as walking velocity increases. In torso/upper-torso coordination as walking velocity increases the proportion of out-of-phase coordination increases from 0.7 to 1.0. A similar pattern is seen in pelvis/upper-torso lateral bend where the change in proportion is even more stark 0.4 to 0.9.

Norm CRP – Proportion of gait cycle spent out-of-phase									
	Torso/Upper-Torso			Pelvis/Upper-Torso			Pelvis/Torso		
	Flex/Ext	**Lat Bend**	**Ax. Rot**	**Flex/Ext**	**Lat Bend**	**Ax. Rot**	**Flex/Ext**	**Lat Bend**	**Ax. Rot**
Slow20	0.0	0.7	0.0	0.0	0.4	0.0	0.0	0.0	0.0
Slow10	0.1	0.7	0.0	0.2	0.3	0.0	0.0	0.0	0.0
SSS	0.0	1.0	0.0	0.0	0.9	0.0	0.0	0.0	0.0
Fast	0.1	1.0	0.0	0.1	0.9	0.0	0.0	0.0	0.0

Table 3.20: Proportion of torso/upper-torso, pelvis/upper-torso, and pelvis/torso coordination patterns spent out-of-phase during overground walking trials with iWalk 2.0 at four speeds. This data was calculated using CRP. Unlike Norm, we see no characteristic

increase in out-of-phase pattern as walking velocity increases. There is a slight increase in pelvis/upper-torso lateral bend however, the percentage of the gait cycle spent out-of-phase is only 10%.

iWalk CRP – Proportion of gait cycle spent out-of-phase									
	Torso/Upper-Torso			Pelvis/Upper-Torso			Pelvis/Torso		
	Flex/Ext	**Lat Bend**	**Ax. Rot**	**Flex/Ext**	**Lat Bend**	**Ax. Rot**	**Flex/Ext**	**Lat Bend**	**Ax. Rot**
Slow20	0.0	0.0	0.0	0.0	0.0	0.0	0.0	0.0	0.0
Slow10	0.0	0.0	0.0	0.0	0.0	0.0	0.0	0.0	0.0
SSS	0.0	0.0	0.0	0.0	0.0	0.0	0.0	0.0	0.0
Fast	0.0	0.0	0.0	0.0	0.1	0.0	0.0	0.0	0.0

5.6 Conclusions

This paper compared three commonly used continuous methods for calculating relative phasing between segments using computer generated data and real data. For RFP, different window types were also compared. CRP and CRP_{HT} were found to produce similar results for both generated and real data. This is in line with other authors who have found that the amplitude centered CRP_{HT} and CRP produce similar results. RFP consistently estimates a higher relative phase than both CRP and CRP_{HT} however, whether this would be inconvenient for the analysis is left for the researcher's discretion. This is because these methods are relative, and their interpretation is study and analysis specific. Whether a 10-15º overestimation of relative phase is significant is subjective. However, when it comes to standard deviations overestimation by RFP may be of greater concern because standard deviation is closely related to stability. Therefore, if the author's objective is to characterize stability, that is, the ability for a group of subjects to transition from one coordination pattern to another, CRP or CRP_{HT} may give more accurate results. This is because RFP assumes that the dominant frequency of the signal accurately describes the movement. This may not be the case especially in instances where higher harmonics are present. Based on their calculation as described in this paper, all these methods provide an intuitive answer. That is, one can easily interpret the coordination patterns between segments or signals of interest using any of these methods.

5.7 References

[1] R. Burgess-Limerick, B. Abernethy, R.J. Neal, Relative phase quantifies interjoint coordination, Journal of Biomechanics. 26 (1993) 91–94. https://doi.org/10.1016/0021-9290(93)90617-N.

[2] S. Choi, S.-K. Kim, G.-J. Lee, H.-K. Park, Paper-based 3D microfluidic device for multiple bioassays, Sensors and Actuators B: Chemical. 219 (2015) 245–250. https://doi.org/10.1016/j.snb.2015.05.035.

[3] J. Hamill, J.M. Haddad, W.J. McDermott, Issues in Quantifying Variability From a Dynamical Systems Perspective, Journal of Applied Biomechanics. 16 (2000) 407.

[4] J. Hamill, R.E.A. van Emmerik, B.C. Heiderscheit, L. Li, A dynamical systems approach to lower extremity running injuries, Clinical Biomechanics. 14 (1999) 297–308. https://doi.org/10.1016/S0268-0033(98)90092-4.

[5] P.F. Lamb, M. Stöckl, On the use of continuous relative phase: Review of current approaches and outline for a new standard, Clinical Biomechanics. 29 (2014) 484–493. https://doi.org/10.1016/j.clinbiomech.2014.03.008.

[6] C.J.C. Lamoth, Pelvis-Thorax Coordination in the Transverse Plane During Walking in Persons With Nonspecific Low Back Pain, Spine (Philadelphia, Pa. 1976). 27 (2002) E92–E99. https://doi.org/10.1097/00007632-200202150-00016.

[7] C.J.C. Lamoth, A. Daffertshofer, O.G. Meijer, G. Lorimer Moseley, P.I.J.M. Wuisman, P.J. Beek, Effects of experimentally induced pain and fear of pain on trunk coordination and back muscle activity during walking, Clinical Biomechanics. 19 (2004) 551–563. https://doi.org/10.1016/j.clinbiomech.2003.10.006.

[8] C.J.C. Lamoth, P.J. Beek, O.G. Meijer, Pelvis–thorax coordination in the transverse plane during gait, Gait & Posture. 16 (2002) 101–114. https://doi.org/10.1016/S0966-6362(01)00146-1.

[9] S. Mehdizadeh, A.R. Arshi, K. Davids, Quantifying coordination and coordination variability in backward versus forward running: Implications for control of motion, Gait & Posture. 42 (2015) 172–177. https://doi.org/10.1016/j.gaitpost.2015.05.006.

[10] S. Mehdizadeh, P.S. Glazier, Order error in the calculation of continuous relative phase, Journal of Biomechanics. 73 (2018) 243–248. https://doi.org/10.1016/j.jbiomech.2018.03.032.

[11] A.R.M. Pelegrinelli, M.F. Silva, L.C. Guenka, A.C. Carrasco, F.A. Moura, J.R. Cardoso, Low back pain affects coordination between the trunk segments but not variability during running, Journal of Biomechanics. 101 (2020) 109605. https://doi.org/10.1016/j.jbiomech.2020.109605.

[12] Z. Sawacha, C.D. Sartor, L.C. Yi, A. Guiotto, F. Spolaor, I.C.N. Sacco, Clustering classification of diabetic walking abnormalities: a new approach taking into account intralimb coordination patterns, Gait & Posture. 79 (2020) 33–40. https://doi.org/10.1016/j.gaitpost.2020.03.016.

[13] J.F. Seay, Influence of Low Back Pain Status on Pelvis-Trunk Coordination During Walking and Running, Spine (Philadelphia, Pa. 1976). 36 (2011) E1070–E1079. https://doi.org/10.1097/BRS.0b013e3182015f7c.

[14] J.F. Seay, R.E.A. Van Emmerik, J. Hamill, Low back pain status affects pelvis-trunk coordination and variability during walking and running, Clinical Biomechanics. 26 (2011) 572–578. https://doi.org/10.1016/j.clinbiomech.2010.11.012.

[15] R.W. Selles, R.C. Wagenaar, T.H. Smit, P.I.J.M. Wuisman, Disorders in trunk rotation during walking in patients with low back pain: a dynamical systems approach, Clinical Biomechanics. 16 (2001) 175–181. https://doi.org/10.1016/S0268-0033(00)00080-2.
[16] I. Shojaei, M. Vazirian, E.G. Salt, L.R. Van Dillen, B. Bazrgari, Timing and magnitude of lumbar spine contribution to trunk forward bending and backward return in patients with acute low back pain, Journal of Biomechanics. 53 (2017) 71–77. https://doi.org/10.1016/j.jbiomech.2016.12.039.
[17] R.E.A. van Emmerik, R.C. Wagenaar, Effects of walking velocity on relative phase dynamics in the trunk in human walking, Journal of Biomechanics. 29 (1996) 1175–1184. https://doi.org/10.1016/0021-9290(95)00128-X.
[18] Y.-T. Yang, Y. Yoshida, T. Hortobágyi, S. Suzuki, Interaction Between Thorax, Lumbar, and Pelvis Movements in the Transverse Plane During Gait at Three Velocities, Journal of Applied Biomechanics. 29 (2013) 261–269. https://doi.org/10.1123/jab.29.3.261.
[19] J.M. Haddad, S. Rietdyk, L.J. Claxton, J.E. Huber, Task-Dependent Postural Control Throughout the Lifespan, Exercise and Sport Sciences Reviews. 41 (2013) 123–132. https://doi.org/10.1097/JES.0b013e3182877cc8.
[20] C.J.C. Lamoth, A. Daffertshofer, O.G. Meijer, P.J. Beek, How do persons with chronic low back pain speed up and slow down? Trunk-pelvis coordination and lumbar erector spinae activity during gait, Gait & Posture. 23 (2006) 230–239. https://doi.org/10.1016/j.gaitpost.2005.02.006.
[21] N.F. Taylor, O.M. Evans, P.A. Goldie, The effect of walking faster on people with acute low back pain, European Spine Journal. 12 (2003) 166–172. https://doi.org/10.1007/s00586-002-0498-3.
[22] B.T. Peters, J.M. Haddad, B.C. Heiderscheit, R.E.A. Van Emmerik, J. Hamill, Limitations in the use and interpretation of continuous relative phase, Journal of Biomechanics. 36 (2003) 271–274. https://doi.org/10.1016/S0021-9290(02)00341-X.
[23] M.J. Kurz, N. Stergiou, Effect of normalization and phase angle calculations on continuous relative phase, Journal of Biomechanics. 35 (2002) 369–374. https://doi.org/10.1016/S0021-9290(01)00211-1.
[24] Y. Li, R.S. Kakar, M.A. Walker, L. Guan, K.J. Simpson, Upper Trunk–Pelvis Coordination During Running Using the Continuous Relative Fourier Phase Method, Journal of Applied Biomechanics. 34 (2018) 312–319.
[25] J.F. Seay, R.E.A. Van Emmerik, J. Hamill, Trunk bend and twist coordination is affected by low back pain status during running, European Journal of Sport Science. 14 (2014) 563–568. https://doi.org/10.1080/17461391.2013.866167.
[26] M. Feldman, HILBERT TRANSFORMS, in: S. Braun (Ed.), Encyclopedia of Vibration, Elsevier, Oxford, 2001: pp. 642–648. https://doi.org/10.1006/rwvb.2001.0057.
[27] C.J.C. Lamoth, O.G. Meijer, A. Daffertshofer, P.I.J.M. Wuisman, P.J. Beek, Effects of chronic low back pain on trunk coordinations and back muscle activity during walking: changes in motor control, European Spine Journal. 15 (2006) 23–40. https://doi.org/10.1007/s00586-004-0825-y.
[28] H.-J. Choi, G. Kim, C.-Y. Ko, Portrait and hilbert transform methods for evaluating continuous relative phase between lower-limb joints in the elderly during walking, J. Mech. Med. Biol. 21 (2021) 2140038. https://doi.org/10.1142/S0219519421400388.

Chapter 6 Conclusions, Limitations & Future Work

6.1 Summary

The overarching goal of the work conducted was to contribute to the knowledge of how unilateral lower-limb amputation affects coordination patterns during running and walking, how different analysis methodologies affect these calculations, and how changes to coordination patterns could be correlated with the development of LBP. This knowledge can be combined with current physical and rehabilitation therapies to create interventions that directly target maladaptive coordination patterns in both amputee and non-amputee populations thereby, decreasing the likelihood of developing LBP. The work proposed here is expected to lead to improvements in physical and rehabilitation therapies.

In the short term, understanding coordination patterns between body segments can lead to a better understanding of other types of joint pain and musculoskeletal disorders including those with a neurological origin. In addition, this work has thoroughly described the different methods used for calculating coordination patterns and described how each method could impact results based on the type of data being analyzed and its purpose. Each chapter addressed an aspect of the specific aims as laid out in Chapter 1.

6.2 Chapter 3: conclusions & limitations

In Chapter 3, Specific Aim 1 was addressed. Upper-torso, torso, and pelvic coordination patterns of a cohort of unilateral-transtibial amputees (UTAs) running at two velocities were characterized. UTAs exhibit velocity dependent changes to coordination patterns that are like those seen in controls [1–4]. This was particularly apparent in mean continuous relative phase (CRP mean), which increased with increasing running velocity. However, this population did not show characteristic changes to CRP variability that have been reported in populations without

LBP. Invariance in CRP variability particularly of the pelvis/torso with increasing walking velocity has been reported in populations with LBP or a history of LBP [2,3,5]. Such changes have also been identified in populations with resolved LBP leading researchers to believe that those with resolved LBP demonstrate characteristics that could predispose one to LBP. If that is the case, changes to coordination patterns in amputees could be indicative of gait adaptations that increase their likelihood of developing LBP later. Whether changes to coordination are lingering adaptations from a pained state or are predictive of future LBP remains unknown. However, this does give physical therapists another target for intervention, and another to assess existing regimens.

This study had three primary limitations. Firstly, the sample size was very small. Within subject statistics were calculated to ensure that a single subject or a single stride did not sway the results of the study. However, the statistical analysis methods used for this analysis are better catered towards larger sample sizes. Secondly, the LBP status of each of these subjects was unknown. While changes to coordination pattern and variability were largely attributed to amputation, the effects of LBP on these measures are very similar and the possibility that they impact these results cannot be ruled out. Lastly, there was no comparison control population. While the results of this study were comparable to others, having a control population of servicemembers would have allowed for internal validation of these results.

6.3 Chapter 4: conclusions & limitations

The remainder of Specific Aim 1 was addressed in Chapter 4, where coordination patterns of healthy controls walking with and without the iWalk 2.0 at four walking velocities were calculated. The iWalk 2.0 is marketed as a crutch alternative. In this study it was used to mimic unilateral LLA through the knee in healthy controls. With the iWalk subjects

demonstrated changes to gait parameters that are normally seen in unilateral LLAs. These included slower preferred walking velocities and increased intact side stance times. Unlike amputees however, while wearing the iWalk subjects maintained symmetrical stride lengths. Studies by other authors have proposed that stride length asymmetries may be due to weak hip abductors rather than amputation [6]. Velocity dependent changes to CRP mean and CRP variability were also reported in this study. During iWalk tasks subjects maintained an overall more in-phase coordination pattern, and reduced CRP variability.

The results of this study are in line with others that have reported velocity dependent changes to coordination patterns, and Chapter 2 which reported changes to coordination patterns in amputees, albeit during running. This study also presented a unique way to isolate the effects of LLA on gait and coordination pattern. Since amputation significantly effects lower limb structure and musculature, some changes to gait and coordination could be attributed to weak muscles, absent joints, or prosthetic design, type, and fit. In addition, it allowed for paired analysis of the data.

This study also had two primary limitations. Firstly, the iWalk 2.0 should not be considered an accurate representation of a prosthetic. The ankle of the prosthetic is stiff and does not allow any movement in the prosthetic side foot. To fit the prosthetic, the knee is bent and strapped essentially bracing the knee so that it cannot flex and extend. Compensatory movements by subjects wearing the iWalk 2.0 are likely more exaggerated than what would be seen in amputee populations. Secondly, there was no amputee population for comparison. Having an amputee population would lend validity to these findings and allow for broader conclusions about amputee gait to be drawn.

6.4 Chapter 5: conclusions & limitations

Specific Aim 2 was addressed in Chapter 5, where computer generated signals with known phase shifts (i.e.: coordination patterns) were analyzed using the three most common continuous methods for calculating relative phasing/coordination patterns. Continuous Relative Phase (CRP), Continuous Relative Phase using the Hilbert Transform (CRP_{HT}) and Relative Fourier Phase (RFP) each address the unique aspects of human movement signals differently. While human movements such as gait are often repetitive, the signals they produce are rarely sinusoidal. Analyzing relative motions between segments is often complicated by the non-sinusoidal nature of these signals. Each method has been used successfully by researchers to characterize pelvis/trunk, and hip and knee coordination by various authors [1–5,7,8]. However, replicating results has often been challenged by questions concerning the mechanics of the methods such as whether to normalize the signals prior to analysis. A fundamental question that has remained unanswered is how each of these methods effects interpretation of coordination patterns, and when it is best to use them. Chapter 5 aimed to address these questions.

Previous authors had discussed the mechanics of CRP and CRP_{HT} in great detail [7–9]. However, to the author's knowledge such consideration had not been given to RFP. At various points in the RFP analysis method windowing is needed. This means that a window type and size need to be selected. Most researchers who have some background in signal processing agree that this decision can be more art than science. A window type is often chosen based on the information that the signal of interest is carrying and whether the researcher prioritizes knowing the signals frequency or amplitude. Window sizes are also of great importance. Picking a window size that is too long can cause important information about the signal to be lost, while a

short window could induce unnecessary artefact. In addition to testing each of these methods, different window types were also tested to see how they would affect RFP analysis

This analysis revealed similarities in CRP and CRP_{HT} which aligned with results reported by other authors [7]. While RFP tended to overestimate relative phase even with the known signals. Whether the overestimation of RFP is concerning is dependent on the goal of the research. Overall, the work Chapter 5 clarifies and provides key considerations for researchers who would like to use CRP, CRP_{HT}, or RFP to analyze coordination between body segments.

6.5 Future work

Previous research has established correlations between LBP and changes to coordination patterns. However, whether these changes are causative or symptomatic is yet unknown. Longitudinal studies that evaluate changes to coordination patterns over time and development of LBP shed more light into this association. These studies should also include LLA populations because of their propensity to experience LBP, and the debilitating nature of their pain

Additional research is also needed to understand the clinical utility of coordination patterns. A focus of rehabilitation for patients with traumatic brain injury is dissociation of head and neck movements. The goal is to re-train patients how to move their head and neck independently. Such a training program may be applicable to LBP and amputee patients who maintain an in-phase coordination pattern. Training patients how to properly counterrotate upper-torso, torso, and pelvic segments may help to relieve LBP and prevent its recurrence regardless of whether these changes are causative of symptomatic.

6.6 References

[1] R.E.A. van Emmerik, R.C. Wagenaar, Effects of walking velocity on relative phase dynamics in the trunk in human walking, Journal of Biomechanics. 29 (1996) 1175–1184. https://doi.org/10.1016/0021-9290(95)00128-X.

[2] J.F. Seay, Influence of Low Back Pain Status on Pelvis-Trunk Coordination During Walking and Running, Spine (Philadelphia, Pa. 1976). 36 (2011) E1070–E1079. https://doi.org/10.1097/BRS.0b013e3182015f7c.

[3] J.F. Seay, R.E.A. Van Emmerik, J. Hamill, Low back pain status affects pelvis-trunk coordination and variability during walking and running, Clinical Biomechanics. 26 (2011) 572–578. https://doi.org/10.1016/j.clinbiomech.2010.11.012.

[4] C.J.C. Lamoth, P.J. Beek, O.G. Meijer, Pelvis–thorax coordination in the transverse plane during gait, Gait & Posture. 16 (2002) 101–114. https://doi.org/10.1016/S0966-6362(01)00146-1.

[5] C.J.C. Lamoth, Pelvis-Thorax Coordination in the Transverse Plane During Walking in Persons With Nonspecific Low Back Pain, Spine (Philadelphia, Pa. 1976). 27 (2002) E92–E99. https://doi.org/10.1097/00007632-200202150-00016.

[6] H. Nadollek, S. Brauer, R. Isles, Outcomes after trans-tibial amputation: the relationship between quiet stance ability, strength of hip abductor muscles and gait, Physiotherapy Research International. 7 (2002) 203. https://doi.org/10.1002/pri.260.

[7] P.F. Lamb, M. Stöckl, On the use of continuous relative phase: Review of current approaches and outline for a new standard, Clinical Biomechanics. 29 (2014) 484–493. https://doi.org/10.1016/j.clinbiomech.2014.03.008.

[8] J. Hamill, R.E.A. van Emmerik, B.C. Heiderscheit, L. Li, A dynamical systems approach to lower extremity running injuries, Clinical Biomechanics. 14 (1999) 297–308. https://doi.org/10.1016/S0268-0033(98)90092-4.

[9] M.J. Kurz, N. Stergiou, Effect of normalization and phase angle calculations on continuous relative phase, Journal of Biomechanics. 35 (2002) 369–374. https://doi.org/10.1016/S0021-9290(01)00211-1.

Chapter 7 Appendix 1 - Supplemental figures & code for amputee runner data

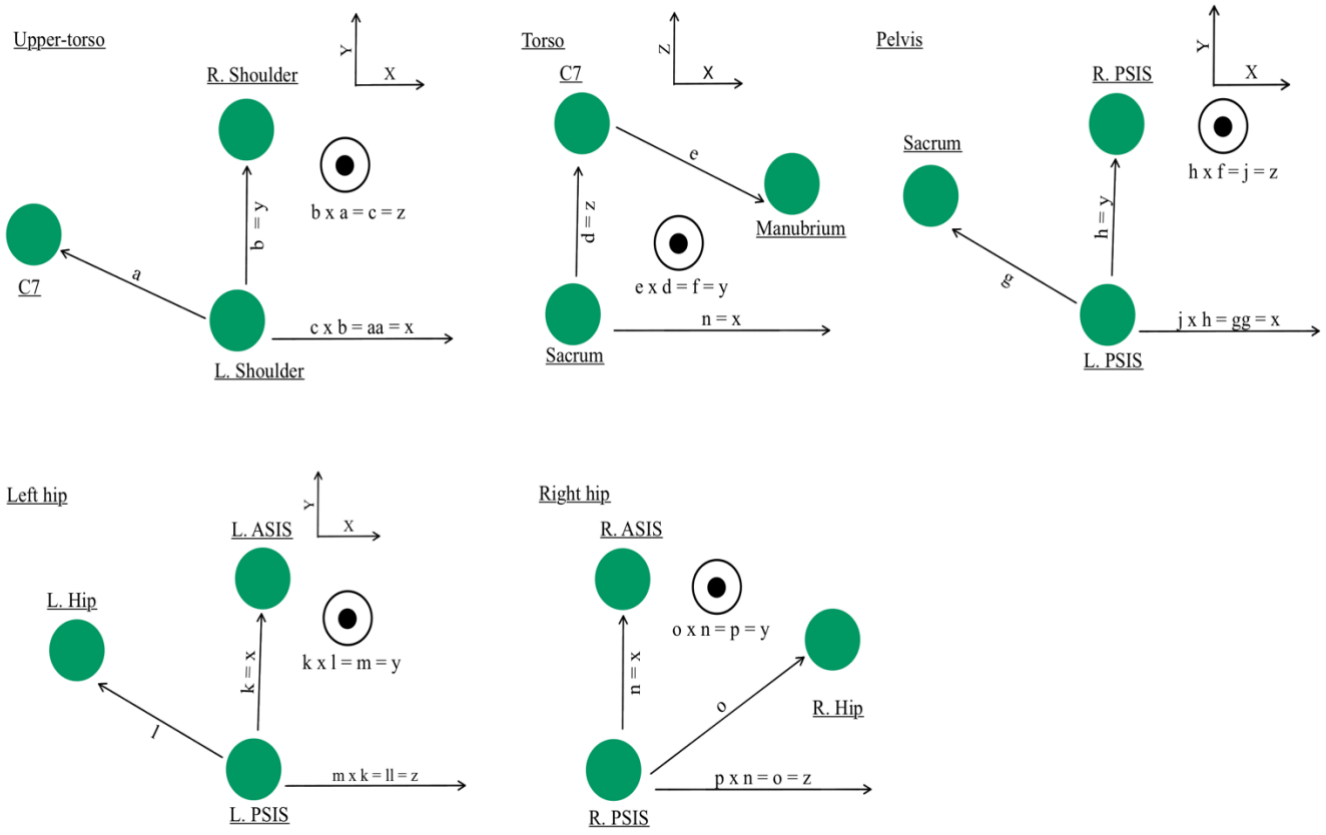

Axes for upper torso, torso, pelvis, and right and left hip segments were created to track the motion of each segment. For example, upper torso axes were built by first drawing a vector from the seventh cervical vertebrae to the left acromioclavicular joint (C7 → LSHO = $\vec{a}$) and from the left to right acromioclavicular joint (LSHO → RSHO = $\vec{b}$). $\vec{b}$ was taken as the y-axis rotations about which represent the upper torso and torso flexion/extension, pelvic and hip anterior/posterior tilt. The cross product of $\vec{a}$ and $\vec{b}$ vectors created a $\vec{c}$ which represented rotations about the z-axis or upper torso, torso and pelvic axial rotations, and hip internal and external rotations ($\vec{a} \times \vec{b} = \vec{c}$). To ensure that vectors were orthogonal $\vec{b} \times \vec{c}$ was taken giving the vector $\overrightarrow{aa}$ which corresponded with the x-axis. Rotations about this axis represented the lateral bend of the upper torso and torso, hip abduction/adduction, and pelvic lateral tilt

Amputee runner MATLAB code

7.1 General processing code

S. Mukui Mutunga
Date created: Wednesday 6 October 2021
Purpose: re-do amputee running analysis
Sensors:

- C7 = dat(:,1:3);
- LSHO = dat(:,4:6);
- RSHO = dat(:,7:9);
- Man = dat(:,10:12);
- LPSIS = dat(:,13:15);
- RPSIS = dat(:,16:18);
- LASIS = dat(:,19:21);
- RASIS = dat(:,22:24);
- LHIP = dat(:,25:27);
- RHIP = dat(:,28:30);
- LTH1 = dat(:,31:33);
- LTH2 = dat(:,34:36);
- LTH3 = dat(:,37:39);
- LTH4 = dat(:,40:42);
- RTH1 = dat(:,43:45);
- RTH2 = dat(:,46:48);
- RTH3 = dat(:,49:51);
- RTH4 = dat(:,52:54);
- LKnee = dat(:,55:57);
- RKnee = dat(:,58:60);
- LSH1 = dat(:,61:63);
- LSH2 = dat(:,64:66);
- LSH3 = dat(:,67:69);
- LSH4 = dat(:,70:72);
- RSH1 = dat(:,73:75);
- RSH2 = dat(:,76:78);
- RSH3 = dat(:,79:81);
- RSH4 = dat(:,82:84);
- LANK = dat(:,85:87);
- RANK = dat(:,88:90);
- LHEEL = dat(:,91:93);
- RHEEL = dat(:,94:96);

- LTOE = dat(:,97:99);
- RTOE = dat(:,100:102);

General analysis notes:

- Sub 3 - has no SSS data
- Sub 6 - missing amputated side ankle data for PS

```
clear; close all; clc

type = 2;      % 1 == Kinematic/sensor data, 2 == Kinetic/FP data
side = 2;
substart = 1; subnum = 9;
tasks = 2;     % 2 tasks, 1 = Prescribed Speed (PS), 2 = Self-selected
speed (SSS)
trials = 6;    % 2-6 depending on subjects
kfreq = 300;   % sensor data collection frequency
```

Reading Data

```
[K_PSdat, K_SSSdat] = AmpRun_SubDatmat05(Kdatpath,Fdatpath, matpath, type,
substart, subnum,tasks, trials);
```

Identify intact and amputated heel strike and toe offs

```
[PS_IntToeHeel, PS_AmpToeHeel, SSS_IntToeHeel, SSS_AmpToeHeel] = ...
    AmpRun_HeelStrike_ToeOff02(matpath, tasks, substart, subnum, side);
```

Calculate gait parameters

```
[PS_Vel, SSS_Vel, PS_IAStrideTime, SSS_IAStrideTime, PS_IAStrideLength,...
    SSS_IAStrideLength,PS_IAStanceTime, PS_IAStanceGC, SSS_IAStanceTime,
...
    SSS_IAStanceGC]  = AmpRun_GaitParam08(kfreq, matpath, side,
tasks,substart, subnum);
```

Segment rotations

Includes interpolation

RotsE = raw rotation data

RotsEi = interpolated rotation data, divided into intact and amputated side strides

```
[PS_RotsE,SSS_RotsE, PS_RotsEi, SSS_RotsEi] = ...
    AmpRun_SegmentRotations6(matpath,substart, subnum, tasks, side);
```

Ensemble average graphs

```
AmpRun_EnsembleAverage01(matpath, figpath, substart, subnum, tasks, side);
```

Rotational amplitude calculations & excel sheet for statisticaly anslysis (R)

```
[Group_RotAmp] = AmpRun_RotationalAmplitudes01(matpath, statpath,
substart, subnum, tasks);
```
e. Coordination patterns

```
[PS_AngPos, PS_AngVel, PS_CRP, SSS_AngPos, SSS_AngVel, SSS_CRP]    =
AmpRun_CRP06(matpath, substart, subnum, tasks);
```
CRPmean, variability and proportion of the gait cycle spent out-of-phase & excel sheet for statistical analysis in R

```
[Group_CRPmean, Group_CRPvar, Group_OOF]...
    = AmpRun_CRPstats02(matpath, statpath, substart, subnum, tasks);
```

7.2 Calculation of coordination patterns

S. Mukui Mutunga
Date created: Friday 19 November 2021
Purpose: coordination pattern calculations
Last major version - v05: fixing angular velocity calculations & adding CRP calculations using the Hilbert transform
New in v06 - Analyzing only intact side strides, and removing hip from coordination analysis , and using interpolated data for analysis

```
function [PS_AngPos, PS_AngVel, PS_CRP, SSS_AngPos, SSS_AngVel, SSS_CRP]
...
    = AmpRun_CRP06(matpath, substart, subnum, tasks)


for isub = substart:subnum


    disp(['Sub' num2str(isub) ' running...']);


    load([matpath 'Sub' num2str(isub) '_Data.mat'], 'PS_RotsEi',
'SSS_RotsEi', 'PS_IntToeHeel', 'SSS_IntToeHeel')


    % PS_RotEi(1,:) = intact side stride
    % PS_RotEi(2,:) = amputated side stride


    for itasks = 1:tasks


        if itasks >= 1
            clear angvel angvel_temp angpos_temp theta omega phi CRP CRPg1
gimbal_CRP CRPg
        end




        if itasks == 1
            task_name = 'PS'; dat = PS_RotsEi(1,:); trial_no =
size(PS_RotsEi,2);
            Heel = PS_IntToeHeel;
        else
            task_name = 'SSS'; dat = SSS_RotsEi(1,:); trial_no =
size(SSS_RotsEi,2);
            Heel = SSS_IntToeHeel;
        end
```

```
        for itrials = 1:trial_no
            for istrides = 1:size(dat{itrials},3)


                h = 1; % resolution for central difference method
                angvel = zeros(size(dat{itrials}(:,:,istrides))); %
preallocate derivative vectors


                for j = 1:size(dat{itrials}(:,:,istrides),2)
                    for i = 1:length(dat{itrials}(:,:,istrides))
                        switch i
                            case 1
                                % use FORWARD difference here for the
first point
                                angvel(i,j) = dat{itrials}(i+1,j,istrides)
- dat{itrials}(i,j,istrides);
                            case  length(dat{itrials}(:,:,istrides))
                                % use BACKWARD difference here for the
last point
                                angvel(i,j) = dat{itrials}(i,j,istrides) -
dat{itrials}(i-1,j,istrides);
                            otherwise
                                % use CENTRAL difference
                                angvel(i,j) =
(dat{itrials}(i+1,j,istrides) - dat{itrials}(i-1,j,istrides))/2/h;
                        end
                    end
                end
```

normalizing angular position and angular velocity

```
                angvel_temp = angvel;
                angpos_temp = dat{itrials}(:,:,istrides);


                for col = 1:size(angvel_temp,2)
                    for row = 1:size(angvel_temp,1)
                        angpos_temp_norm(row,col) = 2 *
((angpos_temp(row,col) - min(angpos_temp(:,col))) ...
                            / (max(angpos_temp(:,col) -
min(angpos_temp(:,col))))) - 1;
                        angvel_temp_norm(row,col) = angvel_temp(row,col)
./ (max(abs(angvel_temp(:,col))));
                    end
                end
```

```
                theta{itrials}(:,:,istrides) = angpos_temp_norm;
                omega{itrials}(:,:,istrides) = angvel_temp_norm;
```

CRP calculations

```
                phi = atan2(omega{itrials}(:,:,istrides),
theta{itrials}(:,:,istrides)) * (180/pi);


                CRP(:,1:3) = abs(phi(:,4:6) -  phi(:,1:3)); % Torso -
Upper-Torso
                CRP(:,4:6) = abs(phi(:,7:9) -  phi(:,1:3)); % Pelvis -
Upper-Torso
                CRP(:,7:9) = abs(phi(:,7:9) -  phi(:,4:6)); % Pelvis -
Torso
                CRPg1 = CRP;


                gimbal_CRP = find(CRP > 180);


                CRPg1(gimbal_CRP) = abs(CRP(gimbal_CRP) - 360);
                CRPg{:,itrials}(:,:,istrides) = CRPg1;
            end
        end
```

Parse into tasks

```
        if itasks == 1
            PS_AngPos = theta;
            PS_AngVel = omega;
            PS_CRP = CRPg;
        elseif itasks == 2
            SSS_AngPos = theta;
            SSS_AngVel= omega;
            SSS_CRP = CRPg;
        end
    end



    save([matpath 'Sub' num2str(isub)
'_Data.mat'],'PS_AngPos','PS_AngVel','PS_CRP',...
        'SSS_AngPos','SSS_AngVel','SSS_CRP','-append');
end
end
```

Chapter 8 Appendix 2 - Analysis of computer-generated signals

8.1 General processing code

S. Mukui Mutunga

Date created: 19 February 2022

Purpose: comparing continuous methods for calculating coordination patterns using known signals

```
clear; close all; clc
t = linspace(0,2*pi,4000);


str_knownSignals = ["Sinusoidal - 0 {\circ} shift","Sinusoidal - 18
{\circ} shift", "Sinusoidal -  {\circ} shift",...
    "Sinusoidal - Sin(2{\pi}t)",  "Sinusoidal - Sin(3{\pi}t)",...
    "Non-Sinusoidal signal - 0 {\circ} shift","Non-Sinusoidal signal - 18
{\circ} shift",...
    "Non-Sinusoidal signal - 126 {\circ} shift"];
```

Scenario 1: 3 signals of the same frequency w/ phase shifts of 0, 18, 126 degrees

```
S1_00 = sin(3 * pi * t);
S1_18 = sin(3 * pi * t - (18 * pi/180));
S1_126  = sin(3 * pi * t - (126 * pi/180));
```

Scenario 2: 2 signals of different frequencies w/o phase shifts

```
S2_2t = sin(3 * pi * t);
S2_3t = sin(4 * pi * t);
```

Scenario 3: 3 non-sinusoidal signals with phase shifts of 0, 18, and 126 degrees

```
S3_00 = cos(3 * pi * t - 0.25 * pi) ./ (sqrt(1 + 0.4148^2 - 2  * 0.4148 *
sin(3 * pi * t - 0.25 * pi)));
S3_18 = cos(3* pi * t - 0.25 * pi + (18 * pi/180)) ./ (sqrt(1 +  0.4148^2
- 2 * 0.4148 * ...
    sin(3 * pi * t - 0.25 * pi + (18 * pi/180))));
S3_126 = cos(3 * pi * t - 0.25 * pi + (126 * pi/180)) ./ (sqrt(1 +
0.4148^2 - 2 * 0.4148 * ...
    sin(3 * pi * t - 0.25 * pi + (126 * pi/180))));


theta = [S1_00; S1_18; S1_126; S2_2t; S2_3t; S3_00; S3_18; S3_126]'; %
angular position
```

Plots of all signals

```
figure(1); subplot(3,2,1); plot(t,S1_00,'k', 'LineWidth',1.5);
           hold on;  plot(t,S1_18, 'k--', 'LineWidth',1.5);
           legend('sin(3{\pi}t)', 'sin(3{\pi}t -
18{\circ})','FontSize',12)
           xlabel('t','FontSize',12); ylabel('x(t)','FontSize',12)
           title('Scenario 1: Sinusoidal signals of same frequency -
18{\circ} phase shift','FontSize',16)
```

```
            subplot(3,2,2); plot(t,S1_00,'k', 'LineWidth',1.5);
            hold on;  plot(t,S1_126, 'k--', 'LineWidth',1.5);
            legend('sin(3{\pi}t)', 'sin(3{\pi}t - 126{\circ})')
            xlabel('t'); ylabel('x(t)')
            title('Scenario 1: Sinusoidal signals of same frequency -
126{\circ} phase shift','FontSize',16)


            subplot(3,2,[3 4]);  plot(t, S2_2t,'k','LineWidth',1.5); hold
on; plot(t, S2_3t,'k--','LineWidth',1.5)
            legend('sin(3{\pi}t)', 'sin(4{\pi}t)','FontSize',12)
            xlabel('t','FontSize',12); ylabel('x(t)','FontSize',12)
            title('Scenario 2: Sinusoidal signals of the different
frequencies without phase shifts','FontSize',16)


            subplot(3,2,5); plot(t, S3_00,'k','LineWidth',1.5);
            hold on; plot(t, S3_18,'k--','LineWidth',1.5)
            legend('non-sinusoidal ', 'non-sinusoidal shifted by
18{\circ}','FontSize',12)
            xlabel('t','FontSize',12); ylabel('x(t)','FontSize',12)
            title('Scenario 3: Non-sinusoidal signals - 18{\circ} phase
shift','FontSize',16)


            subplot(3,2,6); plot(t, S3_00,'k', 'LineWidth',1.5);
            hold on; plot(t, S3_126,'k-- ','LineWidth',1.5);
            legend('non-sinusoidal', 'non-sinusoidal shifted by
126{\circ}','FontSize',12)
            xlabel('t','FontSize',12); ylabel('x(t)','FontSize',12)
            title('Scenario 3: Non-sinusoidal signals - 126{\circ} phase
shift','FontSize',16)


            sgtitle('Known signals used to test continuous
methods','FontSize',20)


            set(gcf, 'Position', get(0, 'Screensize'));
            saveas(gcf, [figpath 'Known Signals plots - All.png'])
```

CRP calculations w/ plots

```
[CRPg] = KS_CRP02(figpath, matpath, t, theta);
```

CRP_HT calculations

```
[CRP_HTg] = KS_CRPHT01(figpath, matpath, t, theta);
```

RFP calcualtions - using a rectangular and Hamming windows

```
[RFP_rectg, RFP_hammg, RFP_hanng] = KS_RFP03(figpath,matpath,t, theta);
```

CRP, CRP_HT & RFP analysis - amputee running example

```
clear; close all; clc
```

```
AmpMatPath = '/Users/Kui/Documents/Amputee Study/AmpRun_Force and
Kinematic Processing/Matfiles2 - 6Oct2021/';
figpath = '/Users/Kui/Documents/Amputee Study/Known Signal
Processing/Known  Signal Plots/';
matpath = '/Users/Kui/Documents/Amputee Study/Known Signal
Processing/Known Signal Matfiles/';


tasks = 2; subs = 1; kfreq = 300;  % sensor data collection frequency


[PS_CRP, PS_CRPHT, PS_RFP, SSS_CRP, SSS_CRPHT, SSS_RFP] = ...
    KS_AmpAnalysis02(AmpMatPath, figpath, matpath, tasks, kfreq, subs);
```

CRP, CRP_HT & RFP analysis - iWalk example

```
clear; close all; clc
iWalkMatPath = '/Users/Kui/Documents/Amputee Study/iWalk Data
Analysis/iWalk Matfiles/';
figpath = '/Users/Kui/Documents/Amputee Study/Known Signal
Processing/Known  Signal Plots/';
matpath = '/Users/Kui/Documents/Amputee Study/Known Signal
Processing/Known Signal Matfiles/';


tasks = 2; subs = 2; speed = 4; trials = 6; kfreq = 60;


[Norm_CRP, Norm_CRPHT, Norm_RFP, iWalk_CRP, iWalk_CRPHT, iWalk_RFP]...
    = KS_iWalkAnalysis01(iWalkMatPath, matpath, figpath, tasks,speed,
trials, kfreq, subs);
```

CRP/CRP_HT & RFP - statistics

```
clear; close all; clc
matpath = '/Users/Kui/Documents/Amputee Study/Known Signal
Processing/Known Signal Matfiles/';
Amp_tasks = 2; methods = 3; iWalk_tasks = 2; speed = 4;


[KS_Means_Std_table, PS_Mean_Std_table, SSS_Mean_Std_table, ...
    NormCRP_Mean_Std_table, NormCRPHT_Mean_Std_table,
NormRFP_Mean_Std_table, ...
    iWalkCRP_Mean_Std_table,
iWalkCRPHT_Mean_Std_table,iWalkRFP_Mean_Std_table,...
    NormCRP_OOF_table, NormCRPHT_OOF_table, NormRFP_OOF_table,...
    iWalkCRP_OOF_table, iWalkCRPHT_OOF_table, iWalkRFP_OOF_table] ...
    = KS_Statistics01(matpath, Amp_tasks, iWalk_tasks, methods, speed);
```

8.2 Computer-generated signals – CRP analysis

S. Mukui Mutunga

Date created: Sunday 1 May 2022

Purpose: Relative phase calculations using CRP - method proposed by Hamill 1999

New in V02: moving omega, theta_norm and omega_norm calculations from the main script here

```
function [CRPg] = KS_CRP02(figpath, matpath, t,theta)


omega = zeros(size(theta)); % preallocate derivative vectors


h = 1; % resolution for central difference method


for j = 1:size(theta,2)
    for i = 1:length(theta)
        switch i
            case 1
                % use FORWARD difference here for the first point
                omega(i,j) = theta(i+1,j) - theta(i,j);
            case length(theta)
                % use BACKWARD difference here for the last point
                omega(i,j) = theta(i,j) - theta(i-1,j);
            otherwise
                % use CENTRAL difference
                omega(i,j) = (theta(i+1,j)-theta(i-1,j))/2/h;
        end
    end
end


clear i j


for k = 1:size(theta,2)
    %     if i == 1 || i == 2 || i == 3 || i == 4 || i == 5
    theta_norm(:,k) = 2 * ((theta(:,k) - min(theta(:,k))) /
(max(theta(:,k) - min(theta(:,k))))) -1;
    omega_norm(:,k) = omega(:,k) / max(abs(omega(:,k)));
end


clear k
```

```
phi = atan2(omega_norm,theta_norm) * (180/pi);


CRP(:,1) = abs(phi(:,2) - phi(:,1)); % S1_18 - S1_00
CRP(:,2) = abs(phi(:,3) - phi(:,1)); % S1_126 - S1_00
CRP(:,3) = abs(phi(:,5) - phi(:,4)); % S2_3t - S2_2t
CRP(:,4) = abs(phi(:,7) - phi(:,6)); % S3_18 - S3_00
CRP(:,5) = abs(phi(:,8) - phi(:,6)); % S3_126 - S3_00


CRP = abs(CRP);
```

CRP Gimbal fix

```
CRPg = CRP;


gimbal = find(CRP > 180);
CRPg(gimbal) = abs(CRP(gimbal) - 360);
```

CRP figures

```
prompt = input('Do you want to output the CRP results [y/n]','s');


if prompt == 'y'
    figure(20); subplot(3,2,1); plot(t, CRP(:,1),'k','LineWidth',1.5);
    xlabel('t')
    ylabel('Relative Phase ({\circ})')
    title('Scenario 1: CRP Sinusoidal signals - 18 {\circ} - 0 {\circ}');


    subplot(3,2,2); plot(t, CRP(:,2),'k','LineWidth',1.5);
    xlabel('t')
    ylabel('Relative Phase ({\circ})')
    title('Scneario 1: CRP Sinusoidal signals - 126 {\circ} - 0 {\circ}');


    subplot(3,2,[3 4]); plot(t, CRP(:,3), 'k','LineWidth',1.5);
    xlabel('t')
    ylabel('Relative Phase ({\circ})')
    title('Scenario 2: CRP Sinusoidal signals - sin(3t) - sin(2t)');


    subplot(3,2,5); plot(t, CRP(:,4),'k','LineWidth',1.5);
    xlabel('t')
    ylabel('Relative Phase ({\circ})')
    title('Scenario 3: CRP Non-sinusoidal signals - 18 {\circ} - 0
{\circ}');


    subplot(3,2,6); plot(t, CRP(:,5),'k','LineWidth',1.5);
```

```
    xlabel('t')
    ylabel('Relative Phase ({\circ})')
    title('Scenario 3: CRP Non-sinusoidal signals - 126 {\circ} - 0
{\circ}');


    sgtitle('|CRP calculations| before gimbal fix');
    set(gcf, 'Position', get(0, 'Screensize'));
    saveas(gcf, [figpath 'CRP before gimbal fix.png'])


    figure(21); subplot(3,2,1); plot(t, CRPg(:,1),'k','LineWidth',1.5);
    xlabel('t')
    ylabel('Relative Phase ({\circ})')
    title('Scenario 1: CRP Sinusoidal signals - 18 {\circ} - 0 {\circ}');


    subplot(3,2,2); plot(t, CRPg(:,2),'k','LineWidth',1.5);
    xlabel('t')
    ylabel('Relative Phase ({\circ})')
    axis([0 7 125.5 126.5])
    title('Scneario 1: CRP Sinusoidal signals - 126 {\circ} - 0 {\circ}');


    subplot(3,2,[3 4]); plot(t, CRPg(:,3),'k','LineWidth',1.5);
    xlabel('t')
    ylabel('Relative Phase ({\circ})')
    title('Scenario 2: CRP Sinusoidal signals - sin(3t) - sin(2t)');


    subplot(3,2,5); plot(t, CRPg(:,4),'k','LineWidth',1.5);
    xlabel('t')
    ylabel('Relative Phase ({\circ})')
    title('Scenario 3: CRP Non-sinusoidal signals - 18 {\circ} - 0
{\circ}');


    subplot(3,2,6); plot(t, CRPg(:,5),'k','LineWidth',1.5);
    xlabel('t')
    ylabel('Relative Phase ({\circ})')
    title('Scenario 3: Non-sinusoidal signals - 126 {\circ} - 0 {\circ}');


    sgtitle('|CRP calculations| after gimbal fix');
    set(gcf, 'Position', get(0, 'Screensize'));
    saveas(gcf, [figpath 'CRP after gimbal fix.png'])
end
```

Save data to matpath

```
save([matpath 'KnownSignals.mat'],"CRPg");
end
```

8.3 Computer-generated signals – CRP_{HT} code

S. Mukui Mutunga

Date created: Sunday 1 May 2022

Purpose: Relative phase calculations using the Hilbert Transform - method proposed by Li and Stockl

```
function [CRP_HTg] = KS_CRPHT01(figpath, matpath, t, theta)
HT_omega = hilbert(theta); % contains both real and imaginary parts
HT_phi = atan2d(imag(HT_omega), real(HT_omega));



CRP_HT(:,1) = abs(HT_phi(:,2) - HT_phi(:,1)); % S1_18 - S1_00
CRP_HT(:,2) = abs(HT_phi(:,3) - HT_phi(:,1)); % S1_126 - S1_00
CRP_HT(:,3) = abs(HT_phi(:,5) - HT_phi(:,4)); % S2_3t - S2_2t
CRP_HT(:,4) = abs(HT_phi(:,7) - HT_phi(:,6)); % S3_18 - S3_00
CRP_HT(:,5) = abs(HT_phi(:,8) - HT_phi(:,6)); % S3_126 - S3_00
```

Fixing gimbal lock

```
CRP_HTg = CRP_HT;


gimbal_170 = find(CRP_HT > 180);
CRP_HTg(gimbal_170) = abs(CRP_HT(gimbal_170) - 360);


clear gimbal_170
```

CRP HT figures

```
prompt = input('Do you want to output the CRP_HT results [y/n]','s');


if prompt == 'y'
    figure(30); subplot(3,2,1); plot(t,CRP_HT(:,1),'k',"LineWidth",1.5);
    xlabel('t')
    ylabel('Relative Phase ({\circ})')
    title('Scenario 1: CRP_{HT} Sinusoidal signals - 18 {\circ} - 0
{\circ}');


    subplot(3,2,2); plot(t,CRP_HT(:,2),'k',"LineWidth",1.5);
    xlabel('t')
    ylabel('Relative Phase ({\circ})')
    title('Scenario 1: CRP_{HT} Sinusoidal signals - 126 {\circ} - 0
{\circ}');
```

```
    subplot(3,2,[3 4]); plot(t,CRP_HT(:,3),'k',"LineWidth",1.5);
    xlabel('t')
    ylabel('Relative Phase ({\circ})')
    title('Scenario 2: CRP_{HT} Sinusoidal signals - sin(3t) - sin(2t)');


    subplot(3,2,5); plot(t,CRP_HT(:,4),'k',"LineWidth",1.5);
    title('Scenario 3: CRP_{HT} Non-sinusoidal signals - 18 {\circ} - 0
{\circ}');


    subplot(3,2,6); plot(t,CRP_HT(:,5),'k',"LineWidth",1.5);
    xlabel('t')
    ylabel('Relative Phase ({\circ})')
    title('Scenario 3: Non-sinusoidal signals - 126 {\circ} - 0 {\circ}');
    sgtitle('|CRP_{HT}| - before gimbal fix')


    set(gcf, 'Position', get(0, 'Screensize'));
    saveas(gcf, [figpath 'CRP_HT before gimbal fix.png']);


    figure(31); subplot(3,2,1); plot(t, CRP_HTg(:,1),'k',"LineWidth",1.5);
    xlabel('t')
    ylabel('Relative Phase ({\circ})')
    title('Scenario 1: CRP_{HT} Sinusoidal signals - 18 {\circ} - 0
{\circ}');


    subplot(3,2,2); plot(t, CRP_HTg(:,2),'k',"LineWidth",1.5);
    xlabel('t')
    ylabel('Relative Phase ({\circ})')
    title('Scenario 1: CRP_{HT}Sinusoidal signals - 126 {\circ} - 0
{\circ}')


    subplot(3,2,[3 4]); plot(t, CRP_HTg(:,3),'k',"LineWidth",1.5);
    xlabel('t')
    ylabel('Relative Phase ({\circ})')
    title('Scenario 2: CRP_{HT} Sinusoidal signals - sin(3t) - sin(2t)');


    subplot(3,2,5); plot(t, CRP_HTg(:,4),'k',"LineWidth",1.5);
    xlabel('t')
    ylabel('Relative Phase ({\circ})')
    title('Scenario 3: CRP_{HT} Non-sinusoidal signals - 18 {\circ} - 0
{\circ}');
```

```
    subplot(3,2,6); plot(t, CRP_HTg(:,5),'k',"LineWidth",1.5);
    xlabel('t')
    ylabel('Relative Phase ({\circ})')
    title('Scenario 3: CRP_{HT} Non-sinusoidal signals - 126 {\circ} - 0
{\circ}');
    sgtitle('|CRP_{HT}| - after gimbal fix');




    set(gcf, 'Position', get(0, 'Screensize'));
    saveas(gcf, [figpath 'CRP_HT after gimbal fix.png']);


end
```

Save to matpath

```
save([matpath 'KnownSignals.mat'],"CRP_HTg", '-append');


end
```

8.4 Computer-generated signals – RFP code

S. Mukui Mutunga

Date created: Monday 2 May 2022

Purpose: RFP analysis using rectangular and hamming windows

New v03: using signal minima to identify window lengths

```
function [RFP_rectg, RFP_hammg, RFP_hanng] = KS_RFP03(figpath,matpath,t,
theta)


Ts = mean(diff(t)); % sampling interval
fs = 1/Ts;


for i = 1:size(theta,2)
    [Pwd(:,i),F(:,i)] = periodogram(theta(:,i),
hann(length(theta)),length(theta),fs);


    % Identifying location of fundamental frequency
    [~, fundamentalfreq(1,i)] = findpeaks(Pwd(:,i),'NPeaks',1);
end
clear i


F6(1,:) = F(fundamentalfreq); % identifying fundamental frequency
F6(2,:) = F6(1,:) * 2; % second harmonic of the funadmental frequency
F6(3,:) = F6(1,:) * 3;
F6(4,:) = F6(1,:) * 4;
F6(5,:) = F6(1,:) * 5;
F6(6,:) = F6(1,:) * 6;


% F6 = F6 * 100;


F6_p = F6 + (0.10 * F6); % 10% + F6 = upper frequency bound
F6_n = F6 - (0.01 * F6); % 10% - F6 = lower frequency bound
```

Calculate average power spectral density over each frequency band & index of harmonicity (IH)

```
for i = 1:size(F6,1)
    for j = 1:size(F6,2)
        PSD(i,j) = bandpower(Pwd(:,j), F(:,j),[F6_n(i,j)
F6_p(i,j)],'psd');
        IH(:,j) = PSD(1,j)/sum(PSD(:,j));
    end
end
```

```
clear i j
```

Windowed Fourier analysis - calculation of phase angles

```
for i = 1:size(theta,2)
    if i == 1 || i == 2 || i == 3
        f1max = max(F6(1,1:3));
    elseif i == 4 || i == 5
        f1max = max(F6(1,4:5));
    elseif i == 6 || i == 7 || i == 8
        f1max = max(F6(1,6:8));
    end


    [~, theta_pklocs] = findpeaks(-theta(:,i));


    windowlength = round(mean(diff(theta_pklocs)));
    %     windowlength = round(4 * (1/f1max) * fs);
    overlap = windowlength-1;


    % short-time Fourier transform


    [Sz_theta_hamm, Sz_fs_hamm] = stft(theta(:,i),
fs,'window',hamming(windowlength),...
        'OverlapLength', overlap);


    [Sz_theta_rectwin, Sz_fs_rectwin] = stft(theta(:,i),fs,'window',
rectwin(windowlength),...
        'OverlapLength',overlap);


    [Sz_theta_hann, Sz_fs_hann] = stft(theta(:,i),fs,'window',
hann(windowlength),...
        'OverlapLength',overlap);


    [~, x_hamm] = min(abs(Sz_fs_hamm - f1max));
    [~ ,x_rectwin] = min(abs(Sz_fs_rectwin - f1max));
    [~, x_hann] = min(abs(Sz_fs_hann - f1max));


    % pulling stft data at f1max
    hamm_theta_f1max = Sz_theta_hamm(x_hamm,:)';
    rect_theta_f1max = Sz_theta_rectwin(x_rectwin,:)';
    hann_theta_f1max = Sz_theta_hann(x_hann,:)';
```

```
    % RFP
    RFP_phi_hamm{i} = angle(hamm_theta_f1max) * (180/pi);
    RFP_phi_rect{i} = angle(rect_theta_f1max) * (180/pi);
    RFP_phi_hann{i} = angle(hann_theta_f1max) * (180/pi);


end


cutlength = min(cellfun('length',RFP_phi_hamm));


for j = 1:size(RFP_phi_rect,2)
    RFP_phi_hamm_cut(:,j) = RFP_phi_hamm{j}(1:cutlength);
    RFP_phi_rect_cut(:,j) = RFP_phi_rect{j}(1:cutlength);
    RFP_phi_hann_cut(:,j) = RFP_phi_hann{j}(1:cutlength);
end


clear i j
```

RFP calculations

```
%% Rectangular window


RFP_rect(:,1) = abs(RFP_phi_rect_cut(:,2) - RFP_phi_rect_cut(:,1));
RFP_rect(:,2) = abs(RFP_phi_rect_cut(:,3) - RFP_phi_rect_cut(:,1));
RFP_rect(:,3) = abs(RFP_phi_rect_cut(:,5) - RFP_phi_rect_cut(:,4));
RFP_rect(:,4) = abs(RFP_phi_rect_cut(:,7) - RFP_phi_rect_cut(:,6));
RFP_rect(:,5) = abs(RFP_phi_rect_cut(:,8) - RFP_phi_rect_cut(:,6));


%% Hamming window
RFP_hamm(:,1) = abs(RFP_phi_hamm_cut(:,2) - RFP_phi_hamm_cut(:,1));
RFP_hamm(:,2) = abs(RFP_phi_hamm_cut(:,3) - RFP_phi_hamm_cut(:,1));
RFP_hamm(:,3) = abs(RFP_phi_hamm_cut(:,5) - RFP_phi_hamm_cut(:,4));
RFP_hamm(:,4) = abs(RFP_phi_hamm_cut(:,7) - RFP_phi_hamm_cut(:,6));
RFP_hamm(:,5) = abs(RFP_phi_hamm_cut(:,8) - RFP_phi_hamm_cut(:,6));


%% Hanning window
RFP_hann(:,1) = abs(RFP_phi_hann_cut(:,2) - RFP_phi_hann_cut(:,1));
RFP_hann(:,2) = abs(RFP_phi_hann_cut(:,3) - RFP_phi_hann_cut(:,1));
RFP_hann(:,3) = abs(RFP_phi_hann_cut(:,5) - RFP_phi_hann_cut(:,4));
RFP_hann(:,4) = abs(RFP_phi_hann_cut(:,7) - RFP_phi_hann_cut(:,6));
RFP_hann(:,5) = abs(RFP_phi_hann_cut(:,8) - RFP_phi_hann_cut(:,6));
```

RFP gimbal fix

```
RFP_rectg = RFP_rect;
RFP_hammg = RFP_hamm;
```

```
RFP_hannng = RFP_hann;




gimbal_rect = find(RFP_rectg > 180);
gimbal_hamm = find(RFP_hammg > 180);
gimbal_hann = find(RFP_hannng > 180);


RFP_rectg(gimbal_rect) = abs(RFP_rect(gimbal_rect) - 360);
RFP_hammg(gimbal_hamm) = abs(RFP_hamm(gimbal_hamm) - 360);
RFP_hannng(gimbal_hann) = abs(RFP_hann(gimbal_hann) - 360);
```

RFP figures

```
prompt = input('Do you want to output the RFP results [y/n]','s');


if prompt == 'y'


    figure(30); subplot(3,2,1); plot(RFP_rect(:,1),'k','LineWidth',1.5);
    xlabel('t')
    ylabel('Relative Phase ({\circ})')
    title('Scenario 1: Sinusoidal signals - 18 {\circ} - 0 {\circ}');


    subplot(3,2,2); plot(RFP_rect(:,2),'k','LineWidth',1.5);
    xlabel('t')
    ylabel('Relative Phase ({\circ})')
    title('Scenario 1: Sinusoidal signals - 126 {\circ} - 0 {\circ}');


    subplot(3,2,[3,4]); plot(RFP_rect(:,3),'k','LineWidth',1.5);

    title('Scenario 2: Sinusoidal signals - sin(3t) - sin(2t)');
    xlabel('t')
    ylabel('Relative Phase ({\circ})')
    subplot(3,2,5); plot(RFP_rect(:,4),'k','LineWidth',1.5);
    title('Scenario 3: Non-sinusoidal signals - 18 {\circ} - 0 {\circ}');


    subplot(3,2,6); plot(RFP_rect(:,5),'k','LineWidth',1.5);
    xlabel('t')
    ylabel('Relative Phase ({\circ})')
    title('Scenario 3: Non-sinusoidal signals - 126 {\circ} - 0 {\circ}');


    sgtitle('RFP w/ rectangular window before gimbal fix');
    set(gcf, 'Position', get(0, 'Screensize'));
```

```
saveas(gcf, [figpath 'RFP rect before gimbal fix.png'])


figure(31); subplot(3,2,1); plot(RFP_hamm(:,1),'k','LineWidth',1.5);
xlabel('t')
ylabel('Relative Phase ({\circ})')
title('Scenario 1: Sinusoidal signals - 18 {\circ} - 0 {\circ}');


subplot(3,2,2); plot(RFP_hamm(:,2),'k','LineWidth',1.5);
xlabel('t')
ylabel('Relative Phase ({\circ})')
title('Scenario 1: Sinusoidal signals - 126 {\circ} - 0 {\circ}');


subplot(3,2,[3,4]); plot(RFP_hamm(:,3),'k','LineWidth',1.5);
xlabel('t')
ylabel('Relative Phase ({\circ})')
title('Scenario 2: Sinusoidal signals - sin(3t) - sin(2t)');


subplot(3,2,5); plot(RFP_hamm(:,4),'k','LineWidth',1.5);
title('Scenario 3: Non-sinusoidal signals - 18 {\circ} - 0 {\circ}');


subplot(3,2,6); plot(RFP_hamm(:,5),'k','LineWidth',1.5);
xlabel('t')
ylabel('Relative Phase ({\circ})')
title('Scenario 3: Non-sinusoidal signals - 126 {\circ} - 0 {\circ}');


sgtitle('RFP w/ Hamm window before gimbal fix');
set(gcf, 'Position', get(0, 'Screensize'));
saveas(gcf, [figpath 'RFP Hamm before gimbal fix.png'])


figure(33); subplot(3,2,1); plot(RFP_hann(:,1),'k','LineWidth',1.5);
xlabel('t')
ylabel('Relative Phase ({\circ})')
title('Scenario 1: Sinusoidal signals - 18 {\circ} - 0 {\circ}');


subplot(3,2,2); plot(RFP_hann(:,2),'k','LineWidth',1.5);
xlabel('t')
ylabel('Relative Phase ({\circ})')
title('Scenario 1: Sinusoidal signals - 126 {\circ} - 0 {\circ}');


subplot(3,2,[3,4]); plot(RFP_hann(:,3),'k','LineWidth',1.5);
```

```
    xlabel('t')
    ylabel('Relative Phase ({\circ})')
    title('Scenario 2: Sinusoidal signals - sin(3t) - sin(2t)');


    subplot(3,2,5); plot(RFP_hann(:,4),'k','LineWidth',1.5);
    xlabel('t')
    ylabel('Relative Phase ({\circ})')
    title('Scenario 3: Non-sinusoidal signals - 18 {\circ} - 0 {\circ}');


    subplot(3,2,6); plot(RFP_hann(:,5),'k','LineWidth',1.5);
    xlabel('t')
    ylabel('Relative Phase ({\circ})')
    title('Scenario 3:  Non-sinusoidal signals - 126 {\circ} - 0
{\circ}');


    sgtitle('RFP w/ Hanning window before gimbal fix');
    set(gcf, 'Position', get(0, 'Screensize'));
    saveas(gcf, [figpath 'RFP Hann before gimbal fix.png'])
```

RFP plots after gimbal fix

```
    figure(34); subplot(3,2,1); plot(RFP_rectg(:,1),'k','LineWidth',1.0);
    xlabel('t')
    ylabel('Relative Phase ({\circ})')
    title('Scenario 1: RFP_{rect} Sinusoidal signals - 18 {\circ} - 0
{\circ}');


    subplot(3,2,2); plot(RFP_rectg(:,2),'k','LineWidth',1.5);
    xlabel('t')
    ylabel('Relative Phase ({\circ})')
    title('Scenario 1: RFP_{rect} Sinusoidal signals - 126 {\circ} - 0
{\circ}');


    subplot(3,2,[3,4]); plot(RFP_rectg(:,3),'k','LineWidth',1.5);
    xlabel('t')
    ylabel('Relative Phase ({\circ})')
    title('Scenario 2: RFP_{rect} Sinusoidal signals - sin(3t) -
sin(2t)');


    subplot(3,2,5); plot(RFP_rectg(:,4),'k','LineWidth',1.5);
    xlabel('t')
    ylabel('Relative Phase ({\circ})')
    title('Scenario 3: RFP_{rect} Non-sinusoidal signals - 18 {\circ} - 0
{\circ}');
```

```
    subplot(3,2,6); plot(RFP_rectg(:,5),'k','LineWidth',1.5);
    xlabel('t')
    ylabel('Relative Phase ({\circ})')
    title('Scenario 3: RFP_{rect} Non-sinusoidal signals - 126 {\circ} - 0
{\circ}');


    sgtitle('RFP w/ rectangular window after gimbal fix')
    set(gcf, 'Position', get(0, 'Screensize'));
    saveas(gcf, [figpath 'RFP rect after gimbal fix.png'])


    figure(35); subplot(3,2,1); plot(RFP_hammg(:,1),'k','LineWidth',1.5);
    xlabel('t')
    ylabel('Relative Phase ({\circ})')
    title('Scenario 1: RFP_{hamm} Sinusoidal signals - 18 {\circ} - 0
{\circ}');


    subplot(3,2,2); plot(RFP_hammg(:,2),'k','LineWidth',1.5);
    xlabel('t')
    ylabel('Relative Phase ({\circ})')
    title('Scenario 1: RFP_{hamm} Sinusoidal signals - 126 {\circ} - 0
{\circ}');


    subplot(3,2,[3,4]); plot(RFP_hammg(:,3),'k','LineWidth',1.5);
    xlabel('t')
    ylabel('Relative Phase ({\circ})')
    title('Scenario 2: RFP_{hamm} Sinusoidal signals - sin(3t) -
sin(2t)');


    subplot(3,2,5); plot(RFP_hammg(:,4),'k','LineWidth',1.5);
    xlabel('t')
    ylabel('Relative Phase ({\circ})')
    title('Scenario 3: RFP_{hamm} Non-sinusoidal signals - 18 {\circ} - 0
{\circ}');


    subplot(3,2,6); plot(RFP_hammg(:,5),'k','LineWidth',1.5);
    xlabel('t')
    ylabel('Relative Phase ({\circ})')
    title('Scenario 3: RFP_{hamm} Non-sinusoidal signals - 126 {\circ} - 0
{\circ}');
```

```
    sgtitle('RFP w/ Hamming window after gimbal fix');
    set(gcf, 'Position', get(0, 'Screensize'));
    saveas(gcf, [figpath 'RFP Hamm gimbal fix.png'])


    figure(36); subplot(3,2,1); plot(RFP_hanng(:,1),'k','LineWidth',1.5);
    title('Scenario 1: RFP_{hann} Sinusoidal signals - 18 {\circ} - 0
{\circ}');


    subplot(3,2,2); plot(RFP_hanng(:,2),'k','LineWidth',1.5);
    xlabel('t')
    ylabel('Relative Phase ({\circ})')
    title('Scenario 1: RFP_{hann} Sinusoidal signals - 126 {\circ} - 0
{\circ}');


    subplot(3,2,[3,4]); plot(RFP_hanng(:,3),'k','LineWidth',1.5);
    xlabel('t')
    ylabel('Relative Phase ({\circ})')
    title('Scenario 2: RFP_{hann} Sinusoidal signals - sin(3t) -
sin(2t)');


    subplot(3,2,5); plot(RFP_hanng(:,4),'k','LineWidth',1.5);
    xlabel('t')
    ylabel('Relative Phase ({\circ})')
    title('Scenario 3: RFP_{hann} Non-sinusoidal signals - 18 {\circ} - 0
{\circ}');


    subplot(3,2,6); plot(RFP_hanng(:,5),'k','LineWidth',1.5);
    xlabel('t')
    ylabel('Relative Phase ({\circ})')
    title('Scenario 3: RFP_{hann} Non-sinusoidal signals - 126 {\circ} - 0
{\circ}');


    sgtitle('RFP w/ Hanning window after gimbal fix');
    set(gcf, 'Position', get(0, 'Screensize'));
    saveas(gcf, [figpath 'RFP Hann gimbal fix.png'])
end
```

Save data to matpath

```
save([matpath 'KnownSignals.mat'],"RFP_hammg", "RFP_hanng", "RFP_rectg",
'-append');


end
```